Conjugation of Mono-Functional Quinone Methides to DNA Ligands for Promotion of Reversible Alkylation

by

Blessing Deeyaa

A dissertation submitted to Johns Hopkins University in conformity with the requirements for the degree of Doctor of Philosophy

Baltimore, Maryland

February, 2017

ABSTRACT

Title of Document: Conjugation of mono-functional quinone methides to DNA ligands for promotion of reversible alkylation

Blessing D. Deeyaa, Doctor of Philosophy, 2017

Directed by: Professor Steven E. Rokita, Department of Chemistry

Quinone methides (QMs) are electrophilic intermediates that alkylate DNA through reaction with the nucleobases. An initial set of kinetic products allow for regeneration of the QM electrophiles which eventually go on to form an alternate set of thermodynamic adducts. Reversibility of QM-DNA adducts is of interest because regeneration of the reactive electrophile may facilitate evasion of DNA repair following excision of adducts. This feature extends the lifetime of a QM drug and is highly advantageous when targeting tumors because the formation of multiple lesions in series by a single molecule lowers the effective dose that is required to trigger apoptosis.

Previous studies in the Rokita lab showed that conjugation of mono-functional quinone methides (mono-QMs) to sequence directing oligonucleotides allowed for reversible alkylation of complementary strands. Although the sequence directing ligands minimizes indiscriminate reactions with endogenous nucleophiles, reversible alkylation is limited to targeted regions of a duplex and QMs are subject

to loss of DNA associating affinity if oligonucleotide ligands are digested by nucleases.

Mono-quinone methides (mono-QM) have now been conjugated to acridine and ammonium ligands that allow the electrophile to move freely along duplex DNA without sequence constraints. Both acridine and diammonium conjugated mono-QMs have been synthesized and shown to alkylate dsDNA reversibly at dG-N7 via transfer of regenerated QMs. The mono-QM acridine conjugate (**QMPAc**) migrates along dsDNA via formation of reversible adducts and the electrophile was able to overcome kinetic barriers without stalling at nicks and bulges. On the other hand, the mono-QM diammonium conjugate (**QMPDA**) provided no evidence of migration. The ability of **QMPAc** to migrate past nicks and bulges suggest that it could also migrate along other nucleic acid structures such as tRNAs, ribozymes or DNAzymes. This may lead to applications of mono-QMs as inhibitors cellular processes of DNA and RNA synthesis.

Formation of dG-N7 adducts by an unsubstituted mono-QM partitions between regeneration of QM and deglycosylation to form G-N7. Within dsDNA, deglycosylation of dG-N7 adducts results in an abasic sites, which destabilize duplexes and may prevent transfer for regenerated QMs between complementary strands. In order to determine if a higher prevalence of deglycosylated adducts limited migration of **QMPDA** over **QMPAc**, the percentage of abasic sites generated in the presence of each mono-QM was quantified. Studies have now shown that both **QMPAc** and **QMPDA** generate similar percentages of abasic sites in ssDNA, while

the percentage of abasic sites generated in dsDNA was higher in **QMPAc** than **QMPDA**. Since the **QMPAc** provided evidence of migration, results from this study suggest that abasic site generation may not be the only factor that impedes migration of **QMPDA**.

In honor of my super lady, Mrs. Grace Omukpai.

Colossians 3:23

ACKNOWLEDGEMENT

I would first like to thank my advisor, Professor Steven Rokita for giving me the opportunity to work on this project. Thank you for your mentorship, patience and support during my graduate studies. I also thank my dissertation committee members, Dr. John Toscano and Dr. Marc Greenberg for their support and guidance.

Thank you to the National Institute of Standards and Technology and Dr. Willie E. May for generously funding the first three years of my graduate research. And I also thank Dr. Edwin Chan and Dr. Peter Johnson for their mentorship during my internship at NIST.

I would like to thank all the Rokita lab members, both past and present for being such great co-workers and making my time at JHU a pleasant learning experience. A special thank you to Abhishek for all your support since our days at UMD, and Patt for being such a great friend both in and out of the Lab. Thank you to Petrina for taking on the challenge of starting a NOBCChE Chapter at JHU with me, and thank you to Shalini for always going above and beyond to lend a helping hand.

I would like to thank all members of NOBCChE-JHU for making my grad school journey exciting. Thank you to my dear friends Darius, Tiana, Phil, Quinton, Heidi and Ebuka for making the organization a huge success. I also thank my friends in the Chemistry Department - Darcie, Diggs, and Pearl- for all their support. You are all such intelligent young ladies and you motivate me to be a better person.

Finally, I would like to thank my parents for their relentless and unconditional love, support and prayers. “Because of You I Can!” And a huge thank you to my friends and extended family - Karen, Helida, and Pelumi, the Awoleye,

Uzosike, Omukpai, and Deeyaa families - for their support and understanding. You all gave me the strength I needed to achieve this goal.

Table of Contents

List of Table

List of Figures

List of Schemes

Abbreviations

*ODN – [^{32}P]-labeled oligonucleotide
APE1 - Human apurinic/apyrimidinic (AP) endonuclease
bis-QMP– bi-functional quinone methide precursor
BME – β-mercaptoethanol
b.p. – base pairs
dA – 2'-deoxyadenosine
dC – 2'-deoxycytidine
dG – 2'-deoxyguanine
DMF – N, N-dimethylformamide
DNA – 2'-deoxyribonucleic acid
dRb – 2'-deoxyribose
dsDNA – double strand DNA
dU – 2'-deoxyuridine
EDTA - ethylenediaminetetraacetic acid
Et743 – ecteinascidin 743
EtOAc – ethyl acetate
g – gram
HPLC – high pressure liquid chromatography
HRFAB-MS – high resolution fast atom bombardment mass spectrometry
L - liter
m – meta
M – molar
MES - 2-(N-morpholino)ethanesulfonic acid
mg - milligram
mL - milliliter
mmol - millimoles
mNBA – *m*- nitrobenzyl alcohol
mono-QM – monofunctional quinone methide
MS – mass spectrometry
nCi – nanocuries
NMR – nuclear magnetic resonance
o – ortho
p – para
pH– -log([H+])
pTsOH – para-toluenesulfonic acid
QM – quinone methide
QMP – quinone methide precursor
ssDNA – single stranded DNA
T – thymidine
T4 PNK – T4 polynucleotide kinase
TBDMS – *tert*-butyldimethylsilyl
TBDMS-Cl – *tert*-butyldimethylsilylchloride
TEAA – triethyl ammonium acetate
UDG – uracil deglycosylase

γ-ATP – gamma - Adenosine triphosphate
μmol – micromoles

Chapter 1: Introduction

1.1 Overview of DNA structure and molecular interactions

The DNA sequence carries the blueprint for synthesis of biomolecules that serve as the basis of gene expression. Therefore, the maintenance of its integrity is critical for the survival and proliferation of cells.[1,2] The DNA polymer is composed of four heterocyclic bases - adenine, guanine, thymine and cytosine - that are each attached to a deoxyribose sugar (Figure 1.1). These units are connected through phosphodiester bonds between the sugar rings, forming a negatively charged backbone. Through hydrogen bonding of purines to pyrimidine bases, two single strands form a double helical, anti-parallel structure that is supercoiled.[3] However, DNA strands are unwound and separated for replication, transcription and repair.

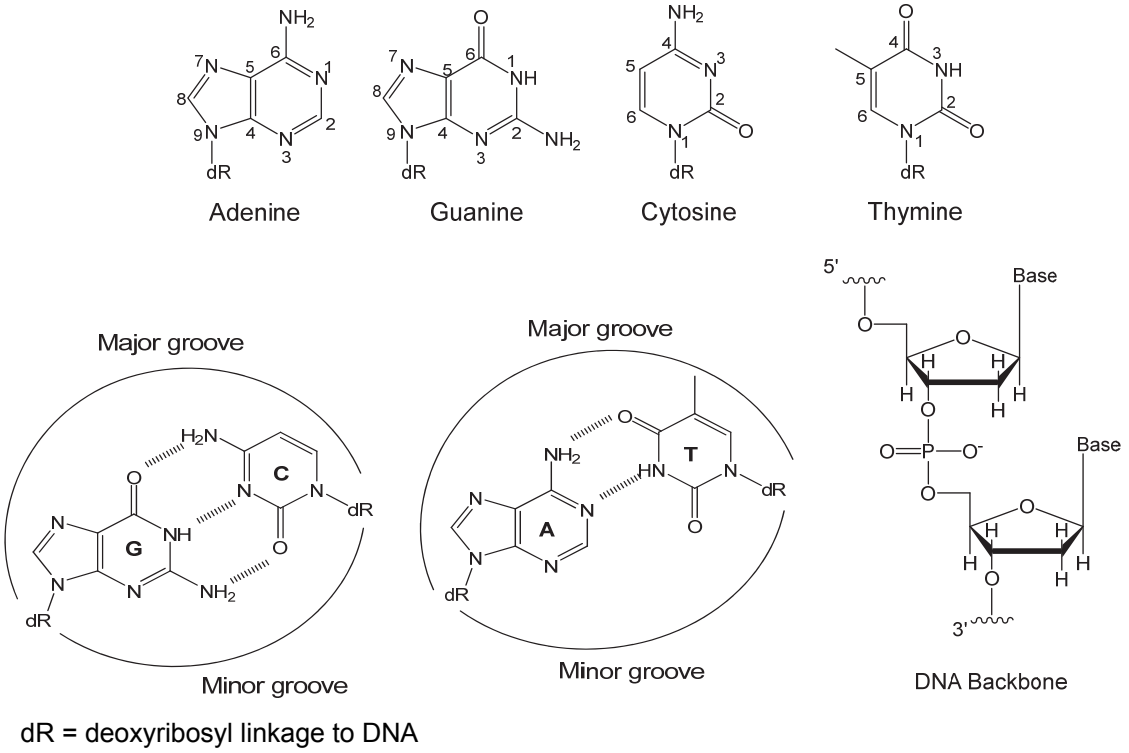

Figure 1.1: DNA base numbering and hydrogen bond association

In order for encoded genes to be expressed, proteins and cofactors associate to DNA via molecular interactions with the heteroatoms of a template strand. Through either electrostatic, covalent or hydrogen bonding, replication, transcription and repair processes can be carried out. Disruption of any of these key interactions could result in genetic mutations or cell death when left unrepaired.[1,4,5] This concept has been applied by researchers to target DNA and induce death of cancer cells. Since the 1910's, DNA targeting small molecules have been used for the treatment of tumors.[6] Localization of small organic compounds to either the major or minor groove, intercalation between the bases, or electrostatic interactions with the negatively charged phosphate groups, can be used to disrupt DNA function (Figure 1.2).[7] For example, alkylating agents that form covalent bonds with DNA bases can consequently generate mismatched bases, abasic sites, or prevent strand separation during DNA replication.[8] In order to maintain a healthy cell cycle, it is necessary that DNA associating proteins are aided in the execution and preservation of genetic information. However, when cells are cancerous, covalent attachment of small molecules to DNA may be utilized to inhibit their growth. Through the use of DNA alkylating agents, proliferation of tumors can be arrested and the harmful effects of cancer can be remedied.

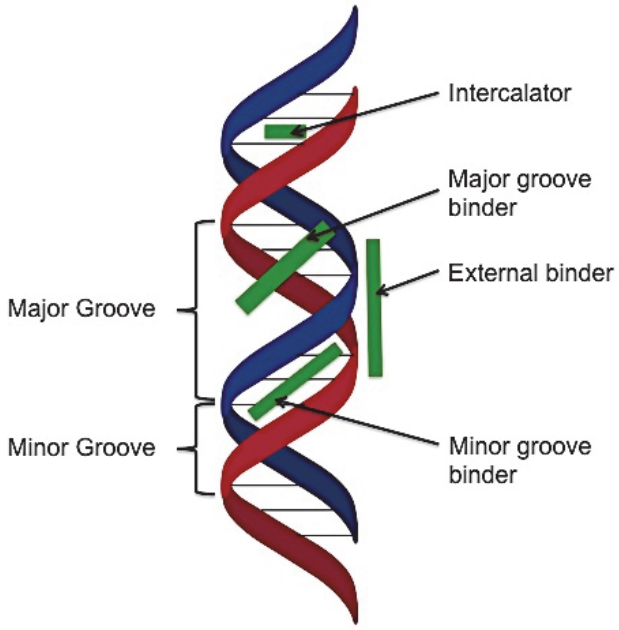

Figure 1.2: DNA structure and various modes of non-covalent molecular interactions [7]

1.2: DNA alkylation is cytotoxic but can be utilized for chemotherapy

Alkylating agents are electrophilic species that undergo nucleophilic attack by DNA bases, proteins, or endogenous nucleophiles to form covalent adducts.[8,9] These species react with the heteroatoms of DNA bases and negatively charged oxygens of the phosphodiesters. Monofunctional alkylating agents form a single covalent adduct with DNA, while bifunctional alkylating agents react with two nucleophiles forming DNA intrastrand or interstand crosslinks (Figure 1.3).[8] These modifications are cytotoxic because they result in formation of abasic sites, base substitutions, strand breaks, and loss of genetic information. Many chemotherapeutic treatments take advantage of these modifications and the resulting toxicities to inhibit growth of tumor cells.[1,2,10] Since DNA alkylating agents possess both carcinogenic and chemotherapeutic properties, it is critical that

researchers elucidate the mechanisms through which these molecules exert toxicity in order to tailor their attributes to remedy illnesses.

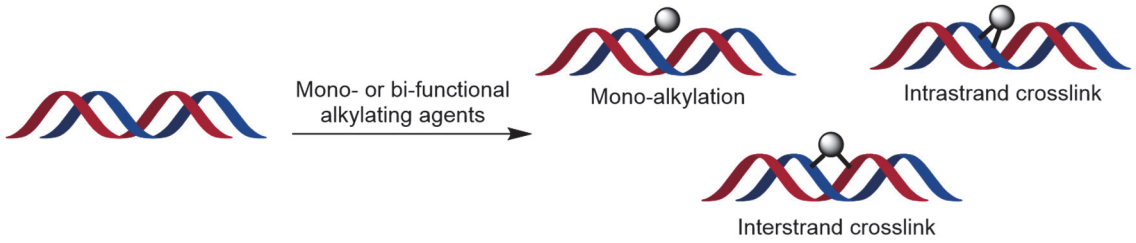

Figure 1.3: Types of DNA alkylation

1.2.1: DNA Alkylation as chemotherapeutic agents

Perhaps the most extensively studied class of alkylating agents are nitrogen mustards. First utilized as a chemical weapon in WWI, their anticancer properties were discovered by military personnel exposed to mustard gas experiencing toxicities.[11] Nitrogen mustards react with DNA by forming adducts at dG-N7. The proposed mechanism of alkylation is via formation of an aziridinium ion by cyclization of the bis(2-chlorethyl) amino motif. Nucleophilic attack of the aziridinium carbons by a DNA base results in the formation of covalent adducts (Scheme 1.1).[12] Nitrogen mustards form both intra- and interstrand crosslinks, with a preference for 5'-GNC-3' sequence interstrand crosslinks.[13,14] In addition to inhibiting DNA strand separation when crosslinks are formed, alkylation of dG-N7 can also result in the formation of abasic sites and ultimately single and double strand breaks.[10,15,16] Over the years, several other nitrogen mustards have been developed for clinical use, demonstrating utility of alkylating agents as potent therapeutic agents, (Figure 1.4).

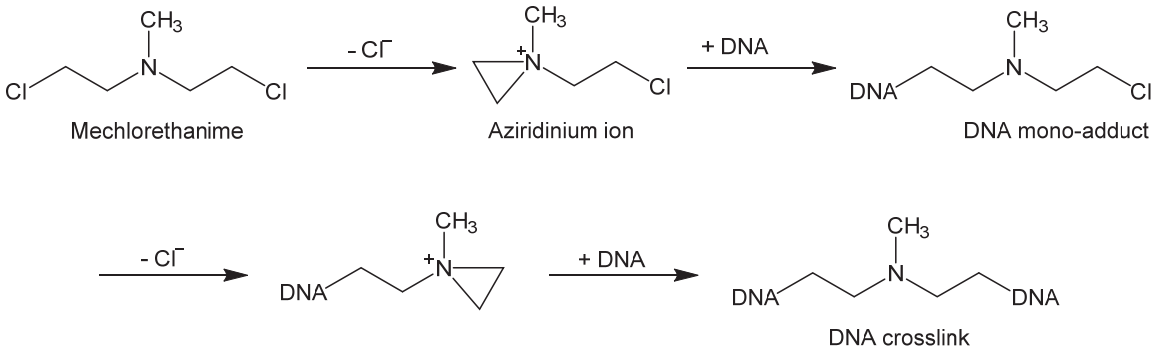

Scheme 1.1: Formation of DNA crosslinks by nitrogen mustards

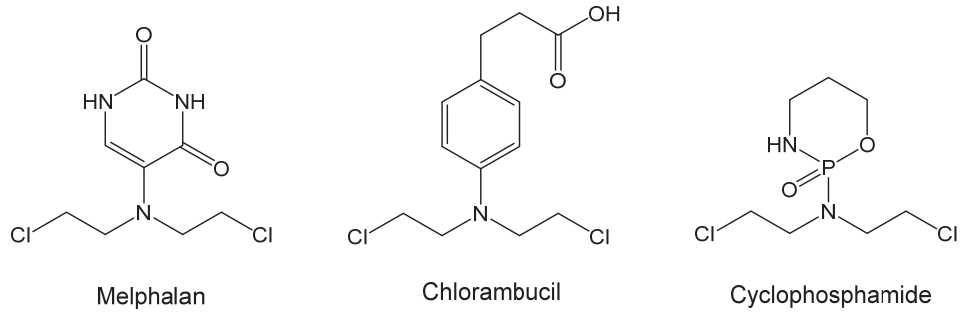

Figure 1.4: Structures of nitrogen mustard

Mitomycin C, a natural product that was first discovered from fermentation cultures of *Streptomyces caespitosus* is another classic example of an alkylating agent that has been utilized as a chemotherapeutic agent.[17] This compound acts as a bifunctional DNA alkylating agent and has been used for the treatment of various adenocarcinomas.[16] Unlike the nitrogen mustards, mitomycin C essentially inert until it is biologically activated. Enzymatic reduction of mitomycin C facilitates opening of the aziridine ring. Nucleophilic attack of the vinylic carbon on the pyrrolizidine moiety leads to the formation of the first DNA adduct (Scheme 1.2). Activation of the second electrophile occurs upon elimination of the carbamate to

form an intra- or interstrand crosslink. Studies have shown that mitomycin C form crosslinks preferentially at 5'-CG-3' sites in the DNA minor groove where it favors the dG-N^2 nucleophile.[18]

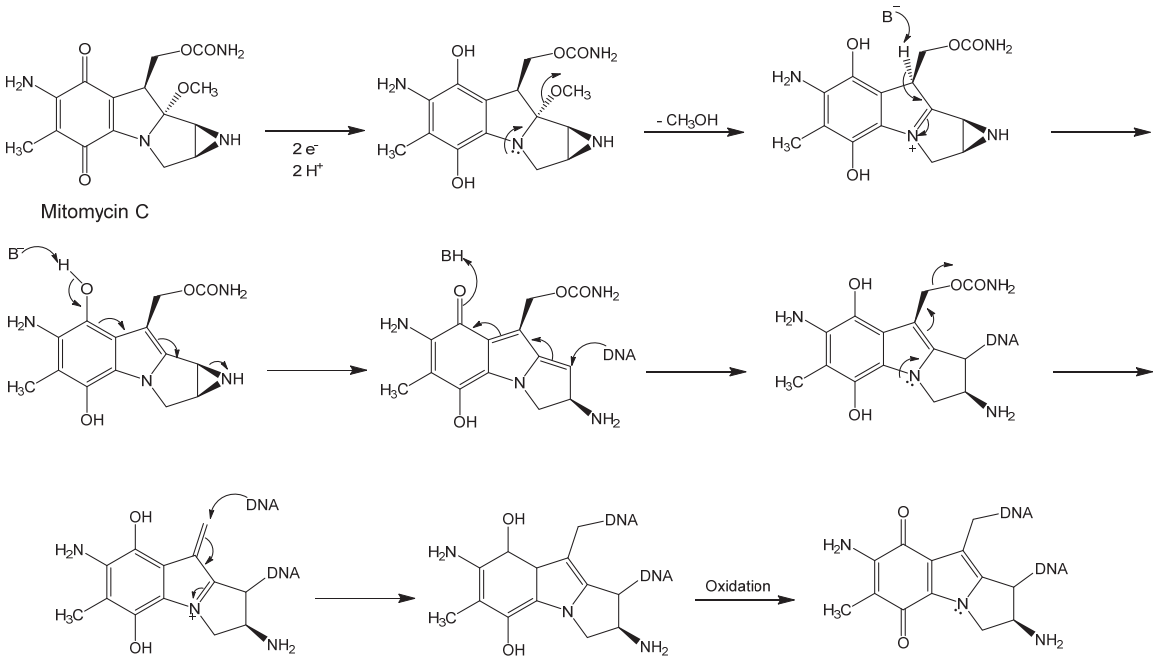

Scheme 1.2: Mechanism of DNA crosslinking by mitomycin C

Another group of DNA alkylating agents that are known to possess antitumor properties are nitrosoureas. Chloroethylnitrosourea (CENU) and other derivatives have shown antiproliferative activity over several cancer cell lines, but are mostly used in the treatment of brain tumors.[8,19] The reactive electrophile is generated via the formation of diazohydroxide (Scheme 1.3). The cation is then susceptible to nucleophilic attack by dG-O6 and dG-N^2 with loss of the chloride. An ethylene linked interstrand crosslink is eventually formed.[8,20] In addition to forming DNA crosslinks, nitrosoureas produce an isocyanate during its activation. This species result in the carbamoylation of DNA and protein residues which consequently impair DNA repair and result in enhanced cytotoxicity.[21]

Since the discovery of the chemotherapeutic properties of nitrogen mustards and the aforementioned compounds, scientific efforts have been directed towards developing new DNA alkylating drugs with improved potency and selectivity towards DNA and tumor cells. This achievement will not only lead to effective treatment, but may also reduce the negative side effects often experienced during chemotherapy due to non-specific alkylation of normal and cancer cells.

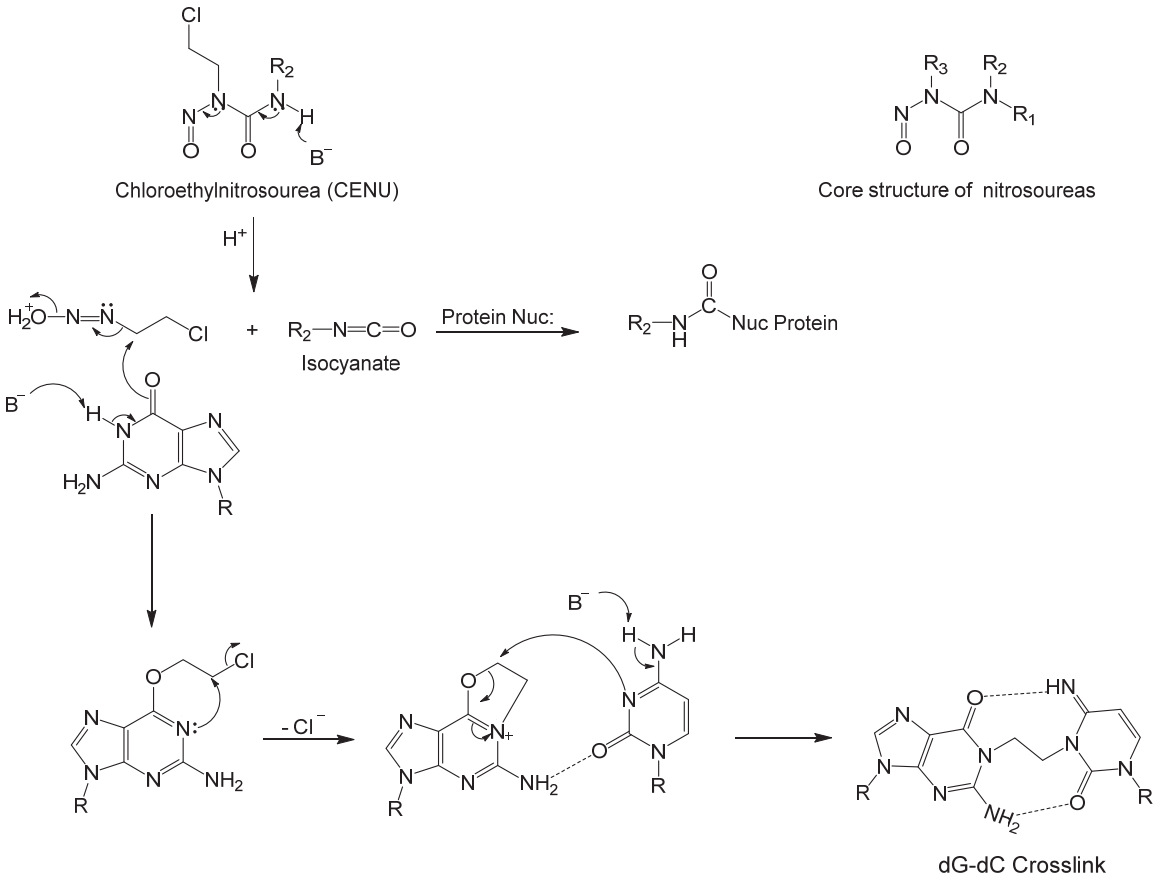

Scheme 1.3: Mechanism of DNA alkylation by nitrosoureas

1.2.2 Reversible DNA alkylation increases potency of chemotherapeutic agents

When DNA adducts are formed by alkylating agents, the reaction can produce either kinetically or thermodynamically stable products. For irreversible alkylating

agents, formation of DNA adducts are thermodynamically stable and lesions can be excised readily by DNA repair enzymes. In contrast, reversible alkylating agents may form an initial set of kinetic products that collapse via regeneration of the reactive electrophile, which then go on to induce further damage of DNA.[22] Reversibility is favorable in tumor treatment because it extends the lifetime of drugs by repeated regeneration and alkylation by the electrophilic species in a targeted oligonucleotide. Unlike irreversible alkylation, this may allow the drug to overcome repair by continuous recycling the electrophile following excision of DNA lesions.

Cyclopropylpyrroloindoles such as duocarmycin, adozelesin, and bizelesin are prime examples of reversible DNA alkylating agents.[23] These compounds bind to the minor groove of DNA, where they exhibit toxicity by forming covalent adducts with the DNA bases. Regeneration of the reactive compound is initiated when oxygen donates a lone pair to form a quinone and displaces the DNA. (Scheme 1.4). Studies indicate that the antitumor potency of a duocarmycin is significantly enhanced by its ability to form reversible DNA adducts.[24] Cytotoxicity of a duocarmycin derivative was also improved when substituents on the indole ring were modified to allow for faster release of the drug.[23,25] This supports the perception that recycling a DNA alkylating agent may be a more effective means of inhibiting tumor growth than the classic irreversible alkylating agent.

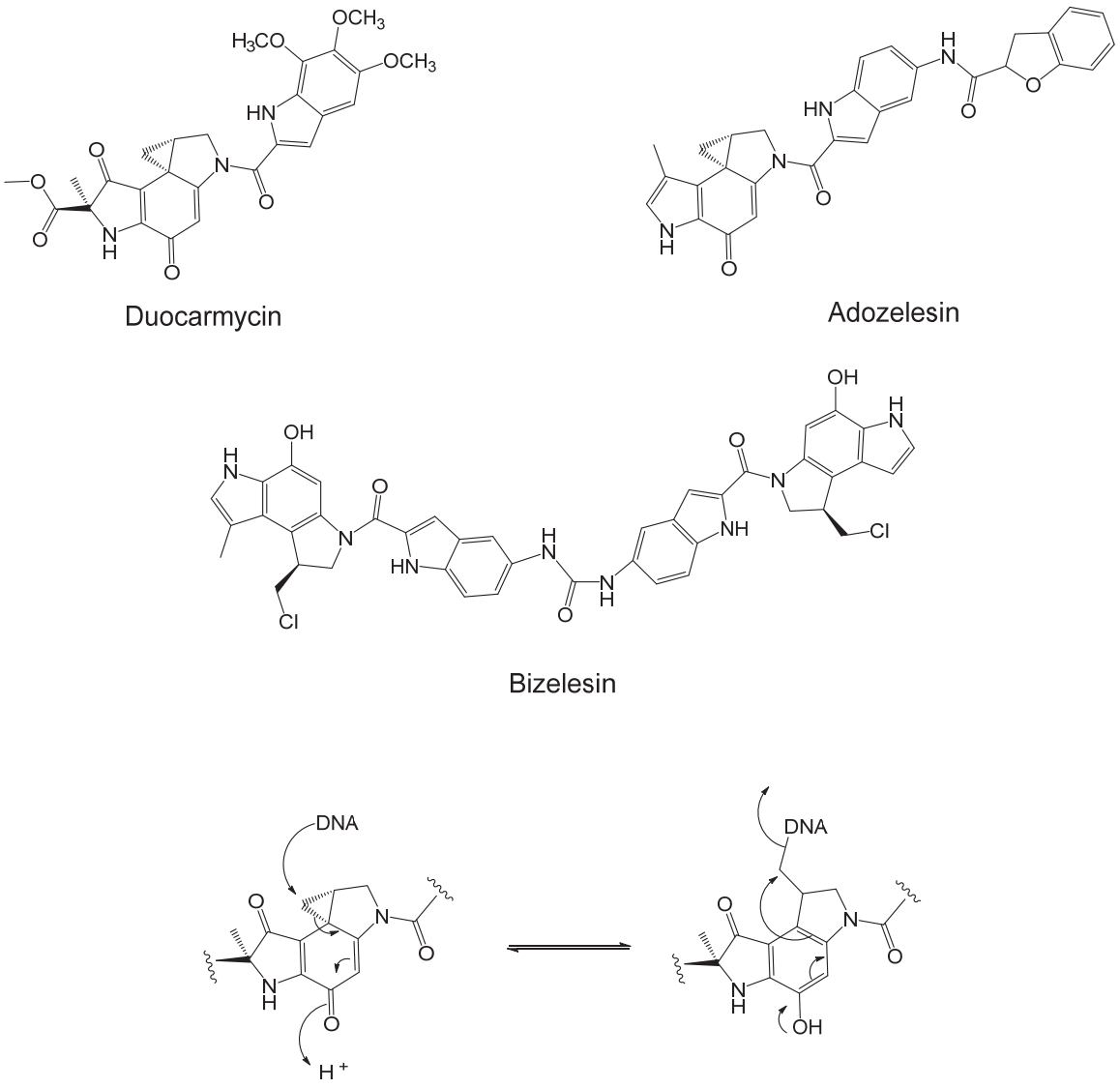

Scheme 1.4: Reversible DNA alkylation by cyclopropylpyrroloindoles

Ecteinascidine 743 (Et743) is another example of a reversible DNA alkylating agents (Scheme 1.5).[26] Formation of a DNA adduct is initiated when the hydroxyl group of the carbinolamine is eliminated to generate a Schiff base that is subject to nucleophilic attack by dG-N^2. The DNA alkylating electrophile is regenerated when nitrogen donates an electron pair to the iminium ion, and the DNA is eliminated. Through repeated capture and release, Et743 is capable of translocating from kinetic to thermodynamic sites on duplex DNA.[27] The ability of Et743 to diffuse

along DNA through repeated alkylation events essentially extends the lifetime of the drug, making them a more desirable therapeutic agents.

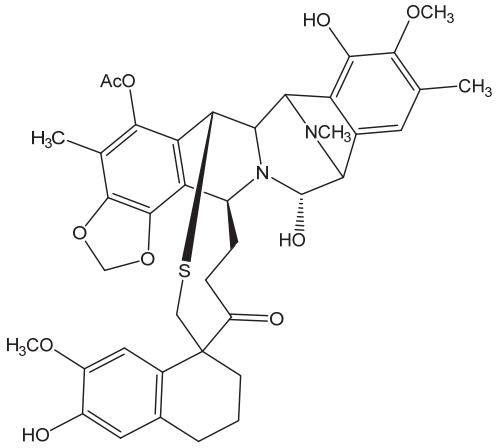

Ecteinascidine 743 (Et743)

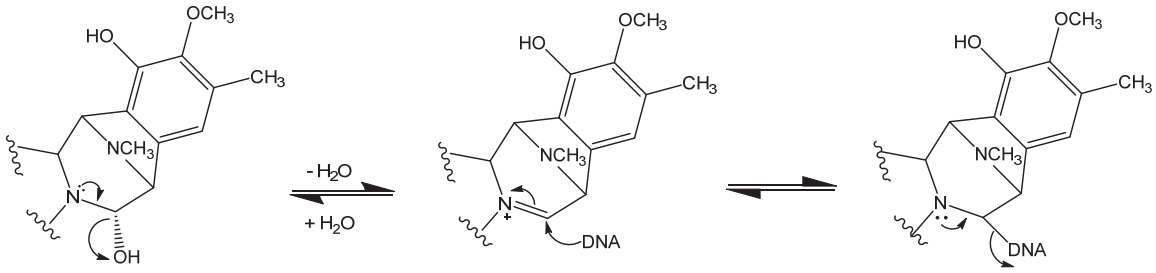

Scheme 1.5: Reversible DNA alkylation by Et743

1.3 Quinone methides alkylate DNA reversibly

Quinone methides (QMs) are electrophilic intermediates that are generated during the metabolism of natural and synthetic products such as acolbifene, taxodone, and butylated hydroxytoulene (BHT).[22,28-30] QMs can exist as either *ortho*- or *para*-isomers (Figure 1.5). Reaction of QMs with DNA has been shown to occur reversibly, and covalent attachment occurs via nucleophilic attack of the electrophilic

methylene carbon.[31] Regeneration of the QM intermediate is driven by the leaving group ability of DNA bases and the electron rich nature of the phenol ring.[32,33] Reformation of the QM is also facilitated by deprotonation of the phenol.

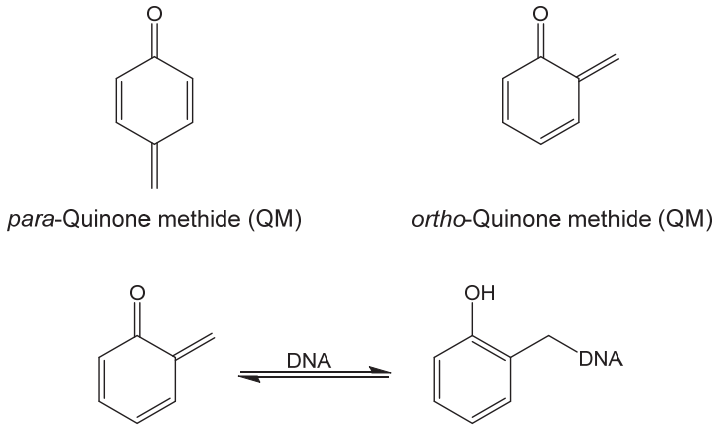

Figure 1.5: Reversible DNA alkylation by quinone methide intermediates

Studies in the Rokita lab have focused on characterizing the reversible DNA alkylating properties of QMs using a model system that initiates the activation of the intermediate via removal of a *tert*-butyldimethylsilyl (TBDMS) protected precursor in the presence of a fluoride anion (Figure 1.6).[34] Studies by Weinert *et al.* showed that reaction of a simple *ortho*-QM with nucleosides formed transient kinetic products that decayed upon regeneration of the electrophile, which then went on to form the thermodynamically stable products.[32] Reversible adducts of QMs were formed at dA-N1, dC-N3, and dG-N7, while irreversible adducts were observed at dG-N^2, dG-N1 and dA-N^6 (Table 1.1). Computations predict the pKa of the conjugate acids of labile bases to be below 5, while the pKa of the exo amino groups of bases with thermodynamically stable adducts are above 9.[35] Coincidentally, the bases with strongest conjugate acids were also the strongest nucleophiles. These strong nucleophiles react with QM more rapidly than the weaker nucleophiles to form

kinetic products. Data gleaned from these studies have now improved our knowledge of the reversible properties of QMs and allowed for selective targeting of nucleic acid sequences that enable repeated capture and release of the intermediate, making QM-drugs attractive candidates for gene-directed therapy.

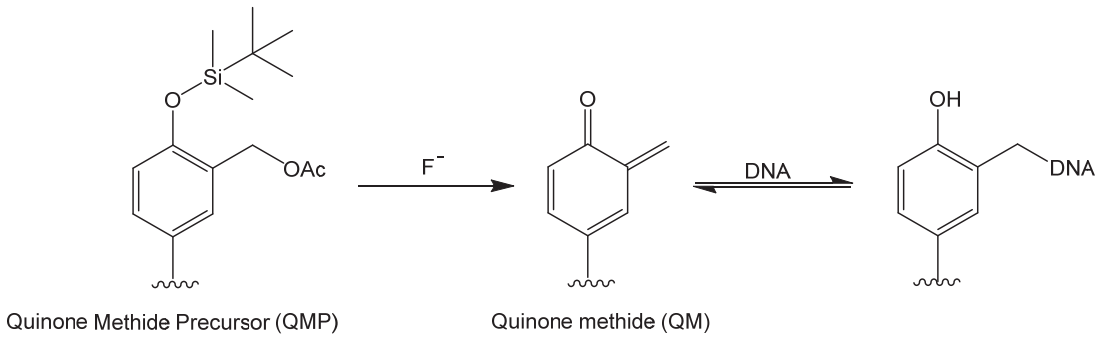

Figure 1.6: *tert*-butyldimethylsilyl (TBDMS) protected quinone methide precursor developed by the Rokita lab

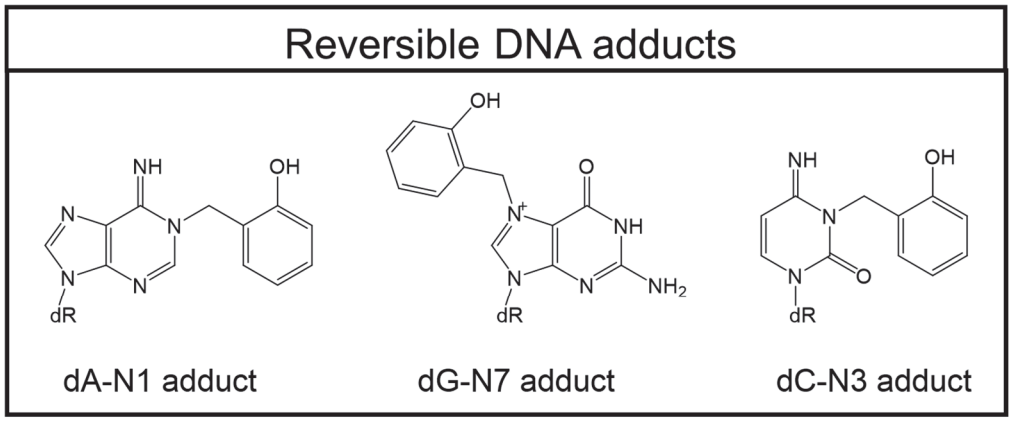

Table 1.1: Reversible and irreversible DNA products of QM [32]

1.3.1: Selected delivery of QM by DNA sequence recognition

Under biologically relevant conditions, alkylating agents are susceptible to react with endogenous nucleophiles in addition to DNA. Off-target reactions by alkylating agents often contribute to negative side effects that typically emerge during and after chemotherapy. To improve the selectivity of alkylating agents towards DNA bases, nucleic acid ligands can be used to deliver drugs to desired sequences. In the case of QMs, oligonucleotide conjugates have been utilized to preserve the electrophile and deliver it to a complementary duplex for efficient crosslinking (Figure 1.7).[36-40] Activation of a silyl protected QM-oligonucleotide conjugate allows for the formation of a self-adduct by alkylating a base nucleophile within its tagged sequence. When the reacted adduct is labile, the QM electrophile can be regenerated and go on to crosslink a complementary strand upon hybridization. This method has also been used to alkylate target sequences through conjugation of QMs to triplex-forming oligonucleotides and protein nucleic acids (PNA).[38,40,41]

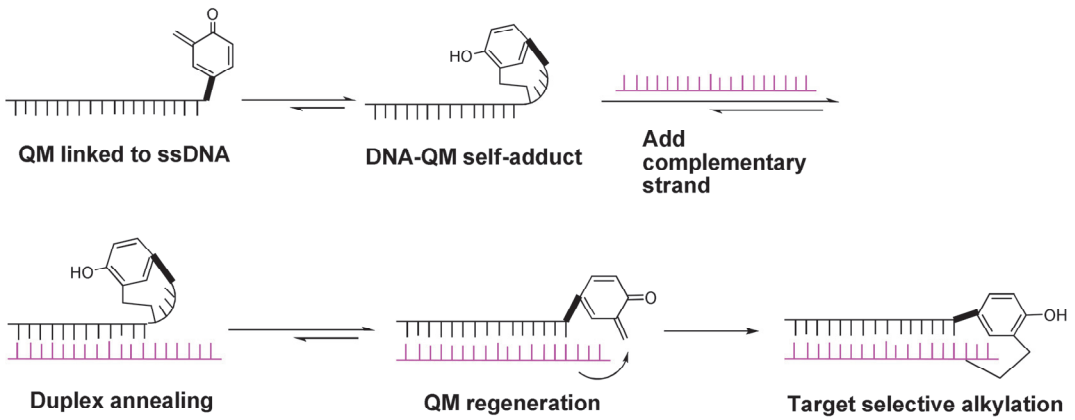

Figure 1.7: Sequence-directed delivery of QM to DNA[37]

Although QM-DNA conjugates provide an effective means of delivering the electrophile to target duplexes *in vitro*, phosphodiester bonds are subject to enzymatic digestion *in vivo* and the alkylating agent may never reach its desired location in the cell.[42] Alternatively, QM-PNA conjugates afford a more stable choice for targeted delivery of the alkylating agent but cellular uptake of the macromolecule is slow due to its low cell permeability and poor solubility in water.[43] The QM electrophile may be trapped irreversibly before the PNA conjugate reaches its target site. More studies directed towards improvement of DNA and PNA drug delivery systems needs to be conducted for applications of these QM conjugates in gene therapy.

1.3.2 Binding localization mediates reversible DNA alkylation

Although sequence-directed drug conjugates provide a means of targeting genes that are specifically associated with an illness, non-specific ligands allow QMs to sample multiple sites on a duplex via reversible reactions before it reaches a thermodynamically stable site. This may offer improved cytotoxicity by allowing the electrophile to evade DNA repair if an adduct is excised but a regenerated QM re-associates to an alternate site on a duplex with the help of a non-specific ligand. Intercalators provide a means of achieving such dynamics by reversibly binding between stacked DNA bases. The Rokita lab has conjugated QM to an acridine intercalator for delivery of the electrophile to the major groove for DNA where reversible alkylation of dG-N7 is highly favored (Figure 1.8).[44] Reaction of the QM in the major groove is necessary for lability of the electrophile across multiple

complementary strands, as reversibility was not observed when QMs were conjugated to a minor groove-binding pyrrole-imidazole polyamide ligand.[45] Conjugation of a bi-functional quinone methide (bis-QMs) to an acridine intercalator was also essential for obtaining interstrand DNA crosslinks. In the absence of the intercalator, less than 1% of crosslinks were detected. However, when QM is conjugated to the acridine ligand, yields of DNA crosslinks increases to 64%.[44] This same bis-QM acridine conjugate has been shown to react reversibly by forming a single strand self-adduct which then crosslinks DNA when a complementary strand is added. Lability of the electrophile was also preserved and persisted through multiple exchanges of complementary DNA strands.[46]

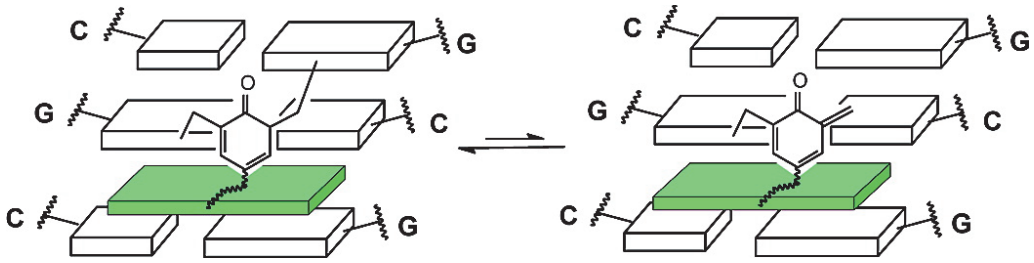

Figure 1.8: Conjugation of QM to an intercalator for reversible DNA alkylation[44]

Most recently, an ether-bridged **bis-QMP2** conjugate was shown to diffuse along dsDNA via stepwise bipedal alkylation and regeneration reactions (Figure 1.9).[47] Migration of the ether bridged bis-QM was facilitated by the electron-rich nature of the reactive electrophile due to the electron donating inductive effect provided by the oxygen lone pairs of the ether substituent. Studies showed that a silyl deprotected methylene-bridged **bis-QMP1** showed no evidence of walking along DNA, whereas the deprotected ether-bridged **bis-QMP2** moved up to 5 bp steps along duplex DNA within 7 days.[47]

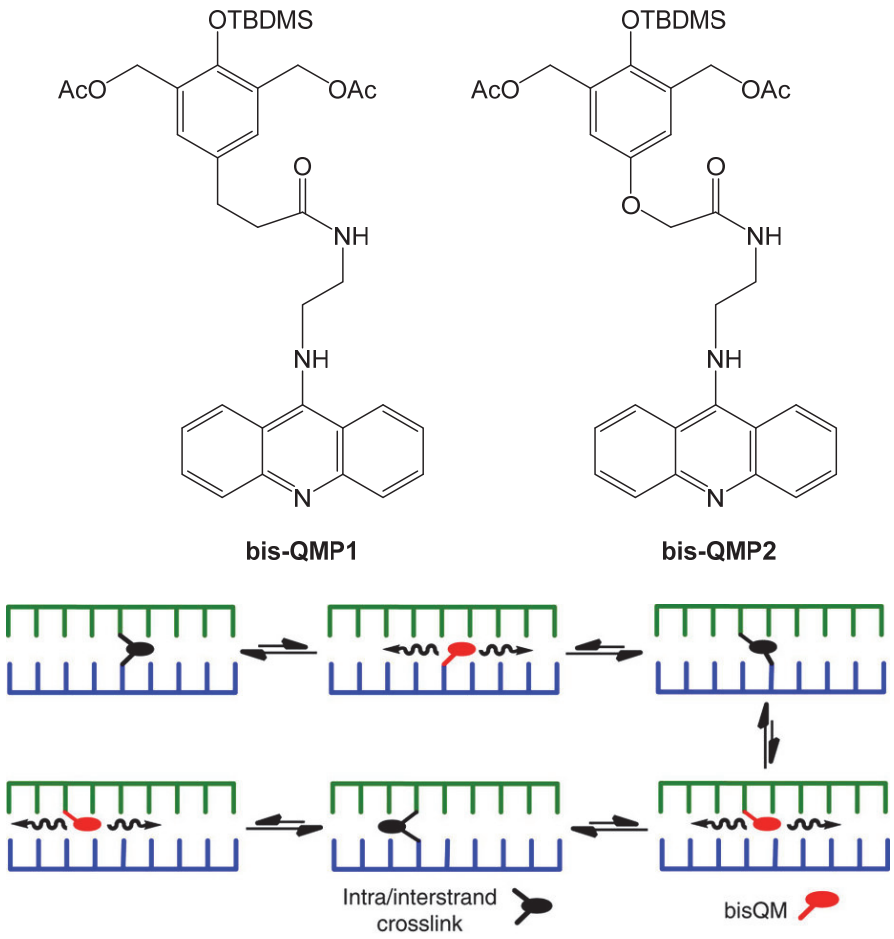

Figure 1.9: Bipedal migration of *tert*-butyldimethylsilyl (TBDMS) deprotected **bis-QMP2** along duplex DNA[47]

Although the electron-rich bis-QM was able to walk along duplex DNA, adducts accumulated at nicks and the electrophile was unable to diffuse past a bulge on the duplex. In order for a bi-functional alkylating agent to migrate from one end of a duplex to another, both electrophilic carbons must be released. However, under biological conditions QMs are prone to nucleophilic attack by strong oxygen, nitrogen, and thiol nucleophiles; it is very likely that the electron-rich QM may be trapped thermodynamically by an endogenous nucleophile before it reaches its desired site of reaction. For this reason, there is a need to develop new QM conjugates that will overcome the kinetic barrier of localization at nicks and bulges,

and also allow for faster regeneration of the electrophile. This may enable QMs migrate along DNA at a much faster rate.

This dissertation was directed towards promoting the diffusion of QM along duplex DNA via modification of the aromatic substituents, and ligand conjugates of synthesized QM precursors. Mono-functional QMs (mono-QMs) were utilized to enable free dissociation and re-association of the reactive electrophile to DNA nucleophiles without having a second carbon center covalently tethered to a DNA base at all times. The feature provides additional lability that may promote movement of QMs past nick and bulges. Motivated by the migration of the ether bridged bis-QM acridine conjugates, reversibility of an ether bridged mono-QM was investigated for enhanced migration along duplex DNA.

In addition, QMs were conjugated to cationic ligands that associate to the negatively charged backbone. It was anticipated that movement of cationic ligands along the DNA backbone may also improve the rate of QM migration in comparison to intercalation and de-intercalation of an acridine ligand. The aim of this study was to determine how various modes of DNA association may affect the initial rate of DNA alkylation, and further influence reversible alkylation along duplex DNA.

Finally, the consequences of DNA alkylation were characterized by determining the percentage of dG-N7 adducts that partition between deglycosylation to form an abasic site and regeneration of the electrophile. Formation of abasic sites affects the stability of duplex DNA[48] and decreases the overall fraction of regenerated QM electrophiles that are available for re-alkylation of DNA. Understanding the partitioning of QM reaction between regeneration and

deglycosylation has improved our understanding of how QMs may exert toxicity *in vivo*, and will ultimately aid the future design of more efficient alkylating and crosslinking agents for applications as therapeutic agents.

Chapter 2: Substituents modulate reversible DNA alkylation by mono-functional quinone methides

2.1: Introduction

Due to their high polarizability, QMs serve a broad range of applications in organic synthesis and molecular biology. Conventional reactions of QMs involve Michael addition by reacting with a nucleophile at its exocyclic methylene (Scheme 2.1). Although QMs are highly transient intermediates, the lifetime of the electrophile can be modulated by aromatic substituents.[33] Such changes can in turn influence the reactivity and selectivity of the electrophile towards nucleophiles.

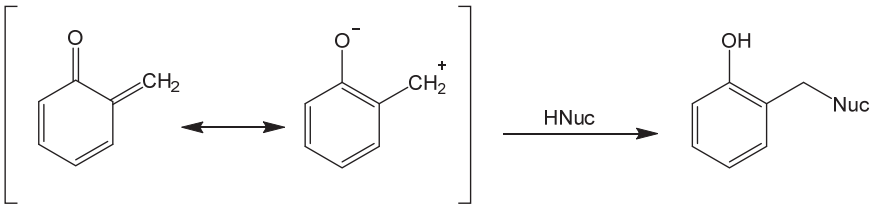

Scheme 2.1: QMs react as Michael acceptors

Earliest known efforts to understand substituent effects on QMs focused on characterizing their reactivity with various nucleophiles.[49-51] The Rokita lab was first to expand the scope of the influence of aromatic substituents on the kinetics and product distribution of QM adducts with deoxynucleosides. Using a collection of QMs with varying electron densities, studies by Weinert et *al.* showed that electron donating aromatic substituents stabilizes QM intermediates, increases their rate of regeneration, and enhances their selectivity towards nucleophilic addition (Figure 2.1). In contrast, electron withdrawing aromatic substituents destabilize these

intermediates, decrease their regeneration, and decrease selectivity towards nucleophiles.[33] In this study, *o*-QMs containing either an electron-donating or withdrawing substituent were reacted with deoxycytidine and the evolution of its dC-N3 adduct was monitored over time (Figure 2.2). **QM2**, composed of an electron donating methyl substituent produced a maximum yield of DNA adducts within an hour but then rapidly decomposed with a half-life of 5 h. Adducts of the unsubstituted **QM1** reached a maximum yield within 4 h, persisted for 6 more hours, before gradual decomposition. Finally, **QM3,** which contained an electron-withdrawing substituent formed a stable dC-N3 adduct that persisted for up to 72 h without decomposing.

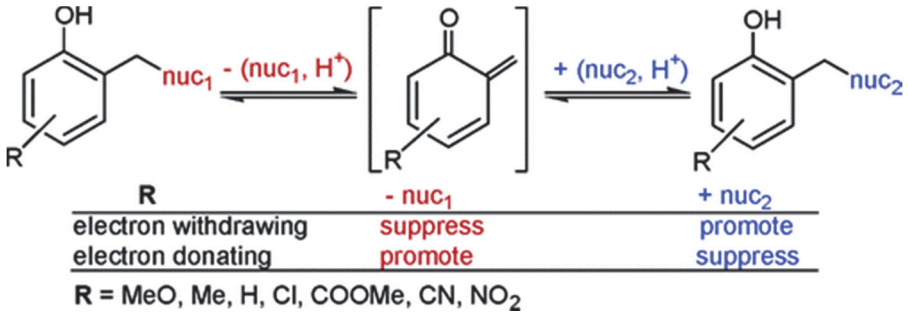

Figure 2.1: Substituent effects on *o*-QM generation and reactivity[33]

The position of an aromatic substituent can also influence the rate of QM generation. Electron-donating substituents placed *para* to the exocyclic methylene are more stabilizing than *meta* substituents. For example, the presence of an ether substituent *para* to the benzylic methylene can participate in resonance stabilization of the QM whereas a *meta* substituent can only stabilize the electrophile through inductive effects (Scheme 2.2).

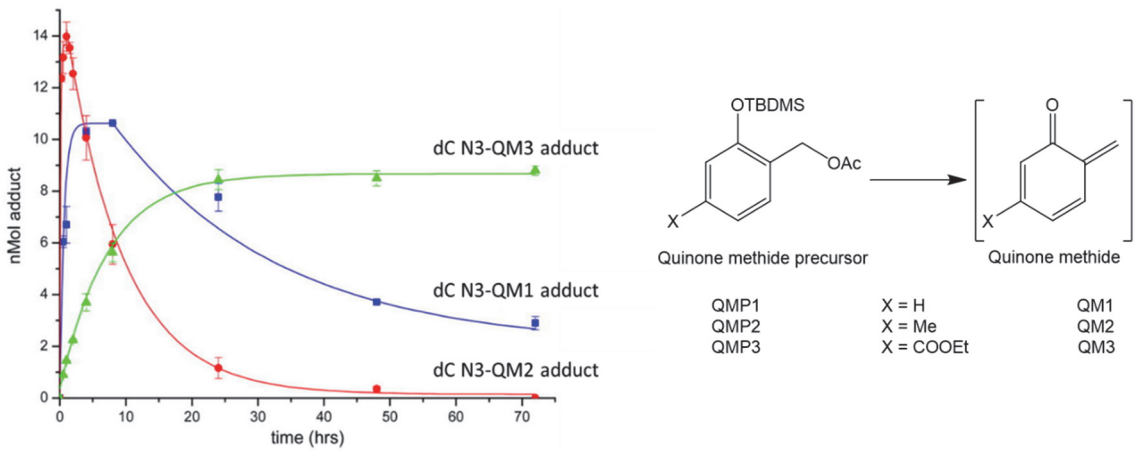

Figure 2.2: Substituent effects on the formation and decomposition of dC N3-QM adduct [33]

The effect of the aromatic substituent placement on the reactivity of QMs was also evaluated by monitoring the kinetic conversion of a morpholino QM precursor to a water adduct upon generation of the reactive intermediate.[33] Results from this study indicated that a *para*-methoxy substituted QM was more labile than the *meta*-substituted QM, with a half-life of 4 mins and 11 mins, respectively. This increase in the rate of QM generation is highly beneficial because formation of reversible DNA adducts depends on both the rate of nucleophilic addition and elimination to regenerate the electrophile. Since the strongest nucleophiles react with QMs more rapidly to form reversible adducts, [33] electron donating substituents may promote migration of QMs along DNA via multiple reversible alkylation events. However, if an electron-donating substituents makes the QM too labile, migration along DNA may be limited as the electrophile might be trapped by other strong endogenous nucleophiles.

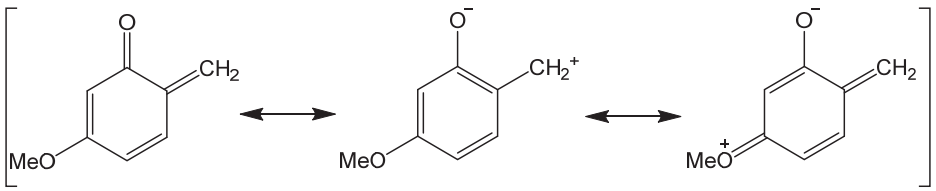

Scheme 2.2: Resonance stabilization of QMs by *para*-methoxy substituents

This chapter focuses on modulating the electronic properties of QM for faster alkylation, regeneration, and migration along DNA. Coupling of a methoxy-bridge QM to a sequence directing oligonucleotide led to an increase in the rate of self-adduct formation in comparison of the methylene-bridges oligonucleotide conjugate (Figure 2.3). [39,40] Similarly, transfer of regenerated QMs onto a complementary strand was significantly faster for the electron-rich QM. However, studies with sequence-directing ligands only allow regenerated QMs to react in one region of a duplex and the DNA associating affinity of QMs is lost if the adducts are excised and oligonucleotide ligands are digested by nucleases.

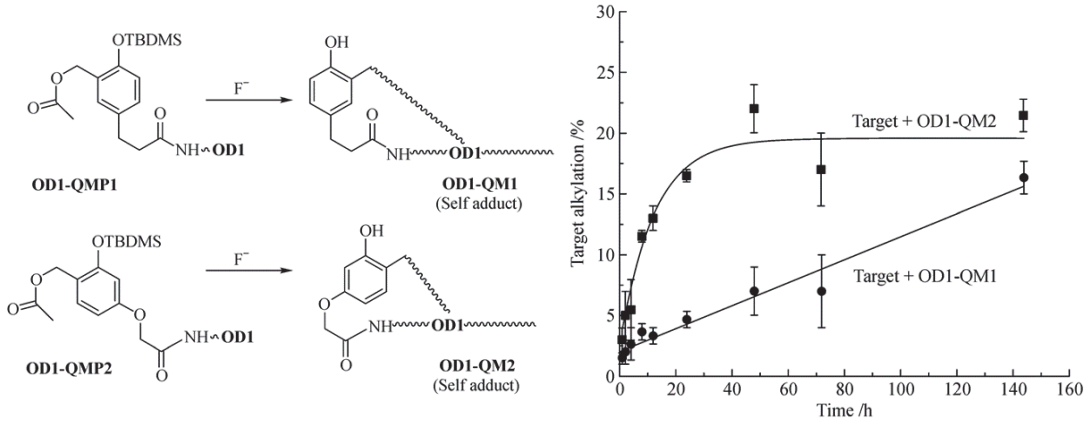

Figure 2.3: Sequence-directed electron-rich QM rapidly crosslinks targeted oligonucleotide[39]

Present work focuses on conjugating a methylene and ether-bridged mono-functional QM (mono-QM) to a non-sequence specific acridine intercalator at the *para* and *meta* positions, respectively. Conjugation of a bi-functional QMs (bis-QM) to an acridine intercalator has been an effective means of delivering the electrophile to the DNA major groove for achieving high yields of reversible dG-N7 adducts.[44,47] While a bi-functional alkylating agent requires the sequential release of two electrophilic carbons from DNA for migration to occur, a mono-QM only needs to be regenerated once. A simple catch and release of mono-QMs could also provide added lability for migration along duplex DNA. Repeated formation of kinetic products will extend the lifetime of QMs. This may also allow QMs to overcome DNA repair enzymes if the electrophile is regenerated following excision of a DNA adduct (Figure 2.4). Ultimately, continuous recycling of QMs will trigger apoptosis of targeted cells.

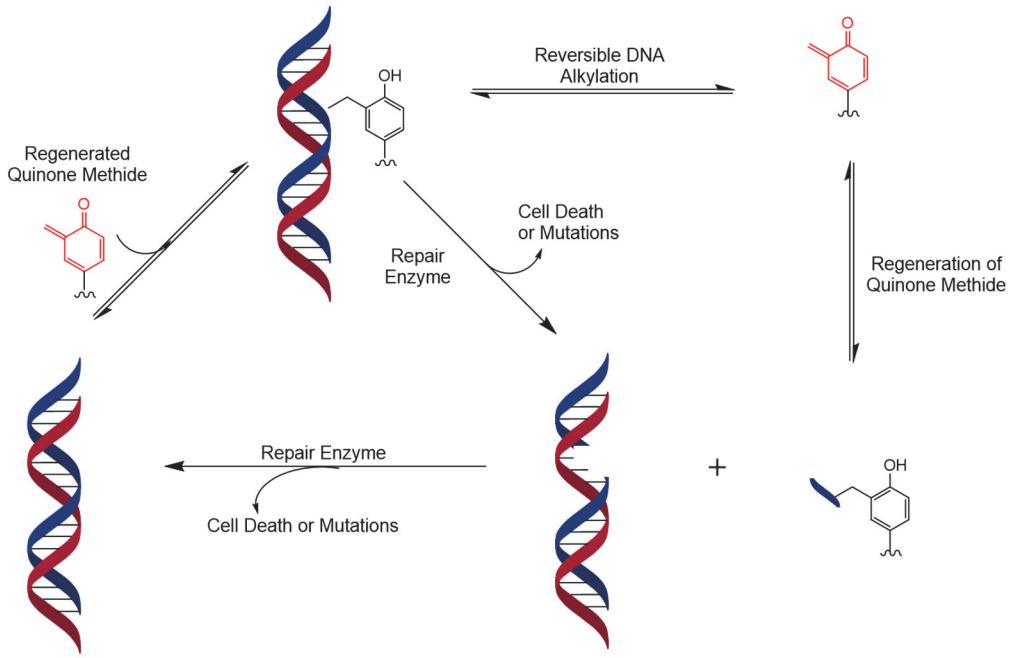

Figure 2.4: Possible evasion of DNA repair by regenerated QMs

2.2: Results and Discussion

2.2.1: Synthesis of acridine conjugated QMs

Synthesis of a methylene bridged mono-QM proceeded in a similar manner as that of the bis-QM acridine conjugate that was previously synthesized in the Rokita lab (Scheme 2.3).[44] The protocol for the synthesis of *N*-hydroxylsuccinimide conjugate of **4** was published by Zhou *et al*.[37] Using this literature protocol, preparation of **1** in the presence of formaldehyde and sodium hydroxide proved to be challenging and produced the di-hydroxymethylated compound as the major product. Following the procedure by Nagata *et al*.,[52] selective activation of the *ortho* position of 3-(4-hydroxyphenyl)propionic acid was achieved using phenylboronic acid, and the yield of **1** increased by 50% without producing the di-hydroxymethylated product. Characterization of **1** via ^{1}H NMR provided evidence of the newly added benzylic carbon at 4.83 ppm and peak assignments corresponded with values in the literature. [37]

Syntheses of compounds **2**, **3**, **4** were relatively straightforward, following procedures by Zhou *et al.*[37] The yield for each step was comparable to literature, with a 40% increase in compound **3** when the reaction time was increased from 30 min to 1 h. All products were characterized via ^{1}H NMR, and the chemical shifts corresponded with values in the literature.[37] Coupling of the terminal amine of **5** to compound **4** was achieved using the previously established protocol for the synthesis of bis-QM[44], to obtain **QMPAc** with a yield of 84%. Characterization of the final product via ^{1}H, ^{13}C NMR and high resolution FAB-MS confirmed **QMPAc**. ^{1}H

NMR chemical shifts showed the presence of the acridine aromatic protons at 6.7 – 8.6 ppm, and the parent ion at 572 m/z matched the exact mass of a protonated **QMPAc** on the MS chromatogram.

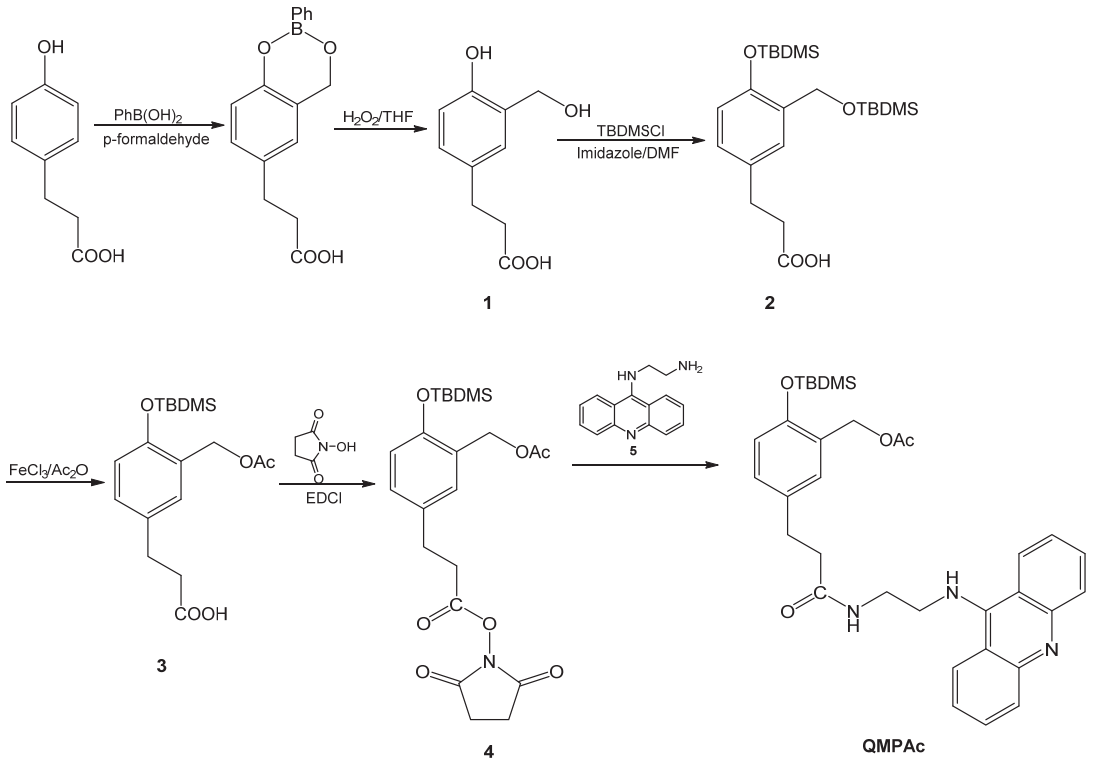

Scheme 2.3: Synthesis of **QMPAc**

Synthesis of the methoxy-bridged electron-rich **eQMPAc** followed a slightly different protocol from **QMPAc** (Scheme 2.4). Compound **11** was previously synthesized in the Rokita lab by Dr. Chengyun Huang.[39] Following this literature procedure, compound **6 - 11** were synthesized with relatively good yields. Coupling of **11** to **5** was achieved using a protocol by Veldhuyzen et *al.*[44] to obtain **eQMPAc** with a 65% yield. The final product and its precursors were characterized using ^{1}H,

^{13}C, HSQC NMR and high resolution FAB-MS. ^{1}H NMR chemical shifts showed the presence of the acridine aromatic protons at 6.7 – 8.6 ppm, and the parent ion at 574 m/z matched the exact mass of protonated **QMPAc** on the MS chromatogram **eQMPAc.**

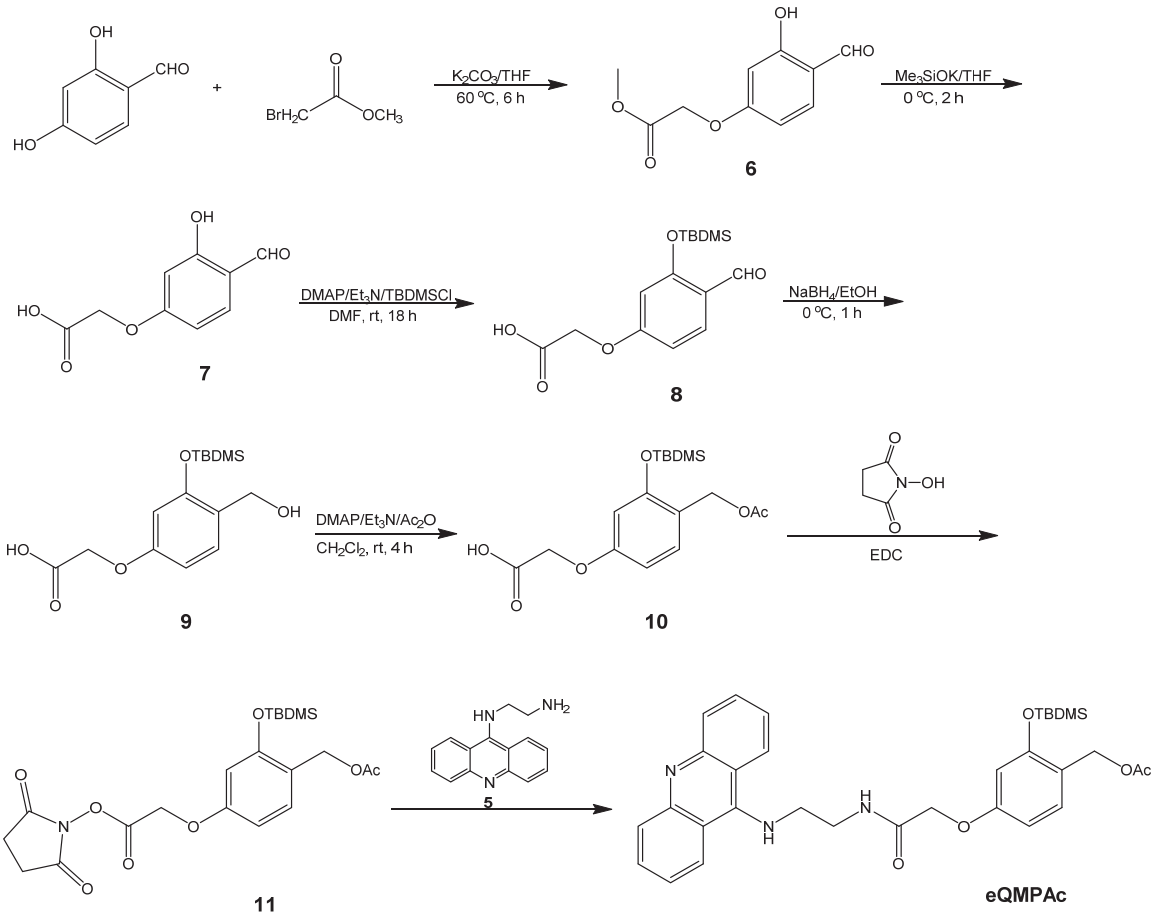

Scheme 2.4: Synthesis of **eQMPAc**

2.2.2: Electron donating substituents promote nucleophilic addition to QMs

The initial rate of QM-DNA adduct formation is governed by the elimination of the benzylic acetate after rapid desilylation.[33] Therefore, the electron-rich **eQMPAc** is expected to generate its reactive intermediate at a faster rate than **QMPAc**

following elimination of the acetate leaving group. To observe this increased rate of DNA alkylation, each alkylating agent was incubated with dsDNA for 0 – 4 h, and then treated with 10% hot piperidine to induce DNA fragmentation when adducts are formed at dG-N7 (Scheme 2.5). Using equimolar reaction concentrations of each alkylating agent, gel image shows that **eQMPAc** reacts at dG-N7 of **5'-[^{32}P]-OD1:OD2** more rapidly than **QMPAc** (Figure 2.5A). Within 4 h, **eQMPAc** produced a total yield of 10% dG-N7 fragments while **QMPAc** produced less than 3% total fragments. This supports previous studies that have shown that methoxy groups stabilize QMs for faster reaction with nucleophiles.[33] However, when the reaction period is extended to 72 h, the yield of DNA fragments by **QMPAc** exceeds that of its electron-rich counterpart with a maximum yield of 46 % total dG-N7 fragments (Figure 2.6). It is also important to note that the yield of dG-N7 adducts in the presence of **eQMPAc** decreased from 10% to 7% from the 24 h to 72 h time period. This could be due to reaction of **eQMPAc** with other non-dG-N7 DNA nucleophiles, or quenching of the intermediate by water as result of the regeneration of the reversible adducts.

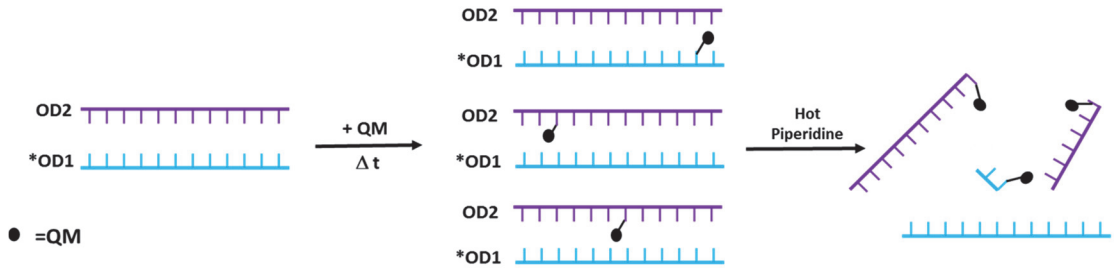

Scheme 2.5: Detection of QM adducts at dG-N7 via piperidine-induced DNA cleavage

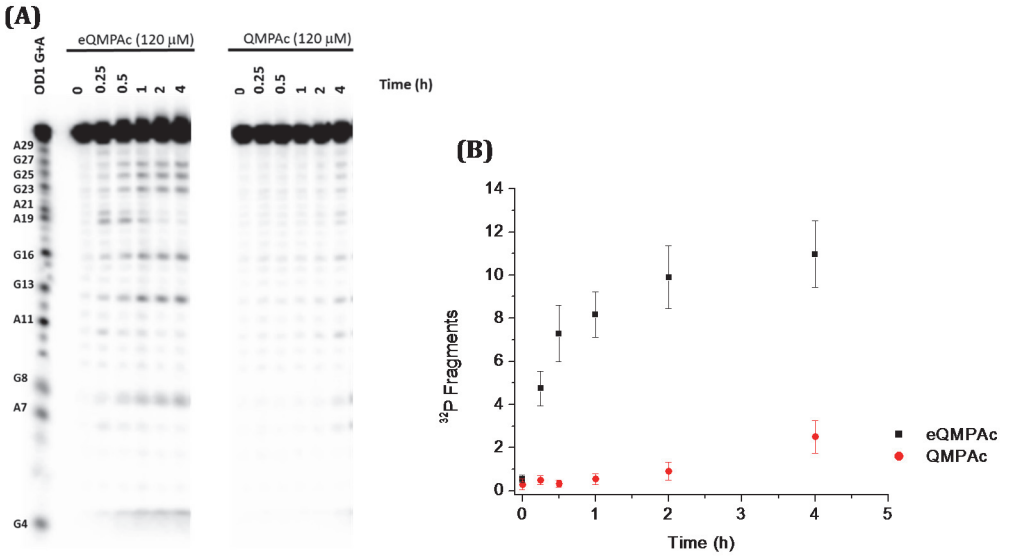

Figure 2.5: Time-dependent alkylation of dsDNA by **QMPAc** and **eQMPAc.** (A.) dsDNA 5'-**[^{32}P]-OD1:OD2** (3.0 μM) was incubated with **eQMPAc** (120 μM), **QMPAc** (120 μM), in the presence of NaF (10 mM) and MES buffer (10 mM, pH 7.0) for 0 – 4 h, followed by 10 % hot piperidine treatment. (B) Rate of dG-N7 alkylation plotted as a percentage of 5'-**[^{32}P]-OD2** fragments for the indicated time periods. Reaction yield is an average of independent three trials, determined by subtracting fragment intensity from t = 0. Error is an average of the standard deviation.

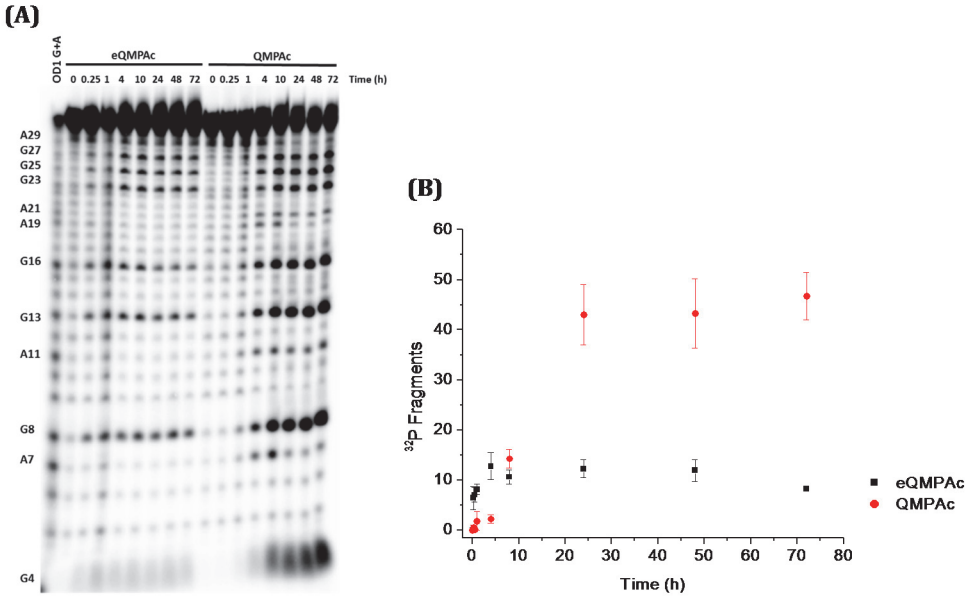

Figure 2.6: Time-dependent alkylation of dsDNA by **QMPAc** and **eQMPAc.** (A.) dsDNA 5'-**[^{32}P]-OD1:OD2** (3.0 μM) was incubated with **eQMPAc** (120 μM), **QMPAc** (120 μM), in the presence of NaF (10 mM) and MES buffer (10 mM, pH 7.0) for 0 – 72 h, followed by 10 % hot piperidine treatment. (B) Rate of dG-N7 alkylation plotted as a percentage of 5'-**[^{32}P]-OD2** fragments for the indicated time periods. Reaction yield is an average of independent three trials, determined by subtracting fragment intensity from t = 0. Error is an average of the standard deviation.

Before proceeding to test for transfer of regenerated QMs between complementary strands, time-dependent quenching of QM precursor in the presence of buffer and sodium fluoride was conducted. This experiment was done to ensure that transfer of QMs from a donor to an acceptor strand was due to regeneration of the electrophile and not unreacted starting material. Reaction of QMs with water has been shown to be thermodynamically stable[28] and should prevents any further reaction of QMs with DNA as hydroxides are not good leaving groups. Incubation of the QM in aqueous buffer before adding DNA oligonucleotides showed that **eQMPAc** was consumed within 1 h, while **QMPAc** was consumed in 24 h (Figure 2.7). This confirms that all mono-QM starting material would either react with water or DNA bases at these time points and any further reaction with nucleophilic bases would be due to regeneration of the reactive electrophile.

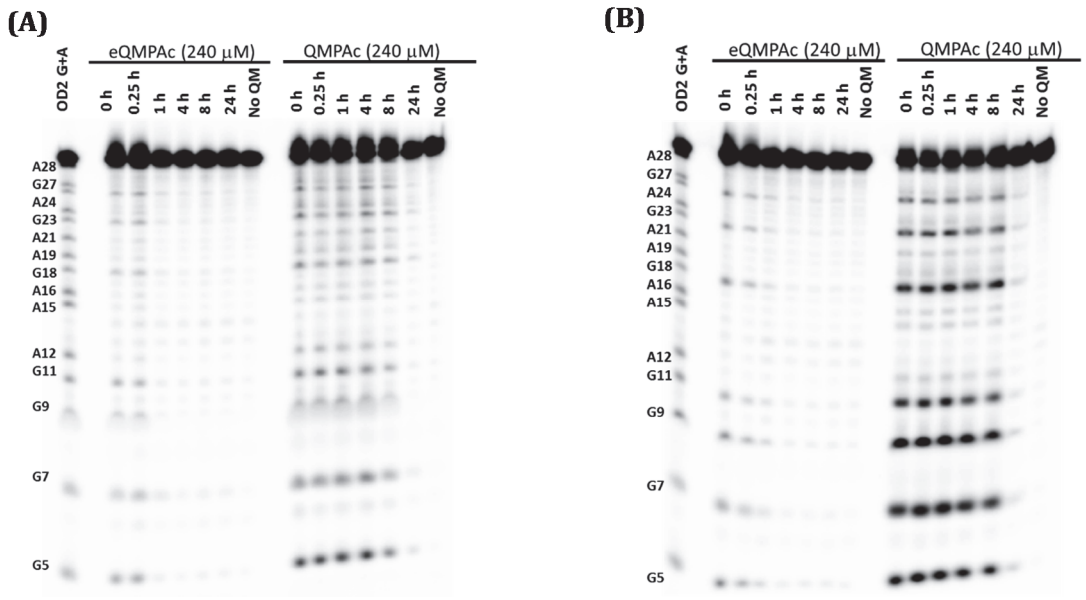

Figure 2.7: Rate of quinone methide (QM) quenching in aqueous buffer. (A.) **eQMPAc** (240 μM) and **QMPAc** (240 μM) was incubated in the presence of NaF (10 mM) and MES buffer (10 mM, pH 7.0) from 0 – 24 h, followed by the addition of either (A) 5'-**[^{32}P]-OD2** (3.0 μM) or (B) 5'-**[^{32}P]-OD2:OD1** (3.0 μM) and then incubated for another 24 h. DNA was then treated with 10 % hot piperidine.

2.2.3: Transfer of ether and methylene-bridged mono-QMs between complementary sequences

Since **eQMPAc** reacts at a faster rate than **QMPAc**, reversible DNA alkylation by the electron-rich compound, **eQMPAc** is also expected to proceed at a faster rate. To observe enhanced reversibility of **eQMPAc** in comparison to **QMPAc**, transfer of each alkylating agent from one complementary strand to another was tested (Scheme 2.6). Each QM was incubated with ssDNA for 24 h, followed by addition of a ^{32}P-labeled complementary stand and further incubation for up to 48 h. Gel image showed an increase in dG-N7 fragments of the radiolabeled strand upon treatment with hot piperidine (Figure 2.8A). Total yield of DNA fragments was 6% and 10% for **eQMPAc** and **QMPAc** treated samples, respectively (Figure 2.8B). Contrary to what was anticipated, electrophoresis studies indicate that transfer of **QMPAc** from one complementary strand to another via regeneration of QMs occurs at a faster rate than the **eQMPAc** when adducts at dG-N7 are detected. However, lower yields of dG-N7 adducts observed with **eQMPAc** could be due to increased lability of the electrophile and formation of water adducts. Quantitation of DNA fragment yields showed that reversible dG-N7 adducts of **eQMPAc** are formed preferentially at G7 of **5'-[^{32}P]-OD2,** within a GC-rich region. This same preference for GC-rich regions was confirmed by observing high yield of G23 adducts on **5'-[^{32}P]-OD4**, when the GC-segment of the oligonucleotide was moved from the 3'-end of the sequence to the 5'-end (Figure 2.9). A graph of the total percentage of dG-N7 fragments in each radiolabeled acceptor strand showed more than 25% of total DNA fragments occurred in the GC-rich regions. It is possible that increased yield of transferred

eQMPAc at GC-rich sequences is due to higher yields of dC-N3 adducts that are regenerated and transferred to dG-N7. Studies showed that reaction at dC-N3 produced the highest yield of adducts when a simple QM was incubated with equimolar concentrations of four deoxynucleosides (dA, dC, dT, dG).[32] Similarly, studies by Lonnberg et *al.* showed higher yields of alkylation by quinone methide cyclen conjugates at CC bulges in comparison to bulges of other bases.[53] The dominance of dC adducts would essentially facilitate reversible alkylation of neighboring nucleophiles upon regeneration of QM. Since piperidine induced DNA fragmentation detects alkylation at dG-N7, it is not surprising that higher yields of fragments are observed at GC-rich regions of our selected sequence.

5'-[^{32}P]-OD2: 3'-GTC CAG TCA GTA CAG CAA TTA GCG CGC GTA TT -5

OD1: 5'-CAG GTC AGT CAT GTC GTT AAT CGC GCG CAT AA -3'

Scheme 2.6: Transfer of QM between complementary strands

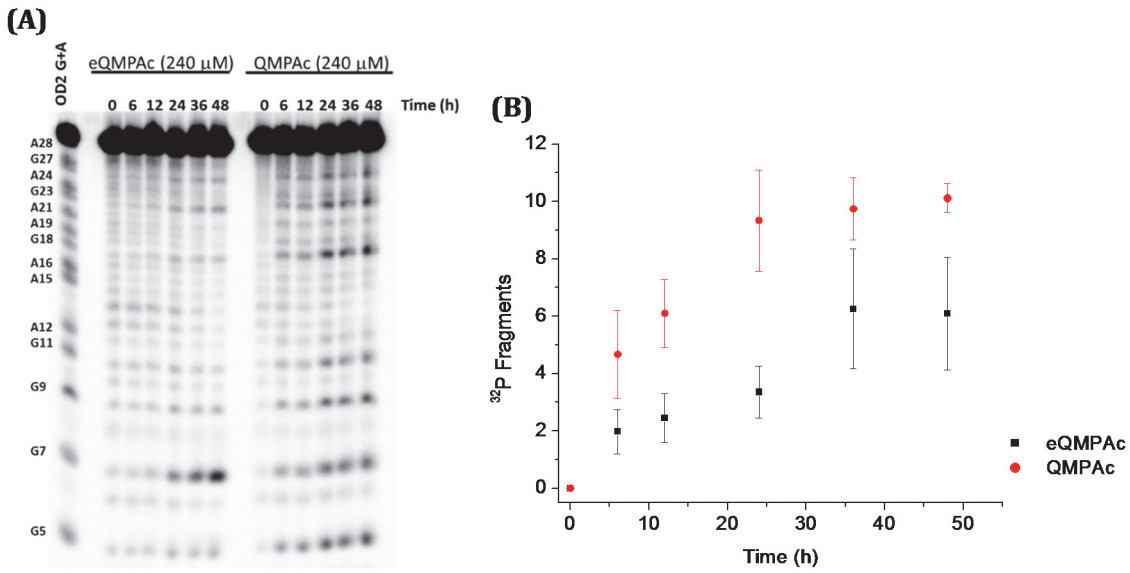

Figure 2.8: Transfer of **eQMPAc** and **QMPAc** between complementary strands. (A) Single strand **OD1** (3.0 μM) was incubated with either **eQMPAc** (240 μM) or **QMPAc** (240 μM), in the presence of NaF (10 mM) and MES buffer (10 mM, pH 7.0) for 24 h, followed by the addition of 5'-**[^{32}P]-OD2** (3.3 μM) for 0 - 48 h and subsequent treamtment with 10 % hot piperidine. (B) Rate of dG-N7 alkylation on 5'-**[^{32}P]-OD2.** Yield of 5'-**[^{32}P]-OD2** is plotted as total percentage of lane intensity for **eQMPAc**, and **QMPAc** treated samples. Reaction yield is an average of independent three trials, determined by subtracting fragment intensity from t = 0. Error is an average of the standard deviation.

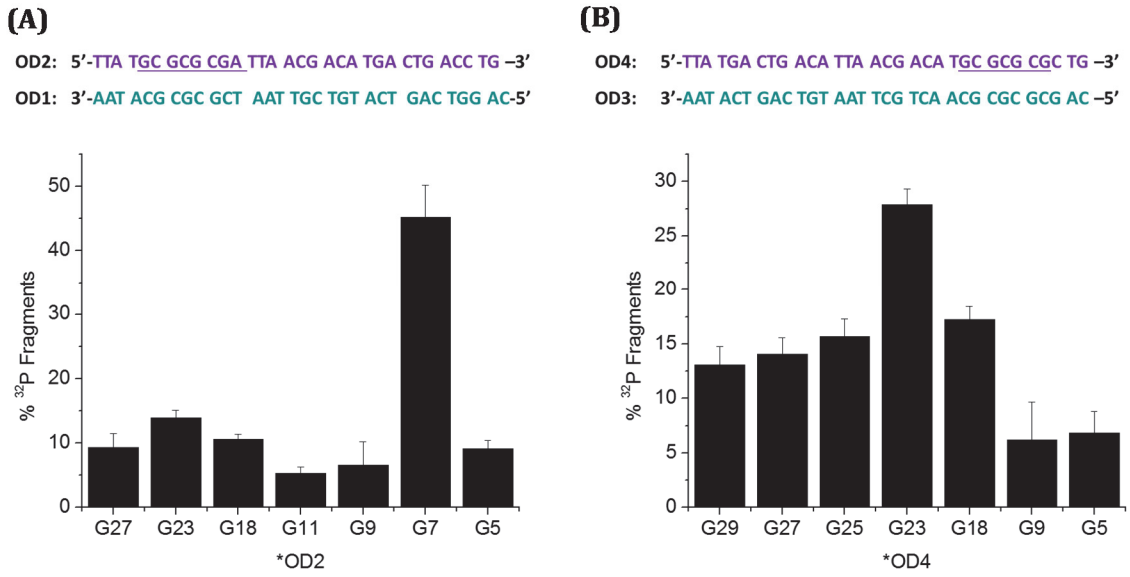

Figure 2.9: Reversible transfer of **eQMPAc** at GC-rich regions. Single strand **OD1** (3.0 μM).or **OD3** (3.0 μM) was incubated with **eQMPAc** (240 μM) in the presence of NaF (10 mM) and MES buffer (10 mM, pH 7.0) for 24 h, followed by the addition of its complement, (A) **5'-[^{32}P]-OD2** (3.3 μM) or (B) **5'-[^{32}P]-OD4** (3.3 μM), and incubating further for 0 - 48 h**.** Subsequent treatment with 10 % hot piperidine product fragments of dG-N7 adducts. Yield is an average of three independent trials and error is the standard deviation.

2.2.4: Electron-rich QMs are susceptible to trapping by strong nucleophiles

Although the electron-rich QM electrophile has been shown to persist for up to 7 days in the presence of DNA nucleophiles, migration along duplex is too slow for biological relevance.[47] Under these circumstances, DNA needs to outcompete irreversible trapping of QMs by endogenous nucleophiles. Even though an electron-rich QM may persist longer, the electrophile is also susceptible to reaction with endogenous strong nucleophiles.[54] Under cellular conditions, trapping of QMs by strong nucleophiles may inhibit reversible alkylation and migration of the electrophile. To observe the competitive reaction of QM with a strong nucleophile versus dG-N7, **eQMPAc** and **QMPAc** were incubated with ssDNA for 24 h, and then 20-fold excess BME (β-mercaptoethanol) was added simultaneously with a complementary strand (Scheme 2.7). BME serves as a good model because thiols are one of the strongest and biologically abundant nucleophiles.[55] In the presence of excess BME, reaction with the thiol nucleophile should prevent reaction of regenerated QMs with the complementary acceptor strand since BME will outcompete the nucleophilic bases. When transfer of either **eQMPAc** or **QMPAc** from one complementary strand to another in the presence of BME was tested, gel image showed minimal alkylation of the acceptor strands, **5'-[^{32}P]-OD2** (Figure 2.10). These results suggests that both **eQMPAc** and **QMPAc** were trapped by BME when the electrophile was released from the DNA bases. This supports previous evidence by Wang *et al.* that showed the inability of a bis-QMs to reversibly alkylate duplex DNA in the presence of BME.[56] While it is possible that minimal reaction at dG-N7 was observed because **eQMPAc** and **QMPAc** have reacted at other

nucleophilic sites of DNA, present data suggest that strong nucleophiles can outcompete DNA bases to react with mono-QMs and inhibit transfer of regenerated QMs within dsDNA.

Scheme 2.7: Trapping regenerate QMs with BME

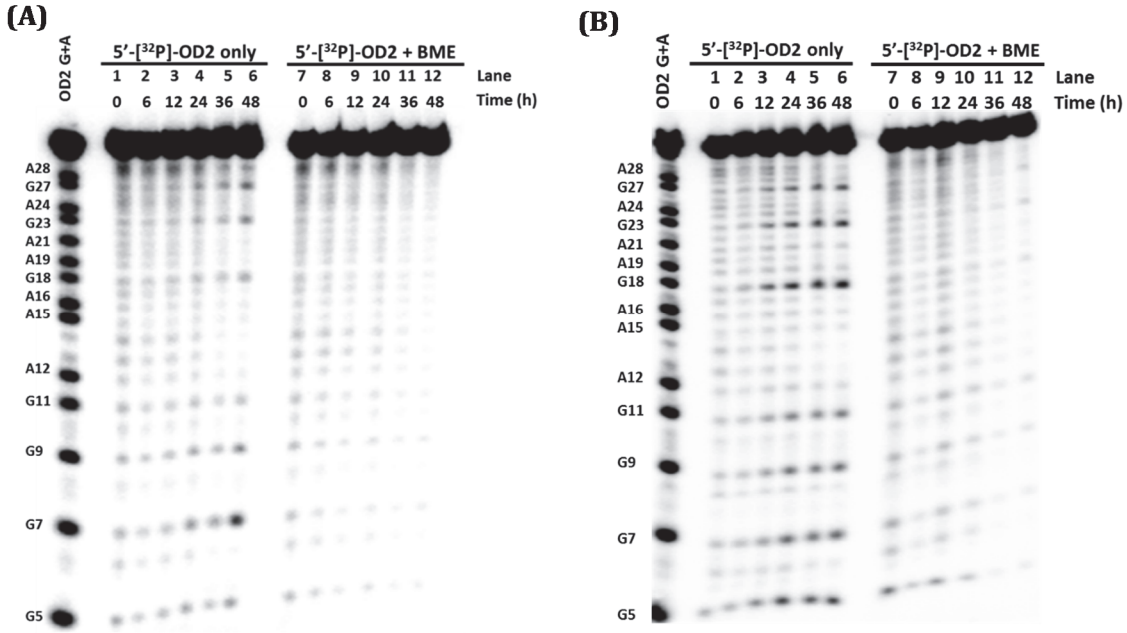

Figure 2.10: Quenching of regenerated **eQMPAc** and **QMPAc** by BME. Single strand **OD1** (3.0 μM) was incubated with either (A) **eQMPAc** (240 μM) or (B) **QMPAc** (240 μM), in the presence of NaF (10 mM) and MES buffer (10 mM, pH 7.0) for 24 h, followed by the addition of either **5'-[^{32}P]-OD2** (3.3 μM), lanes 1 – 6, or **5'-[^{32}P]-OD2** (3.3 μM) and BME (5.0 mM), lanes 7 - 12 for 0 - 48 h. Subsequently, samples were treated with 10% hot piperidine.

2.3: Conclusion

In this chapter, the influence of electron-donating aromatic substituents on the kinetics of reversible DNA alkylation by mono-QM acridine conjugates was evaluated. Studies have shown that the presence of an ether substituent

dramatically promotes initial DNA alkylation at dG-N7. However, this improved reactivity of **eQMPAc** resulted in lower yields of DNA adducts in comparison to the methylene-substituted **QMPAc** at longer incubation periods. Release of the electrophile from kinetically favored reaction sites would allow for the formation of thermodynamically stable adducts with DNA bases, water or endogenous nucleophiles. Since adducts at dG-N7 are kinetic products, this could be the reason for the decrease in **eQMPAc** adducts at extended time periods.

This work also demonstrated that reversible DNA alkylation by mono-QM intermediates is governed by the nucleophilic environment. The ether substituted **eQMPAc** showed a preference for reversible alkylation of dG-N7 at GC-rich sequences, whereas **QMPAc** was more promiscuous. In the future, quantifying the yield of adducts at each base via HPLC-MS will help elucidate the reason for this trend. Studies also indicated that presence of strong nucleophiles like BME trap the electrophile and hinder migration of QM along DNA. However, this may be circumvented if a QM drug is delivered exclusively to GC-rich sequences and under conditions of low thiol concentration.

2.4: Materials and Methods

General Methods

Absorbance spectra were recorded on a Hewlett-Packard 8453 UV/Vis spectrophotometer. High resolution mass spectra (HRMS) by Fast Atom

Bombardment (FAB) were determined on a VG70S magnetic sector spectrometer. Nuclear magnetic resonance (NMR) were recorded on a Bruker Avance spectrometer (^{1}H: 400 MHz, ^{13}C: 100 MHz). Buffers and salts were prepared using water that was purified to a resistivity of 18 MΩ.cm. DNA oligonucleotides were radiolabeled by incubating primers with [γ-^{32}P]-ATP, and T4 polynucleotide kinase (PNK) enzyme in T4 PNK buffer. Radiolabeled DNA samples were separated using 20% denaturing polyacrylamide gel (40 % acrylamide (19:1 acrylamide:bis-acrylamide) electrophoresis. DNA alkylation samples dissolved in loading dye (0.05 % bromophenol blue, 0.05 % xylene cyanol FF, 10 mM EDTA, in formamide)) were loaded into the gel wells and electrophoresis was conducted at 1200 V for 4 h. Gels were then transferred onto a Molecular Dynamics phosphoimager screen for 4 hours, and images was scanned on a Typhoon 9410 Variable Mode Imager. DNA fragments were quantified using ImageQuant TL software.

General Materials

Sodium fluoride, 2-(*N*-morpholino)ethanesulfonic acid (MES), boric acid, and Tris base were purchased from Fisher Scientific. Buffers and salts were prepared using water that was purified to a resistivity of 18 MΩ.cm. DNA oligonucleotides were synthesized by Integrated DNA technologies (Coraville IA). Radioactive [γ-^{32}P]-dATP was purchased from Perkin Elmer. T4 PNK and T4 PNK buffer were purchased from New England Biolabs (Beverly, MA). Polyacrylamide gel (40% acrylamide (19:1 acrylamide:bis-acrylamide)) was purchased from Bio-Rad (Hercules, California).

3-(3-Hydroxymethyl-4-hydroxyphenyl)propionic acid (1) [52]

3-(4-Hydroxyphenyl)propionic acid (3.00 g, 18.1 mmol) was added to a solution of phenylboronic acid (2.30 g, 19.0 mmol), trichloroacetic acid (1.47 g, 9.00 mmol), and paraformaldehyde (2.80 g, 90.0 mmol) in benzene (30.0 mL). The reaction was heated to reflux for 4 h, cooled to room temperature, and solvent was evaporated under reduced pressure. A white solid was collected, dissolved in ether (50 mL), washed with water (50 mL), and saturated aqueous sodium bicarbonate (3 × 50 mL). The organic layer was dried over $MgSO_4$. Solvent was evaporated, and a white solid was collected. The residue was then dissolved in THF (10 mL). Hydrogen peroxide (30 %, 5 mL) was added, and the solution was stirred at 0 ^oC for 2 h. The reaction was diluted with water (50 mL), and extracted with ether (3 × 50 mL). The organic layers were combined, dried over $MgSO_4$, and concentrated under reduced pressure. A light beige oil was collected, and purified by a silica gel column (2:1 hexanes in ethyl acetate and 0.5% acetic acid) to yield **1**, the desired white solid (2.56 g, 72%). ^1H NMR (400 MHz, CD_3OD) d ppm 2.54 (t, *J*=7.6 Hz, 2 H), 2.82 (t, *J*=7.6 Hz, 2 H), 4.62 (br. s., 2 H), 6.68 (d, *J*=8.2 Hz, 1 H), 6.95 (d, *J*=8.0 Hz, 1 H), 7.12 (br. s., 1 H)

3-(3-*tert*-Butyldimethylsilyoxymethyl-4-*tert*-butyldimethylsilyloxyphenyl)-propionic acid (2) [37]

Imidazole (3.00 g, 43.8 mmol) and *tert*-butyldimethylsilyl chloride (TBDMSCl, 3.30 g, 21.9 mmol) was added to a solution of **1** (1.00 g, 5.10 mmol) in DMF (6 mL). The reaction was stirred under nitrogen (N_2) for 18 h, diluted with brine (50 mL), and

extracted with ether (3 × 50 mL). The organic layers were combined, washed with saturated aqueous sodium bicarbonate (2 × 50 mL), dried over $MgSO_4$ and solvent was removed under reduced pressure to yield **2** as a colorless oil product (3.27 g, 66 %). ^{1}H NMR (400 MHz, $CDCl_3$) δ ppm -0.01 - 0.04 (m, 6 H), 0.26 (s, 6 H), 0.87 (s, 9 H), 0.93 (s, 9 H), 2.61 (t, *J*=7.8 Hz, 1 H), 2.87 (t, *J*=7.8 Hz, 1 H), 4.72 (s, 1 H), 6.65 (d, *J*=8.2 Hz, 1 H), 6.92 (d, *J*=8.0 Hz, 1 H), 7.27 (s, 1 H)

3-(3-Acetoxymethyl-4-*tert*-butyldimethylsilyloxyphenyl)propionic acid (3) [37]

Ferric chloride (15 mg, 0.10 mmol) was added to a solution of **3** (1.00 g, 2.36 mmol) in acetic anhydride (2 mL) at 0 °C. The reaction was stirred for 1 h, diluted with ether (50 mL), washed with water (50 mL), and saturated aqueous sodium bicarbonate (50 mL). The organic layer was dried over $MgSO_4$, filtered, and evaporated under reduced pressure to yield **3** as a colorless oil (0.72 g, 87%). ^{1}H NMR (400 MHz, $CDCl_3$) δ ppm 0.27 (s, 5 H), 0.97 (s, 9 H), 2.09 (s, 3 H), 2.74 (d, *J*=8.0 Hz, 2 H), 2.90 (t, *J*=7.7 Hz, 2 H), 5.08 (br. s., 2 H), 6.75 (d, *J*=8.0 Hz, 1 H), 6.99 - 7.08 (m, 1 H), 7.14 (br. s., 1 H)

***N*-Succinimidyl-3-(3-acetoxymethyl-4-*tert*-butyldimethylsilyloxyphenyl) propionate (4)** [37]

N-Hydroxysuccinimide (680 mg, 6.4 mmol) was added to a solution of **3** (580 mg, 1.65 mmol) and 1-ethyl-3-(3-dimethylaminopropyl)carbodiimide (EDCl, 450 mg, 3.91 mmol) in DMF (5 mL). The reaction was cooled to 0 °C and stirred under N_2 for 22 h. The mixture was diluted with brine (30 mL), and extracted with ether (3 × 30 mL). The organic layers were combined, washed with saturated ammonium

chloride, and dried over $MgSO_4$. The solvent was evaporated under reduced pressure, to yield **4** as a viscous colorless oil (400 mg, 54%).^{1}H NMR (400 MHz, $CDCl_3$) d ppm 0.23 (s, 6 H), 0.97 (s, 10 H), 2.09 (s, 3 H), 2.77 - 2.91 (m, 8 H), 2.93 - 3.03 (m, 2 H), 5.09 (s, 2 H), 6.76 (d, *J*=8.4 Hz, 2 H), 7.06 (dd, *J*=8.2, 2.2 Hz, 2 H), 7.16 (d, *J*=2.2 Hz, 2 H)

5-(3-((2-(Acridin-9-ylamino)ethyl)amino)-3-oxopropyl)-2-((*tert*-butyldimethylsilyl)oxy)benzyl acetate (QMPAc)

To a mixture of *N*'-(acridin-9-yl)ethane-1,2-diamine hydrochloride **5** (50 mg, 0.21 mmol), supplied by Dr. Qingping Zeng (Rokita Lab), in methanol (10 mL), trimethylamine (350 μL, 2.5 mmol) was added and stirred at room temperature. Compound **4** (400 mg, 0.890 mmol) was dissolved in acetonitrile (8 mL) and added dropwise to the methanol mixture. The reaction was stirred for 30 min, and then acetic acid (35 μL, 0.56 mmol) was added dropwise, over 5 min. The solvent was removed under reduced pressure, and the collected residue was dissolved in CH_2Cl_2 (30 mL), washed with water (1 × 30 mL), and brine (2 × 30 mL). The organic layer was dried over Na_2SO_4, and concentrated under reduced pressure. A yellow paste was collected and recrystallized in CH_2Cl_2 and ether (1:2), to yield **QMPAc**, a yellow crystal (101 mg, 84%). ^{1}H NMR (400 MHz, $CDCl_3$) δ ppm 0.21 (s, 6 H), 0.97 (s, 10 H), 2.06 (s, 3 H), 2.77 (t, *J*=7.7 Hz, 2 H), 3.02 (t, *J*=7.7 Hz, 2 H), 3.89 (br. s., 2 H), 4.29 (br. s., 2 H), 5.04 (s, 2 H), 6.69 (d, *J*=8.0 Hz, 1 H), 7.10 (d, *J*=8.2 Hz, 1 H), 7.20 (br. s., 3 H), 7.51 (t, *J*=6.7 Hz, 2 H), 8.18 (d, *J*=8.2 Hz, 2 H), 8.27 (d, *J*=7.0 Hz, 2 H), 8.59 (br. s., 1 H), 9.48 (br. s, 1 H). ^{13}C NMR (100 MHz, $CDCl_3$) δ -4.05, 18.37, 21.28, 25.84, 31.11, 38.14,

39.72, 52.57, 62.48, 118.74, 119.69, 126.53, 129.56, 130.53, 133.28, 134.50, 152.63, 171.17, 178.00. HRMS (FAB, mNBA) m/z 572.2938. Calcd for $C_{33}H_{42}N_3O_4Si$ ($M + H^+$) 572.2945

Methyl (2-(4-formyl-3-hydroxyphenoxy) acetate) (6) [39]

To a solution of 2, 4-dihydroxybenezaldehyde (3.00 g, 21.7 mmol) and potassium carbonate (3.00 g, 21.7 mmol) in THF (50 mL), methylbromoacetate (2.00 mL, 20.0 mmol) was added dropwise over 3 minutes and stirred on ice. The mixture was heated under reflux to 60 ^oC for 16 h, cooled to room temperature, and potassium carbonate was removed via vacuum filtration. The filtrate was collected and the solvent was removed under reduced pressure to yield a yellow oil. The product was purified via silica column chromatography using methylene chloride and ethyl acetate (20:1) to provide a white solid. (3.19 g, 70%). ^1H NMR (400 MHz, $CDCl_3$) δ ppm 3.83 (s, 3 H), 4.70 (s, 2 H), 6.39 (d, *J*=2.3 Hz, 1 H), 6.60 (dd, *J*=8.7, 2.4 Hz, 1 H), 7.48 (d, *J*=8.7 Hz, 1 H), 9.75 (s, 1 H), 11.45 (s, 1 H)

2-(4-Formyl-3-hydroxyphenoxy)acetic acid (7) [39]

Potassium trimethylsilanolate (5.50 g, 43.0 mmol) was added to compound **6** (3.19 g, 15.2 mmol) in THF (40 mL), cooled to 0 ^oC. The mixture was stirred on ice for 4 h until the starting material was consumed (monitored by TLC). The solution was adjusted to pH 2.0 using aqueous citric acid (0.1 M), and extracted with ether (3 × 50 ml). The organic layer was dried over sodium sulfate and concentrated under reduced pressure. A crude solid was collected and recrystallized in hexane:ethanol (10:1) to yield a white solid (3.00 g, quantitative yield). ^1H NMR (300 MHz, CD_3CN) δ

ppm 4.72 (s, 2 H), 6.42 (d, *J*=2.4 Hz, 1 H), 6.52 - 6.61 (m, 1 H), 7.59 (d, *J*=8.7 Hz, 1 H), 9.74 (d, *J*=0.5 Hz, 1 H), 11.36 (s, 1 H)

2-(3-*tert*-Butyldimethylsilyloxy-4-formylphenoxy)acetic acid (8) [39]

Triethylamine (4.0 mL, 28.4 mmol) and 4-dimethylaminopyridine (DMAP, 0.39 g, 320 mmol) were added to a solution of **7** (3.00g, 15. 2 mmol) in DMF (30 mL). TBDMSCl (6.72 g, 45.7 mmol) was then added to the solution and stirred under N_2 for 20 h. The reaction was quenched with water (50 mL) and extracted with ether (3 × 50 mL). The organic phases were combined, washed with saturated ammonium chloride (2 × 50 mL), washed with brine (50 mL) and dried over sodium sulfate. The mixture was filtered and the solvent was removed under reduced pressure. The crude product was purified through silica gel column chromatography using hexane and ethylacetate (2:1, 1% acetic acid) to yield a white solid (4.21 g, 88%). ^{1}H NMR (400 MHz, $CDCl_3$) δ ppm 0.29 (s, 6 H), 1.03 (s, 10 H), 4.73 (s, 2 H), 6.40 (d, *J*=2.3 Hz, 1 H), 6.57 - 6.61 (m, 1 H), 7.82 (d, *J*=8.7 Hz, 1 H), 10.31 (s, 1 H)

2-(3-*tert*-Butyldimethylsiloxy-4-(hydroxymethyl)phenoxy)acetic acid (9) [39]

Compound **8** (2.00 g, 6.36 mmol) was dissolved in ethanol (20 mL) and cooled to 0 ^{o}C). Sodium borohydride (240 mg, 6.46 mmol) was then added to the mixture and stirred for 2 h until the starting material was consumed (monitored via TLC). The reaction was quenched with water (20 mL) and ethanol was removed under reduced pressure. The aqueous layer was washed with ether, and acidified with citric acid (1 M). The solution was then extracted with ether (3 x 30 mL), the organic layers were combined, dried over sodium sulfate, and solvent was removed under

reduced pressure to yield a white solid (1.54 g, 78 %). ^{1}H NMR (300 MHz, CD_3CN) δ ppm 0.23 (s, 6 H), 0.94 (s, 9 H), 4.56 (s, 2 H), 4.61 (s, 2H), 6.36 (d, *J*=2.5 Hz, 1 H), 6.52 (dd, *J*=8.5, 2.5 Hz, 1 H), 7.25 (d, *J*=8.5 Hz, 1 H)

2-(3-*tert*-Butyldimethylsiloxy-4-(acetoxymethyl)phenoxy)acetic acid (9) [39]

Triethylamine (400 μL, 2.64 mmol) and DMAP (32 mg, 0.28 mmol) were added to a solution of **8** (250 mg, 0.79 mmol) in CH_2Cl_2 (10 mL). Excess acetic anhydride (1 mL, 10 mmol) was added to the mixture ad stirred at room temperature for 2 h. The reaction was quenched with water (30 mL), and extracted with CH_2Cl_2 (3 × 30 mL). The organic phases were combined, dried over sodium sulfate, and concentrated under reduced pressure. The crude product was purified via silica column chromatography using hexanes and ethylacetate (1:1) to yield a white solid (140 mg, 50%). ^{1}H NMR (300 MHz, $CDCl_3$) d ppm 0.24 (s, 6 H), 1.00 (s, 9 H), 2.05 (s, 3 H), 2.27 (s, 2 H), 4.70 (s, 2 H), 5.03 (s, 2 H), 6.42 - 6.50 (m, 2 H), 7.23 (d, *J*=8.3 Hz, 3 H)

***N*-Hydroxylsuccinimide-2-(3-*tert*-butyldimethylsiloxy-4-(acetoxymethyl)phenoxy)-acetate (10)** [39]

Synthesis of **10** was carried out using the same procedure as that described above for **4**. Activation of the carboxylate of **9** (140 mg, 0.395 mmol) using *N*-hydroxysuccinimide (68 mg, 60 mmol) and 1-ethyl-3-(3-dimethylaminopropyl)carbodiimide (EDC, 116 mg, 60 mmol) yielded **11** (160 mg, 89%) as a viscous clear oil. ^{1}H NMR (300 MHz, $CDCl_3$) δ ppm 1.00 (s, 9 H), 2.05 (s, 3

H), 2.82 - 2.87 (m, 4 H), 4.93 (s, 2 H), 5.04 (s, 2 H), 6.40 - 6.48 (m, 1 H), 6.52 (dd, *J*=8.4, 2.5 Hz, 1 H), 7.27 (s, 1 H)

4-(2-((2-(Acridin-9-ylamino)ethyl)amino)-2-oxoethoxy)-2-((*tert*-butyldimentylsilyl)oxy)benzyl acetate (eQMPAc)

Addition of the acridine group to **10** (160 mg, 0.41 mmol) was conducted using a modified from that procedure describe above for **QMPAc**. *N*'-(Acridin-9-yl)ethane-1,2-diamine hydrochloride **5** (28 mg, 0.12 mmol) in methanol (10 mL), and trimethylamine (64 mg, 0.64 mmol) were mixed until it was homogenous. Compound **10** was dissolved in acetonitrile (10 mL) and added dropwise to the methanol mixture. The reaction was stirred for 1 h, and then acetic acid (0.025 g, 0.41 mmol) was added dropwise, over 5 min. The solvent was removed under reduced pressure, and the collected residue was dissolved in CH_2Cl_2 (20 mL), washed with water (1 × 20 mL), and brine (2 × 20 mL). The organic layer was dried over Na_2SO_4, and concentrated under reduced pressure. A yellow paste was collected and recrystallized in CH_2Cl_2 and ether (1:2), to yield **eQMPAc**, a yellow crystal (30 mg, 65%). ^{1}H NMR (400 MHz, $CDCl_3$) δ ppm 0.21 (s, 6 H), 0.95 (s, 9 H), 1.99 (s, 3 H), 4.07 (dd, *J*=5.0 Hz, 2 H), 4.40 (dd, *J*=4.5 Hz, 2 H), 4.59 (s, 2 H), 4.97 (s, 2 H), 6.53 - 6.61 (m, 2 H), 7.12 (t, *J*=7.7 Hz, 2 H), 7.17 (d, *J*=8.3 Hz, 1 H), 7.39 (t, *J*=7.6 Hz, 2 H), 8.08 (d, *J*=8.4 Hz, 2 H), 8.27 (d, *J*=8.7 Hz, 2 H), 8.61 (br. t, *J*=1.0, 1.0 Hz, 1 H), 9.33 (br. t, *J*=1.0, 1.0 Hz, 1 H) ^{13}C NMR (100 MHz, $CDCl_3$) δ 4.25, 18.15, 21.01, 25.57, 39.15, 50.80, 61.87, 67.05, 106.05, 119.38, 120.52, 123.44, 131.70, 133.98, 155.43,

158.16, 170.99, 171.10. HRMS (FAB, mNBA) m/z: 574.2738. Calcd for $C_{33}H_{42}N_3O_4Si$ ($M + H^+$): 574.2737

Alkylation of ss and dsDNA with QMPAc and eQMPAc

The desired ^{32}P radiolabeled ss or dsDNA (3.0 μM, 50 nCi) was incubated under ambient temperature with the indicated concentration of alkylating agent (0 – 240 μM) in presence of NaF (10 mM), MES (10 mM, pH 7), and 20% acetonitrile. Following a 24 h incubation period, samples were dried with a speedvac, and treated with 10% hot piperidine, at 90 ^oC for 30 min. The resulting samples were dried, resuspended in formamide loading solution, and subjected to 20% denaturing polyacrylamide gel electrophoresis.

Transfer of Alkylating Agent from Donor to Acceptor Strand

The indicated donor ssDNA, **OD1** or **OD3** (3.0 μM) was pre-incubated with each alkylating agent (**eQMPAc** or **QMPAc**, 240 μM) in the presence of NaF (10 mM), MES (10 mM, pH 7.0) and 20% acetonitrile for 24 h, under ambient temperature. Following pre-incubation, the radiolabeled ^{32}P acceptor strand (**OD2** or **OD4,** 3.3 μM, 50 nCi) was added to the samples and incubated for 0 - 48 h under ambient temperature. DNA was then treated with hot piperidine treatment (90 ^oC, 30 min), dried on the speedvac, resuspended in formamide loading solution, and then subjected to 20% denaturing gel electrophoresis.

Quenching regenerated QMs with BME

The donor ssDNA, **OD1** (3.0 μM) was pre-incubated with each alkylating agent, **eQMPAc** or **QMPAc** (240 μM), in the presence of NaF (10 mM), MES (10 mM, pH 7.0) and 20% acetonitrile for 24 h, under ambient temperature. Following pre-incubation, the radiolabeled ^{32}P acceptor strand (**OD2**, 3.3 μM, 50 nCi) and/or β-mercaptoethanol (BME, 5 mM) was added to the samples and incubated for 0 - 48 h under ambient temperature. DNA was then treated with hot piperidine (90 ^{o}C, 30 min), dried on the speedvac, resuspended in formamide loading solution, and then subjected to 20% denaturing gel electrophoresis.

Chapter 3: Migration of mono-QMs along duplex DNA

3.1: Introduction

Non-covalent localization of alkylating agents to DNA has been a means of achieving enhanced reactivity and maximizing cytotoxicity for therapeutic purposes.[57] For example, the chemotherapeutic agent chlorambucil crosslinks DNA more efficiently by a factor of 10^4 *in vitro* when it is conjugated to a spermidine polyamine DNA ligand, relative to the parent compound.[58] The covalent linkage of polycationic amines to chlorambucil promotes association of the alkylating agent to the negatively charged phosphate backbone of DNA, thereby placing the electrophilic species in close proximity to react with the nucleophilic bases. The DNA associating affinity provided to alkylating agents by ligands is advantageous because it reduces the effective dose of DNA targeting drugs and minimizes indiscriminate reactions with endogenous nucleophiles.

By taking advantage of the diverse functional groups available within DNA, non-covalent associations by small molecule ligands may improve localization of alkylating agents to targeted sequences. For example, Cullis *et al*. exploited the affinity of polyamines for DNA by adding an extra cationic charge to the spermidine-conjugated chlorambucil, to achieve a spermine conjugate. [59,60] The addition of an extra ammonium group led to an increase in the DNA alkylating efficiency of chlorambucil while maintaining the same sequence specificity at 5'-GNC-3'as the non-conjugated compound. The chlorambucil-spermidine conjugate was also 35-fold more cytotoxic than the non-conjugated chlorambucil and cytotoxicity of the

alkylating agent also increased by 200-fold when the ligand-conjugated compound was delivered to polyamine-depleted cells. Polyamines are essential for cell proliferation and its depletion triggers arrest of cell growth.[61] By utilizing the cellular polyamine uptake system alkylating agents conjugated to these ligands could exhibit increased formation of DNA adducts and cytotoxicity.

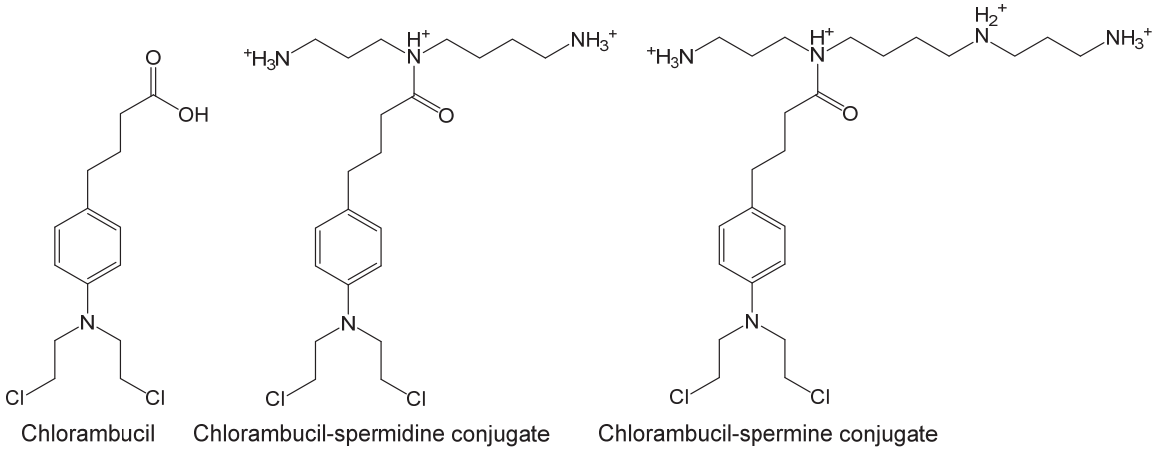

Figure 3.1: Conjugation of chlorambucil to polyammonium ligands

The addition of a trimethylammonium substituent to the peripheral end of a group of CC-1065 CBI analogs also increases their DNA alkylation efficiency by over 100-fold without altering their sequence specificity at AT-rich regions, in comparison to the parent compound.[62] The improved DNA alkylation was attributed to the high affinity of the cationic substituent for the negatively charged phosphate groups. Once bound to DNA, polyamines still possess freedom of motion traverse the phosphate backbone until the alkylating agent to reaches its preferred reaction site.[63] This is likely why both the CC-1065 and chlorambucil ammonium conjugates maintained similar sequence specificity as their parent compounds despite changes in their DNA association mode.

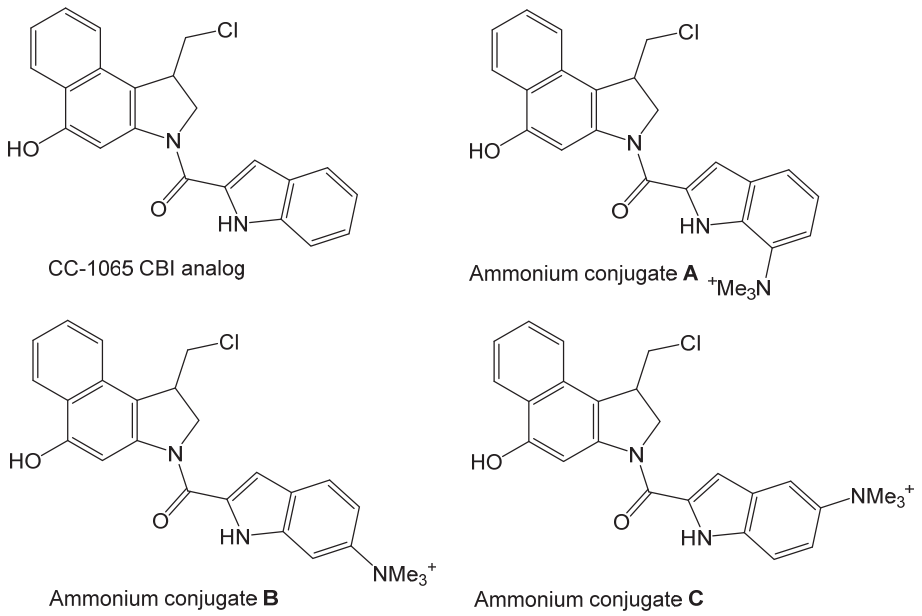

Figure 3.2: Comparison of ammonium substituents on CC-1065 CBI analogs

Conjugation of QMs to di- and trimethylammonium cations has been used for generating the reactive intermediate upon UV irradiation or thermal activation.[64-66] Although research was not directly motivated by association of the ammonium group to the DNA backbone, it has been an effective means of placing QMs in close proximity to nucleophilic base upon activation of the intermediate via displacement of the ammonium cations. However, through activation of the intermediate, QMs may suffer a loss in DNA affinity as the ammonium cations are released. This may also decrease yields of reversible adducts as QMs are regenerated, and limit migration of the electrophile along DNA via multiple reversible alkylation events. However, if QMs are conjugated to ammonium cations in which generation the intermediate is independent of its ligand, DNA alkylation efficiency may be enhanced and migration of the electrophile along duplex DNA may also benefit from the free movement of cations along the DNA backbone.

This chapter focuses on evaluating the ability of non-sequence specific cationic and intercalating ligands to enhance the DNA alkylating efficiency monofunctional QMs (mono-QM) and furthermore, promote reversible alkylation and migration of QMs along duplex DNA. Similar to the ammonium conjugated chlorambucil and CC-1065, a mono- and di-cationic trialkylammonium ligand has been conjugated to QMs to determine their ability to promote DNA alkylation (Figure 4). Polyammonium cations retain freedom of motion within DNA that may aid in maximizing the dynamic properties of QMs by promoting migration along dsDNA while forming multiple reversible adducts.[63,67]

Report have shown that bi-functional QM acridine conjugate (bis-QM) alkylated and migrated along duplex DNA via bipedal reversible reactions. Efforts to elucidate the mode of association suggests that acridine intercalates between DNA bases.[5,68] The stabilization provided by pi-pi stacking interactions between the aromatic bases increases its affinity towards DNA, thereby improving the alkylating efficiency of QM conjugates.[44,47] Through intercalation and de-intercalation of acridine, regenerated bis-QMs migrated by reacting from one DNA base to another. However, studies by Fakhari *et al*. showed that migration of a bis-QM acridine conjugate was limited due to kinetic localization of the intercalator on the 3'-end of a TT-bulge.[47] In order to fully exploit the reversible properties of QMs as a potential chemotherapeutic agent, it is necessary to explore the use of alternative DNA ligands that may enhance migration of the intermediate along duplex DNA. This chapter expands on the lability of the previously studied **QMPAc** by comparing its

ability to migrate along DNA to the newly synthesized ammonium conjugates, **QMPDA** and **QMPMA**.

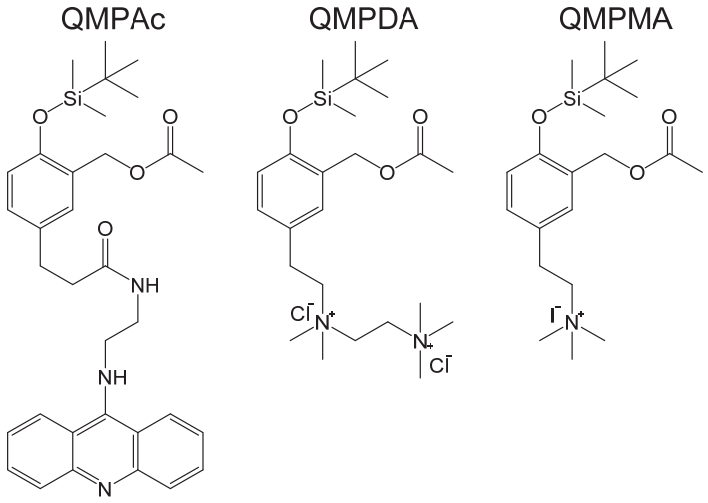

Figure 3.3: Conjugation of mono-QM precursors to DNA ligands

3.2: Results and Discussion

3.2.1: Synthesis of Aminated QMP

A conjugated mono-QM of interest, **QMPMA,** was initially synthesized by Dr. Mark Hutchinson in the Rokita lab. ^{1}H and ^{13}C showed that the final product was composed of roughly a 50:50 mixture of **QMPMA** and a non-acetylated product. Separation of both products proved to be difficult due to the presence of the charged ammonium ion, which caused both compounds to be strongly retained on a silica gel column. Since purity of the compound was crucial for DNA alkylation studies, **QMPMA** was re-synthesized with slight modifications to Dr. Hutchinson's protocol (Scheme 3.1). Selective hydroxymethylation was achieved through activation of the *ortho* position on the phenol through the use of phenyl boronic acid. [52] This was

followed by protection of the phenol with TBDMS[37], and then substitution of the bromine for an amine. The benzylic TBDMS of **14**was selectively hydrolyzed with the use of *p*-toluenesulfonic acid (pTsOH) to produce **15**. The benzyl alcohol was then acetylated with acyl chloride. Extending the reaction time when synthesizing **16** from 30 min to 14 h ensured full conversion of the starting material, and yielded 50% of the desired product. Finally, **16** was methylated to produce the ammonium salt of **QMPMA** with a yield of 50%. Methylation of **16** to produce **QMPMA** was confirmed by a change in the chemical shift of the two methyl groups attached to the amine from 2.37 ppm to a trimethylammonium at 3.26 ppm. High resolution fast atom bombardment mass spectrometry (HRFAB-MS) also provided evidence of the parent ion at 366 m/z for the deiodinated cationic product.

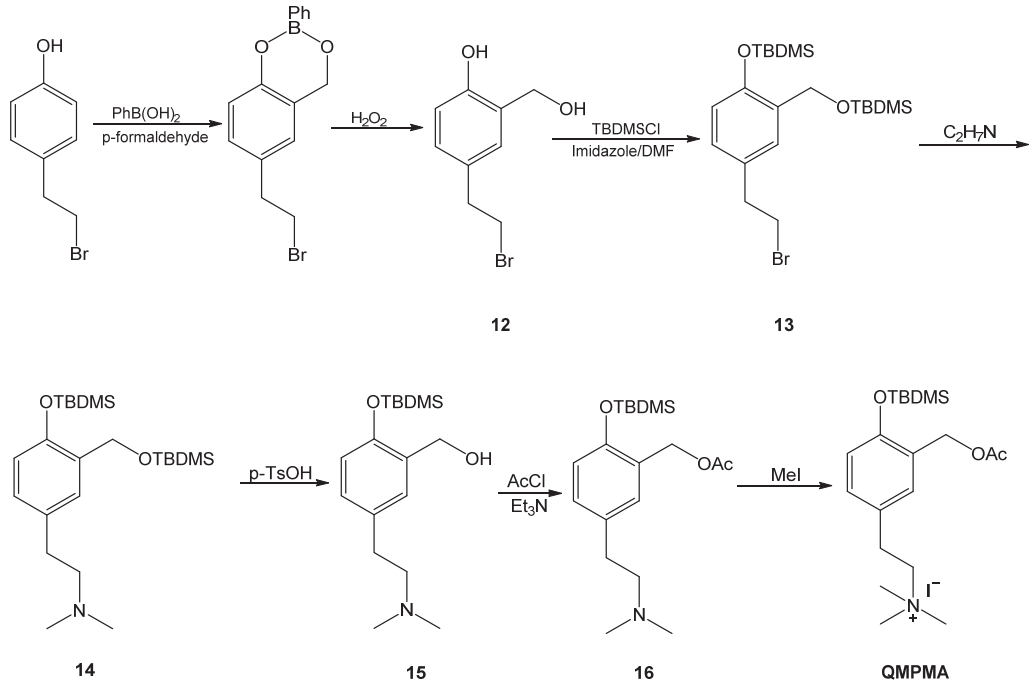

Scheme 3.1: Synthesis of **QMPMA**

Synthesis of **QMPDA** was commenced by a summer undergraduate researcher, Ms. Sierra Williams. Direct synthesis of the diammonium, **QMPDA**, was achieved using similar protocols as that described for **QMPMA** (Scheme 3.2). Addition of the diamine moiety increased the polarity of **17** making it difficult to purify subsequent products via silica gel chromatography. The use of excess reagents for the syntheses of **18**, **19,** and **QMPDA** ensured complete consumption of starting material to produce the desired product, without further purification. **QMPDA** was purified through anion exchange of the iodide to obtain a chloride salt. This also aided in preventing oxidation of the iodide anion and the production unwanted side products in DNA alkylation studies. Characterization of **QMPDA** by ^{1}H NMR showed changes in the methylene amine protons from 2.70 to 3.88 ppm. The di- and trimethylammonium protons were also present at 3.19 and 3.15 ppm, respectively. Integration of ^{1}H NMR signals showed an increase in methyl protons indicative of methylated final products. Chemical shift signals also matched predictions by ChemBioDraw Ultra 14.0. The mass spectrum of **QMPDA** showed no evidence of the expected molecular ion peak at 219 m/z, for the doubly charged state. However, a signal at 455 m/z, which correlates with the loss of both chloride anions and the presence of a hydroxide was observed. It is likely that the detection of this species was due to the isolation of the product from water as the lone pair electrons on the hydroxide oxygen could coordinate to either one or both of the nitrogen cations to form a hydroxide species. Nonetheless, chemical shifts observed on ^{1}H and ^{13}C NMR spectra provided conclusive evidence of **QMPDA**.

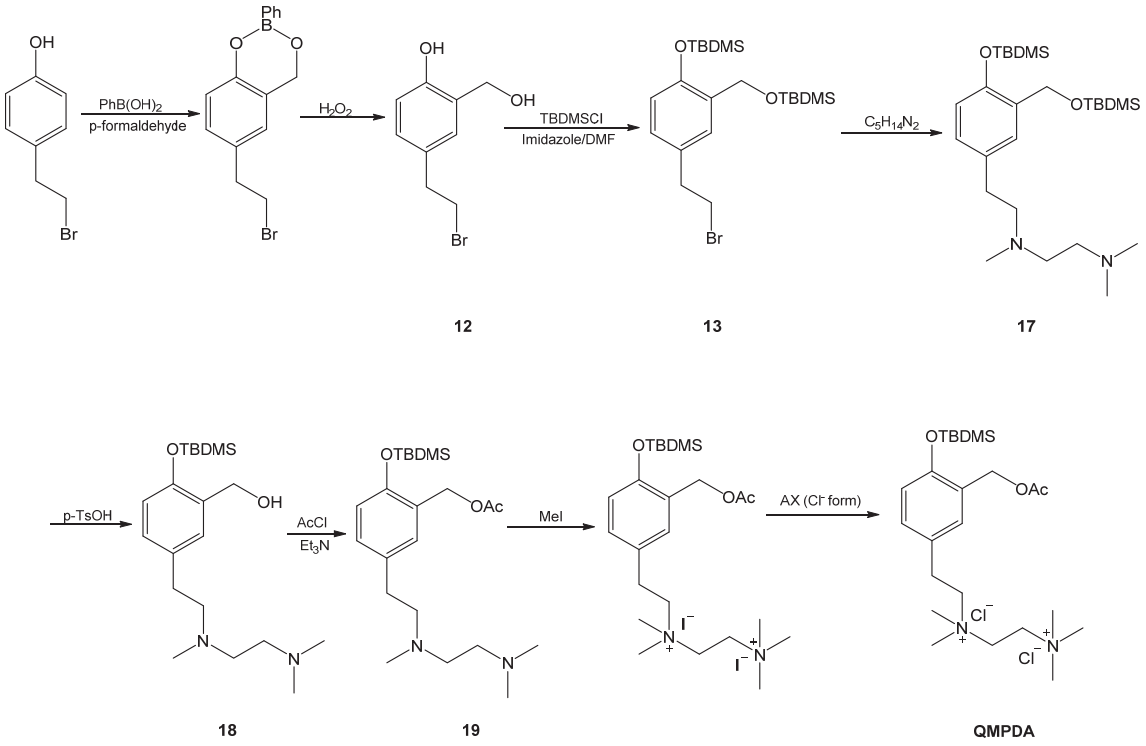

Scheme 3.2: Synthesis of **QMPDA**

3.3.2: Conjugation of mono-QMs facilitates efficient alkylation of ssDNA and dsDNA

Initial efforts to determine the effect of mono-QM localization on the rate of alkylation and migration focused on defining optimal concentrations at which **QMPAc**, **QMPDA**, and **QMPMA** alkylated ss and dsDNA at dG-N7. Covalent adducts at dG-N7 are highly labile and subject to strand cleavage in the presence of a mild base like hot piperidine (Scheme 3.3). Separation of DNA fragments via denaturing polyacrylamide gel electrophoresis allowed for quantitation of reaction at dG-N7. DNA alkylation studies were conducted using a randomized 32-base oligomer containing equal ratios dGs, dAs, dCs, and dTs. Incubation of ssDNA or dsDNA with varying concentrations of either **QMPAc**, **QMPDA** or **QMPMA** resulted in

fragmentation of radiolabeled ^{32}P strands when subject to hot piperidine treatment. In the presence of ssDNA and dsDNA, analysis of the gel showed an increase fragments with increasing concentrations of either **QMPAc**, **QMPDA** or **QMPMA**. (Figure 3.4). In addition, DNA fragment intensities were much stronger for reactions with dsDNA than ssDNA for **QMPAc** and **QMPDA** treated samples. This suggests that the mono-QMs alkylate dsDNA more efficiently than ssDNA. However, fragments of **QMPMA** produced similar yields in ssDNA and dsDNA. Reaction yields of **QMPAc**, **QMPDA** and **QMPMA** with DNA was confirmed by a plot of the total number of dG-N7 fragments as a function of the concentration of each alkylating agent (Figure 3.5). Both **QMPAc** and **QMPDA** alkylated dsDNA more efficiently than ssDNA, with increasing yields of dG-N7 fragments at higher concentrations of each alkylating agent. This may be due to increased stability of the ligand in dsDNA than ssDNA and also the availability of more reaction sites in dsDNA than ssDNA. However, thermodynamic binding studies would be needed to determine the degree of ligand association in single versus double stranded DNA and how it may affect alkylation by mono-QMs. Comparison of the fragment yields at the highest concentration of each alkylating agent indicates that **QMPAc** was more efficient than **QMPDA**, requiring only half the quantity of the electrophile (120 μM) to produce similar reaction yields (~40% ^{32}P fragments) as **QMPDA** when reacted with dsDNA. **QMPDA** also produced higher yields (4x) of DNA fragments than the singly charged conjugate, **QMPMA**, at 240 μM of each alkylating agent when reacted with dsDNA. Similar to the increase in the DNA alkylating efficiency of a quadruple charged spermine-conjugated chlorambucil over the triple charged spermidine conjugate,

the increase in reaction yield with **QMPDA** may be due to higher affinity of the doubly-charged ammonium ligand for DNA over the singly-charged **QMPMA**.

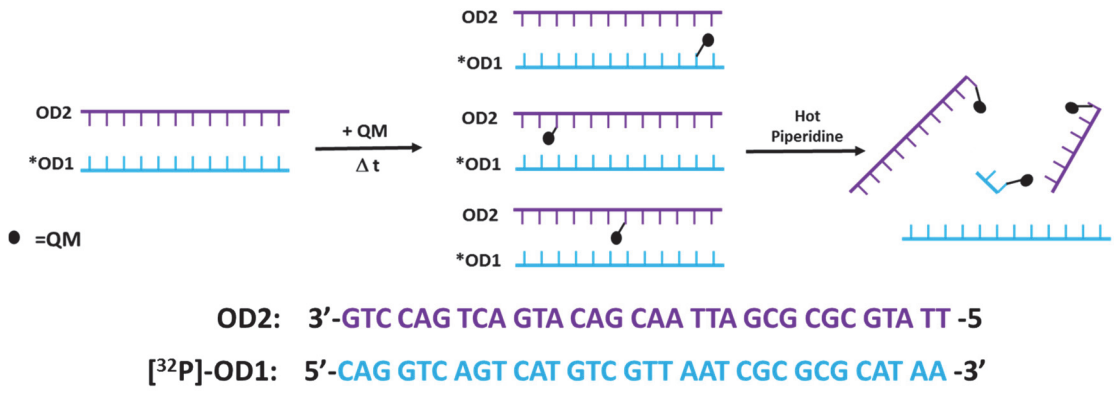

Scheme 3.3: Piperidine-induced DNA fragmentation at dG-N7 adducts

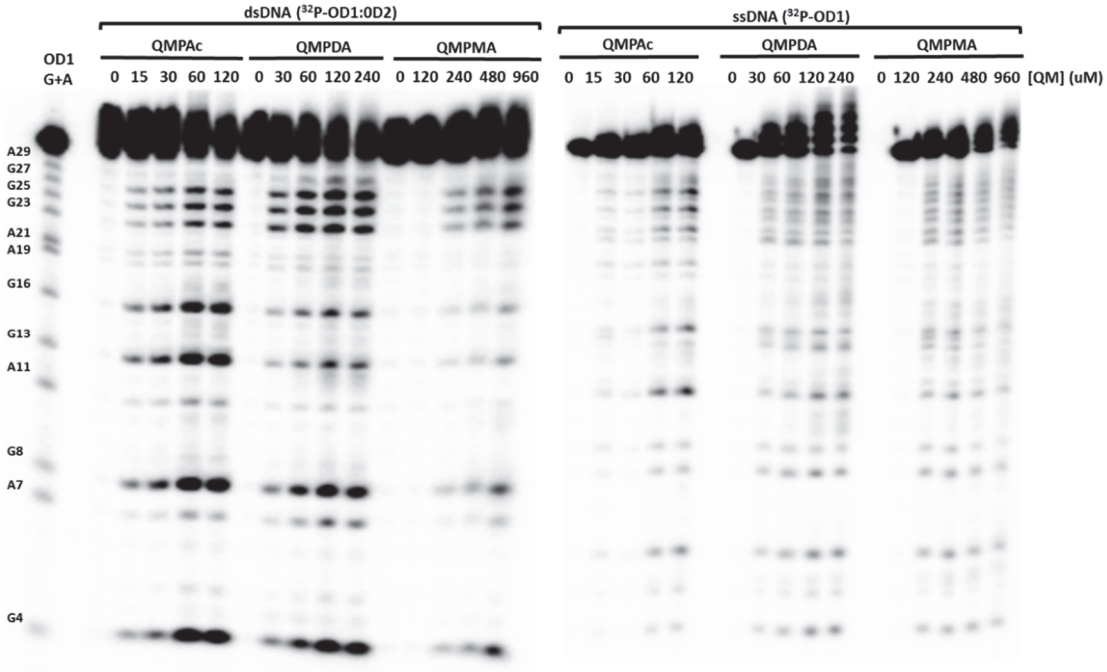

Figure 3.4: Concentration dependent alkylation of DNA by mono-QMs. Reaction at dG-N7 of dsDNA **5'-[32P]-OD1:OD2** (3.0 μM) and ssDNA **5'-[32P]-OD1** (3.0 μM) with **QMPAc** (0 - 120 μM), **QMPDA** (0 – 240 μM), and **QMPMA** (0 – 960 μM), in the presence of NaF (10 mM) and MES buffer (10 mM, pH 7.0) for 24 h, followed by 10 % hot piperidine.

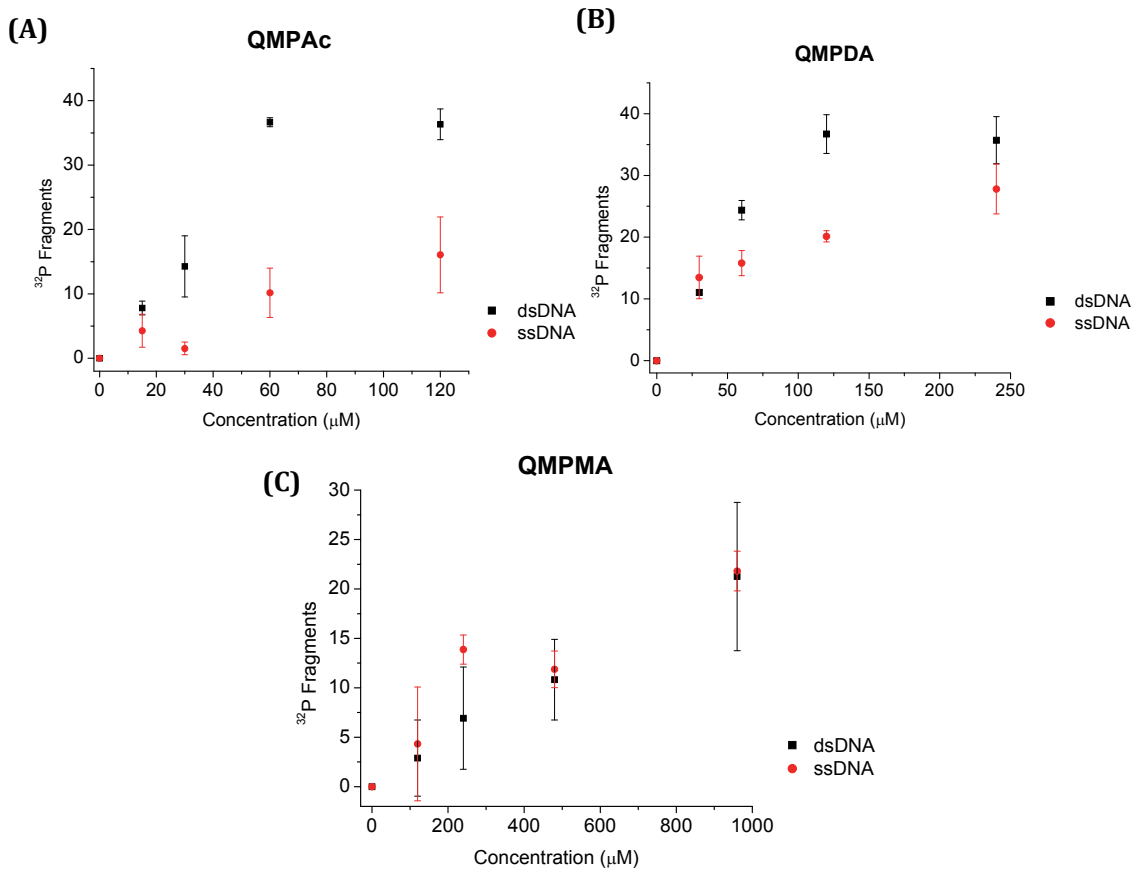

Figure 3.5: Rate of single and double strand DNA alkylation by mono-QMs. Yield of **5'-[^{32}P]-OD1** fragments as total percentage of lane intensity for ssDNA and dsDNA alkylation of (A) **QMPAc**, (B) **QMPDA** and (C) **QMPMA** treated samples. Reaction yield is an average of independent three trials, determined by subtracting fragment intensity from t = 0. Error is an average of the standard deviation.

Comparison of the ability of the ammonium and acridine ligands to enhance the rate of initial DNA alkylation following deprotection of the precursors was probed via time-dependent reactions of each mono-QM with ssDNA and dsDNA. Incubation of either **QMPAc**, **QMPDA**, or **QMPMA** with DNA for 0 – 48 h resulted in the formation of dG-N7 adducts that fragmented in the presence of hot piperidine. Analysis of total ^{32}P labeled DNA fragments showed that reaction of all three mono-QMs with dsDNA reached completion at 24 h, with half-lives of approximately 6 h (Figure 3.6). This indicated that the ligands did not influence the rate of DNA

alkylation. However, in order to test for reversible DNA alkylation, it was necessary to determine the rate at which all activated desilylated QMs either formed adducts with the nucleobases or reacted with water. Formation of QM-water adducts are thermodynamically stable and consumption of all starting material ensures that within complementary strands, transfer of QMs from a donor to an acceptor strand would be due to regeneration of the electrophile that had previously reacted with the donor strand. By initiating the desilylation of QMs in the presence of the fluoride anion and aqueous buffer for 0-24 h, the subsequent addition of DNA oligonucleotide produced low yields of dG-N7 adducts as a function of time (Figure 3.7). For both single- and double-stranded DNA samples, gel image shows that QMs were completely quenched by water in 24 h. Fragment intensities at 24 h were comparable to that of DNA samples lacking a QM alkylating agent. This confirms that within 24 h the deprotected starting material would have either reacted with water or the DNA bases and any further evidence of alkylation would be due to regeneration of the reactive electrophile.

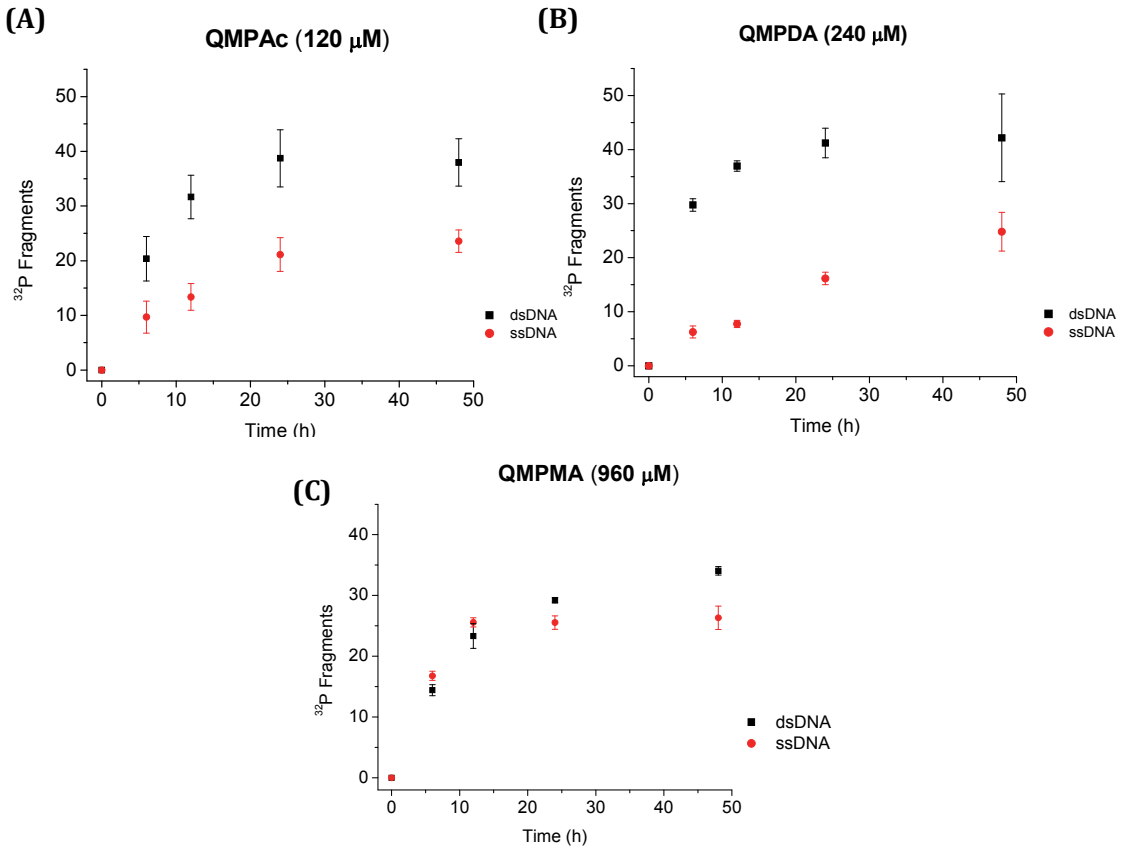

Figure 3.6: Rate of ssDNA and dsDNA alkylation at dG-N7 by **QMPAc**, **QMPDA** and **QMPMA**. dsDNA **5'-[^{32}P]-OD1:OD2** (3.0 μM) and ssDNA **5'-[^{32}P]-OD1** (3.0 μM) were incubated with either (A) **QMPAc** (120 μM), (B) **QMPDA** (240 μM), or (C) **QMPMA** (960 μM) in the presence of NaF (10 mM) and MES buffer (10 mM, pH 7.0) from 0 – 72 h, followed by 10 % hot piperidine. Plot of **5'-[^{32}P]-OD1** fragments as total percentage of lane intensity from 20% denaturing polyacrylamide gel image. Reaction yield is an average of independent three trials, determined by subtracting fragment intensity from t = 0. Error is an average of the standard deviation.

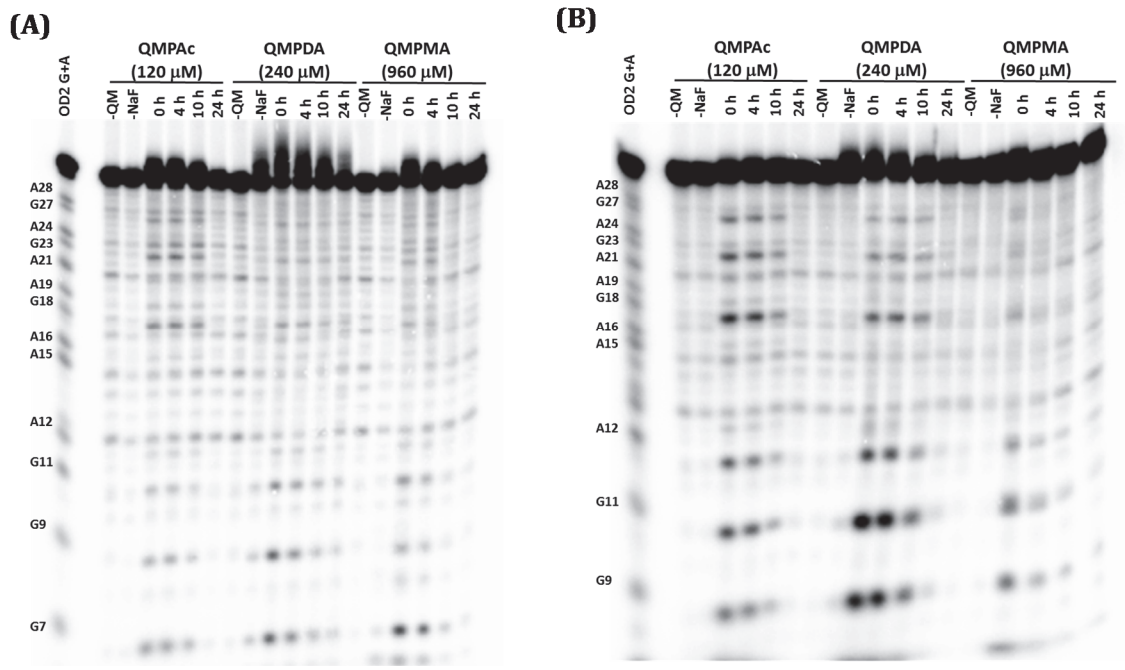

Figure 3.7: Quenching of quinone methide (QM) in aqueous buffer. **QMPAc** (120 μM), **QMPDA** (240 μM), and **QMPMA** (960 μM) were individually incubated in the presence of NaF (10 mM) and MES buffer (10 mM, pH 7.0) from 0 – 24 h, followed by the addition of either (A) **5'-[^{32}P]-OD2** (3.0 μM) or (B) **5'-[^{32}P]-OD2:OD1** (3.0 μM) and further incubation for 24 h. DNA was then treated with 10 % hot piperidine.

3.2.3: Acridine and quaternary diammonium QM conjugates alkylate complementary strands reversibly

Time-dependent transfer of QMs in ammonium and acridine conjugates from one complementary DNA strand to another were executed in order to compare the ability of these conjugates to promote reversible DNA alkylation (Scheme 3.4). In this study, each QM was incubated with a ssDNA donor strand, **OD1**, for 24 h. Subsequent addition of a radiolabeled complementary acceptor strand, **^{32}P-OD2**, which hybridizes to the donor strand, was expected to trap the regenerated electrophile through attack of the nucleophilic bases. Incubation of the acceptor

strand, **^{32}P-OD2**, in a solution of **QM-OD1** for up to 48 h showed a gradual increase in DNA fragments as a function of time (Figure 3.8A). Yields of transferred adducts reached a maximum of 10% and 12% total DNA fragments for **QMPAc-** and **QMPDA-**treated samples, respectively (Figure 3.8B). **QMPMA**-treated samples produced low yields of transfer with 5% total DNA fragments. This is not surprising considering the fact that **QMPMA** had the weakest DNA alkylating efficiency. However, the yield of fragments for **QMPAc** and **QMPDA** were within error of each other, despite the variation in it DNA ligand; it appears that having an ammonium vs. acridine ligand conjugate has minimal influence on transfer of the QM.

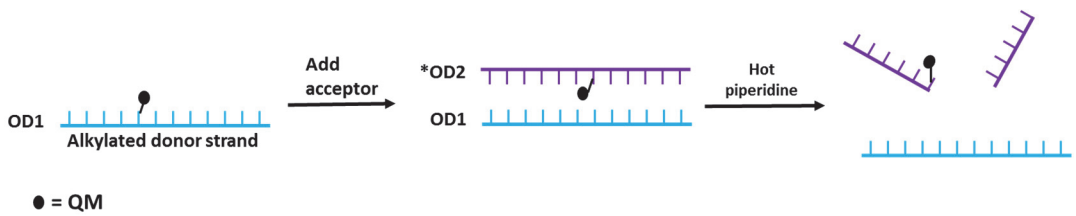

5'-[^{32}P]-OD2: 3'-GTC CAG TCA GTA CAG CAA TTA GCG CGC GTA TT -5

OD1: 5'-CAG GTC AGT CAT GTC GTT AAT CGC GCG CAT AA -3'

Scheme 3.4: Transfer of QM between complementary strands

At equal molar concentration of **QMPAc** and **QMPDA,** reaction of each alkylating agent with ssDNA produced 21% and 30% total DNA fragments at dG-N7, respectively (Appendix B, Figure B2). Transfer of half of these dG-N7 adducts from a donor ssDNA to an acceptor strands, would produce a yield of 10 -15%. However, it is possible that reversible adducts of dA-N1 and dC-N3 are also transferred to dG-N7. Nonetheless, the reported yields of transferred **QMPAc** and **QMPDA** suggest that slightly less than 50% of initial dG-N7 adducts on the donor strand were

transferred onto the acceptor strand. The rest of the regenerated mono-QMs may have formed hydroxide adducts or reacted with other DNA nucleophiles beside dG-N7.

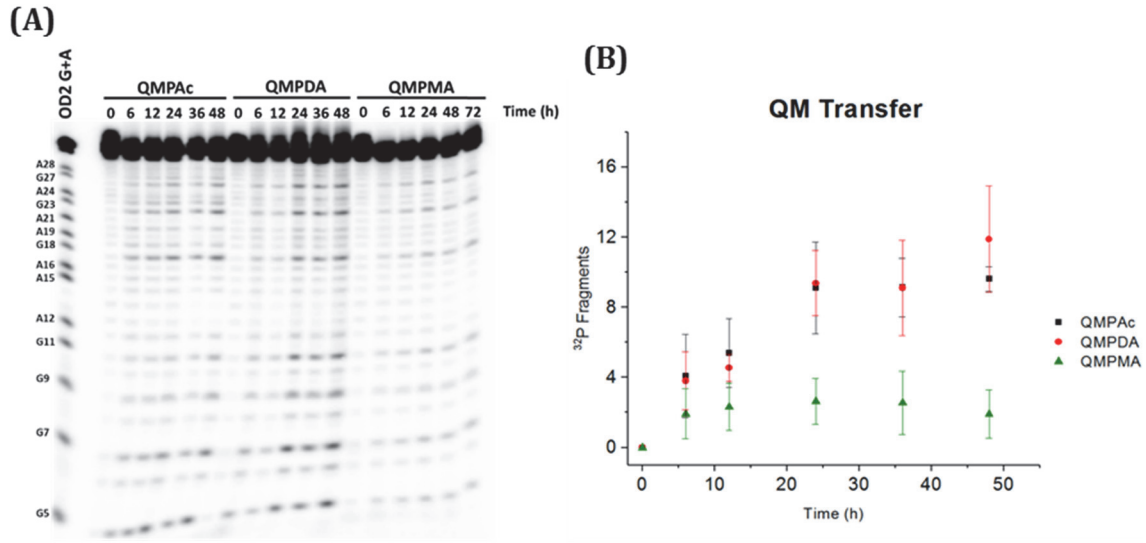

Figure 3.8: Reversible transfer of QMs between complementary strands. (A) Time-dependent alkylation of acceptor strand, **5'-[^{32}P]-OD2** (3.3 μM), following transfer of regenerated QM from donor strand **OD1** (3.0 μM). Single strand **OD1** (3.0 μM) was incubated with either **QMPAc** (240 μM), **QMPDA** (240 μM), or **QMPMA** (960 μM), in the presence of NaF (10 mM) and MES buffer (10 mM, pH 7.0) for 24 h, followed by the addition of **5'-[^{32}P]-OD2** for 0 - 48 h**.** Subsequently, samples were treated with 10 % hot piperidine. (B) Rate of QM transfer from donor to acceptor strands plotted as total percentage **5'-[^{32}P]-OD2** fragments **QMPAc**, **QMPDA** and **QMPMA** treated samples. Reaction yield is an average of independent three trials, determined by subtracting fragment intensity from t = 0. Error is an average of the standard deviation.

3.2.4: QMPAc migrates along a nicked duplex via formation of reversible adducts

Although both **QMPAc** and **QMPDA** seem to transfer from one complementary strand to another at similar rates, migration of the QM electrophile from the 3'- to 5'-end of a helix may be influenced by the freedom of movement of the ammonium vs acridine ligand. To test the ability of **QMPAc** and **QMPDA** to migrate from the 3'-

end to the 5'-end of a helix (Scheme 3.5), each QM was first incubated with a donor strand for 24 h. Subsequently, a complementary mediator strand composed of a toehold region was added for an additional 24 h. Finally, an acceptor strand that anneals to the toehold region was added to the reaction mixture. Regenerated QM electrophiles should first alkylate the donor strand (**OD5**), then the mediator strand (**OD6**), and finally the radiolabeled acceptor strand (**OD7**). Gel image shows an increase in dG-N7 fragments as a function of time for **QMPAc** treated samples, while no distinct changes are detected in **QMPDA-**treated samples over time (Figure 3.9A). Quantitation of **5'-[^{32}P]-OD7** DNA band intensities showed that transfer of **QMPAc** to the acceptor strand reached a maximum of 11% total DNA fragments at the end of a 6-day incubation period (Figure 3.9B). In contrast, the maximum yield of DNA fragments for transferred **QMPDA** was below 3%. These results indicate that **QMPAc** was capable of migrating along a nicked duplex via alkylation and regeneration of DNA adducts. Unlike a previously studied electron-rich bifunctional QM-acridine (bis-QMPAc) conjugate in which alkylation at the nick was thermodynamically favored,[47] monofuntional **QMPAc** shows little preference for the nick region at G20 of **OD7**, as DNA adducts are detected at both the 3'-end and 5'-end of the acceptor strand. The differences in reactivity observed between the mono- and bifunctional-acridine conjugates may be explained through potential disparities in the reversibility of alkylation by these agents. The mono-QM can undergo simple catch and release, allowing it to be released from the DNA and readily bypass nick regions whereas release of the bis-QM is dependent on the regeneration of both electrophilic carbons. If only one of the electrophiles are

released, the compound is still effectively tethered to the DNA until the second electrophile is released. For the diammonium conjugated **QMPDA**, yields of transferred adducts at dG-N7 were too low to determine if the electrophile had migrated via reversible alkylation. Reasons for this observation will be explored further in the following chapter.

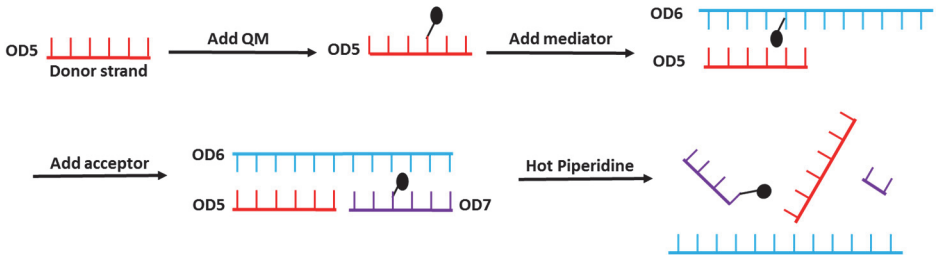

OD6: 5'-TTA TGC GCG CGA TTA ACG ACA T GAC TGA CCT GTG TGA GCC ATA C-3'

OD5/7: 3'-AAT ACG CGC GCT AAT TGC TGT A CTG ACT GGA CAC ACT CGG TAT G-5'

Scheme 3.5: Migration of mono-QM along duplex DNA

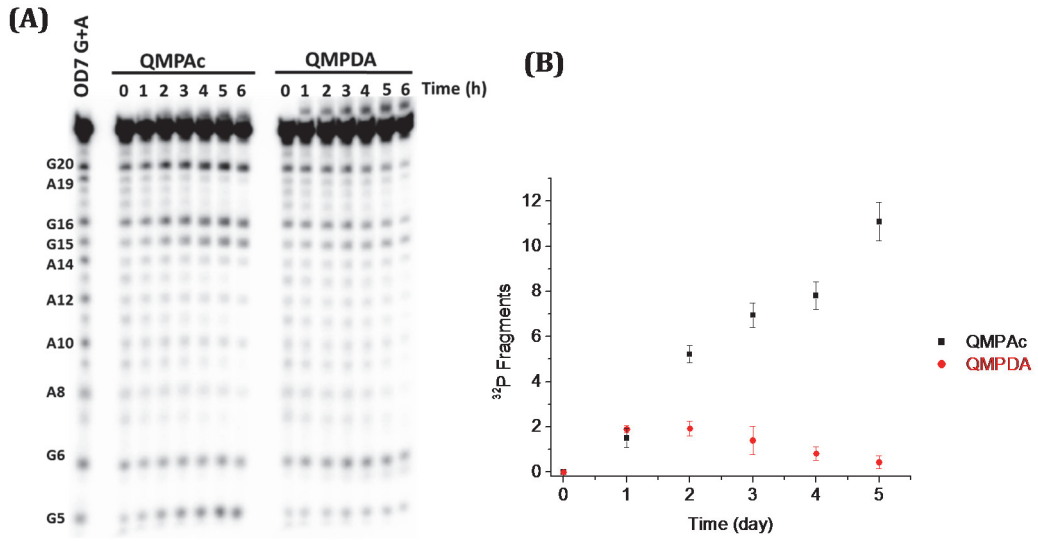

Figure 3.9: Migration of **QMPAc** and **QMPDA** along a nicked duplex. (A) Single strand **OD5** (3.0 μM) was incubated with either **QMPAc** (240 μM), or **QMPDA** (240 μM), NaF (10 mM), MES (10 mM, pH 7.0) for 24 h before addition of **OD6** (3.0 μM) and incubating for 24 h. Then **5'-[^{32}P]-OD7** was added to each samples. DNA was then treated with hot piperidine. (B) Yield of total percentage of **[^{32}P]-OD7** fragments for migration of **QMPAc** and **QMPDA.** Reaction yield is an average of independent three trials, determined by subtracting fragment intensity from t = 0. Error is an average of the standard deviation.

3.2.5: QMPAc migrates past bulge on duplex via formation of reversible adducts

To examine the ability of **QMPAc** to migrate past other complex DNA secondary structures, diffusion of the electrophile past an extrahelical thymine-thymine (TT) bulge was assessed. Since **QMPAc** possessed the lability to migrate past nicks, it may also possess the ability to migrate from the 3'-end to the 5'-end of a duplex, past a TT-bulged. Migration was initiated by incubating **QMPAc** with the same initial donor strand (**OD5**) for 24 h, followed by the addition of a mediator strand (**OD6**), which contains a toehold, and incubation for another 24 h period. Finally, an acceptor strand (**OD8**) was added to the reaction and incubated for 0-6 days. Hybridization of the acceptor strand to the toehold of the mediator strand thermodynamically drives the displacement of the donor strand (Scheme 3.6). Gel image shows an increase in DNA fragments as a function of time for alkylation of the acceptor strand, **5'-[^{32}P]-OD8** by **QMPAc** (Figure 3.10A). Analysis of the gel image showed that **OD8** is fragmented at both the 3'- and 5'-ends of the acceptor strands. This suggests that regenerated **QMPAc** was transferred from the donor strand onto the 5'-end on mediator strand, and from the 5'-end of the mediator strand to the 3'-end of the acceptor strand. Reversible alkylation of both the mediator and acceptor strands enabled **QMPAc** to migrate from the 3'-end to 5'-end of the acceptor strand, past a TT-bulge on **OD8**. Quantitation of DNA fragment intensities showed that total yield of transferred **QMPAc** reach of maximum of 20% at the 6-day incubation period (Figure 3.10B).

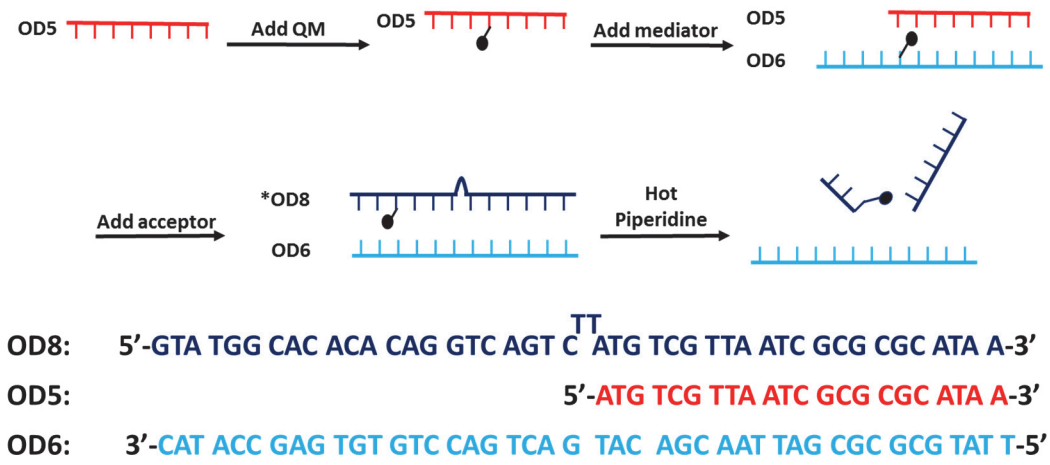

Scheme 3.6: Migration of **QMPAc** past TT-bulges

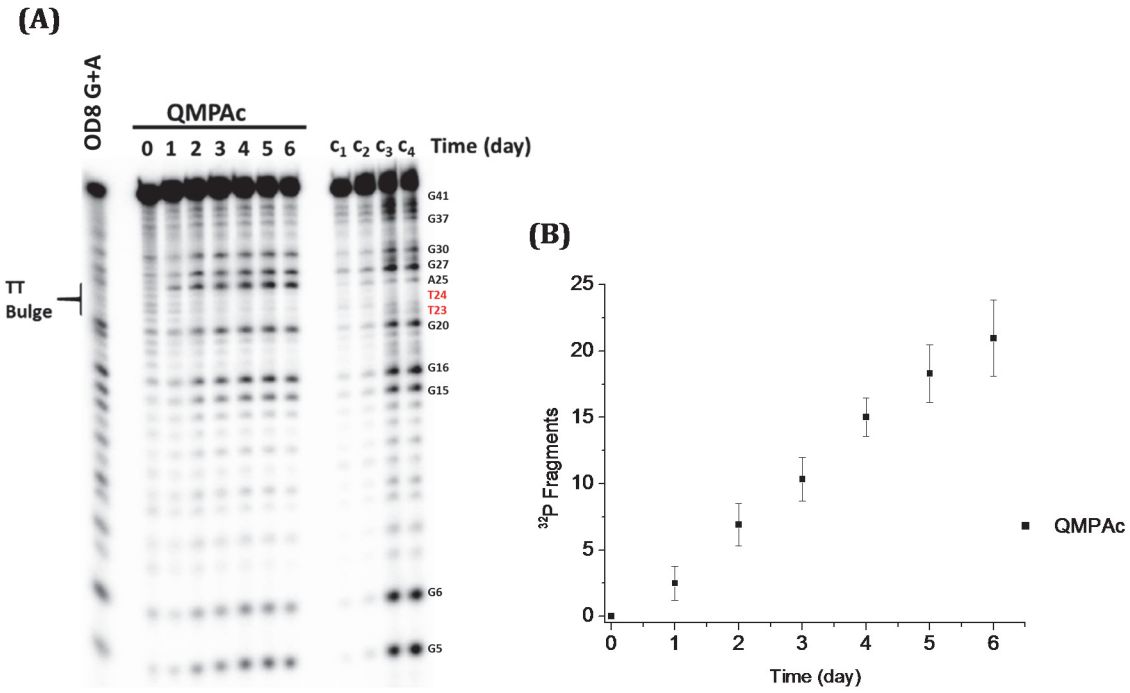

Figure 3.10: Migration of **QMPAc** along a bulge duplex. (A) Single strand **OD5** (3.0 μM) was incubated with alkylating agent (240 μM), NaF (10 mM), MES (10 mM, pH 7.0) for 24 h before addition of **OD6** (3.0 μM) and incubating for 24 h. Then **5'-[^{32}P]-OD8** (3.3 μM) was added to each samples and incubated for 0 – 6 days. DNA was then treated with hot piperidine. Lanes c_1 and c_2 represent quenching of **QMPAc** (240 μM) in MES (10 mM, pH 7.0) and NaF (10 mM) for 48 h, followed by the addition of **5'-[^{32}P]-OD8** and **5'-[^{32}P]-OD8:OD6** for 6 days**,** respectively**.** Lanes c_3 and c_4 represent incubation of **QMPAc** (240 μM) in MES (10 mM, pH 7.0) and NaF (10 mM) with **5'-[^{32}P]-OD8** and **5'-[^{32}P]-OD8:OD6** for 6 days**,** respectively. (B) Yield of **5'-[^{32}P]-OD8** fragments for migration of **QMPAc** along a bulge duplex**.** Reaction yield is an average of independent three trials, determined by subtrating fragment intensity from t = 0. Error is an average of the standard deviation.

Although studies have shown that acridines preferentially localize at bulges,[69] and the bis-QM-acridine conjugate was unable to migrate past a TT-bulge[47] to reach its thermodynamically favored site of reaction, this experiment demonstrated that **QMPAc** possesses the labilityy to migrate past a TT-bulge via reversible DNA alkylation without distinct accumulation of adducts. Such lability may provide **QMPAc** with improved biological activity as navigates through different secondary structures of dsDNA to reach sites of favorable reaction.

3.3: Conclusion

In this study, quaternary ammonium ligands were utilized to deliver mono-QMs to the backbone of DNA. It was anticipated that these ligands would allow the electrophile to freely traverse the phosphodiester backbone without being trapped at nicks or bulges. However, studies have now shown that while the ammonium conjugate, **QMPDA,** is capable of alkylating complementary strand reversibly, migration along duplex DNA was not detected. In contrast, the acridine conjugate, **QMPAc,** alkylated complementary strands reversibly and possessed the kinetic lability to can migrate past nicks and bulges on a duplex without a strong preference for reaction at these sites. In the future, the ability of **QMPAc** to migrate along other complex DNA and RNA secondary structure may be tested. This could open new possibilities for applications of mono-QMs as ribozyme or DNAzyme inhibitors.

3.4: Materials and Methods

4-(2-Bromoethyl)-2-(hydroxymethyl)phenol (12)[52]

4-(2-Bromoethyl)phenol (6.00 g, 29.8 mmol) was added to a solution of phenylboronic acid (3.80 g, 31.2 mmol), trichloroacetic acid (2.10 g, 10.6 mmol), and paraformaldehyde (3.2 g, 1.00 mmol) in benzene (30 mL). The mixture was heated to reflux for 4 h, cooled to room temperature, and solvent was removed under reduced pressure. A solid residue was collected, dissolved in ether (100 mL), washed with water (100 mL), and saturated aqueous sodium bicarbonate (3 X 100 mL). The organic layers were dried over $MgSO_4$ and solvent was evaporated under reduced pressure. A white solid residue was collected and dissolved in THF (10 mL). Hydrogen peroxide (30%, 5 mL) was added, and the solution was stirred at 0^oC for 2 h. The reaction was then diluted with water (50 mL), and extracted with ether (3 X 50 mL). The organic layers were combined, dried over $MgSO_4$, and concentrated under reduced pressure. The resulting brown oil was purified via silica gel column chromatography (5:1 hexanes in ethyl acetate), which yielded **12**, the desired beige solid (4.36 g, 63.4%). ^1H NMR (400 MHz, CD_3OD) δ ppm 3.04 (t, *J*=7.6 Hz, 2 H), 3.54 (t, *J*=7.6 Hz, 2 H), 4.63 (s, 2 H), 6.71 (d, *J*=8.0 Hz, 3 H), 6.74 - 6.81 (m, 1 H), 6.97 (dd, *J*=8.2, 2.2 Hz, 4 H)

(4-(2-Bromoethyl)-2-(((*tert*-butyldimethylsilyl)oxy)methyl)phenoxy)(*tert*-butyl)dimethylsilane (13)[37]

tert-Butyldimethylsilyl chloride (TBDMSCl, 13.5 g, 21.9 mmol) and imidazole (12.5 g, 43.8 mmol) was added to a solution of **12** (4.36 g, 18.9 mmol) in DMF (6 mL). The reaction was stirred under nitrogen for 15 h, diluted with brine (50 mL), and extracted with ether (3 X 50 mL). The organic layers were combined, washed with saturated aqueous sodium bicarbonate (2 X 50 mL), dried over $MgSO_4$, and solvent was removed under reduced pressure to yield **13** as a colorless oil product (7.60 g, 87%). ^{1}H NMR (300 MHz, $CDCl_3$) δ ppm 0.09 (m, 6 H), 0.23 (m, 6 H), 0.94 - 1.03 (m, 18 H), 2.95-3.15 (m, 2 H), 3.45 - 3.74 (m, 2 H), 4.74 (s, 2 H), 6.68 (d, *J*=8.1 Hz, 1 H), 6.90 - 6.98 (m, 1 H), 7.29 (s, 2 H)

***N*^{1}-(4-((*tert*-Butyldimethylsilyl)oxy)-3-(((*tert*-butyldimethylsilyl)oxy)methyl)phenethyl)-N^1,N^2,N^2-trimethylethane-1,2-diamine (17)**

N, N, N'-Trimethylethylenediamine (1.00 mL, 7.69 mmol) was added to a solution of **13** (3.00 g, 6.55 mmol) in acetonitrile (10 mL) and heated to 75 ^{o}C for 16 h. The reaction was diluted with saturated aqueous sodium bicarbonate (50 mL) and extracted with chloroform (3 X 50 mL). The organic layers were combined and dried over Na_2SO_4. The solvent was evaporated under reduced pressure to yield a crude orange oil. The residue was collected and subjected to silica gel column chromatography (2:1 hexane: ethylacetate) to yield **17** as a light orange oil (700 mg, 22%). ^{1}H NMR (400 MHz, CD_3OD) δ ppm 0.10 (s, 6 H), 0.23 (s, 6 H), 0.96 (s, 9 H),

0.99 (m, 9 H), 2.28 (s, 6 H), 2.34 (s, 3 H), 2.47 - 2.55 (m, 2 H), 2.57 - 2.69 (m, 4 H), 2.69 - 2.79 (m, 2 H), 4.72 (s, 2 H), 6.72 (d, *J*=8.2 Hz, 1 H), 6.98 (dd, *J*=8.1, 2.1 Hz, 1 H), 7.26 (s, 1 H). ^{13}C NMR (100 MHz, $CDCl_3$) δ -4.91, -3.91, 19.27, 19.48, 26.42, 26.66, 33.77, 42.83, 45.90, 55.85, 57.66, 61.24, 61.91, 119.43, 128.93, 129.06, 133.08, 133.99, 151.87. HRMS (FAB, mNBA) m/z 481.3638. Calc'd for $C_{26}H_{53}N_2O_2Si_2$ (M + H^+) 481.3646.

(2-((*tert*-Butyldimethylsilyl)oxy)-5-(2-((2-(dimethylamino)ethyl)(methyl)amino)ethyl)phenyl)methanol (18)

p-Toluenesulfonic acid (pTsOH, 260 mg, 1.51 mmol) was added to a solution of **17** (700 mg, 1.46 mmol) in methanol (5 mL). The reaction was stirred at room temperature for 1 h, diluted with ethyl acetate (50 mL), and washed with saturated aqueous sodium bicarbonate (2 X 50 mL). The organic layer was dried over $MgSO_4$, and concentrated under reduced pressure. The residue was collected, dissolved in methanol (50 mL), and washed with hexane (3 X 50 mL). The methanol layer was collected and evaporated under reduced pressure to yield **18** as a clear oil (520 mg, 97%). ^{1}H NMR (400 MHz, CD_3OD) δ ppm 0.23 (s, 6 H), 0.99 (s, 9 H), 2.31 (s, 6 H), 2.32 (s, 9 H), 2.56 (d, *J*=3.3 Hz, 2 H), 2.59 - 2.69 (m, 4 H), 2.70 - 2.78 (m, 2 H), 4.61 (s, 2 H), 6.73 (d, *J*=8.2 Hz, 1 H), 6.99 (dd, *J*=8.2, 2.2 Hz, 1 H), 7.27 (s, 1 H). ^{13}C NMR (100 MHz, CD_3OD) δ -2.86, 20.32, 27.50, 34.63, 43.71, 46.77, 56.58, 58.47, 61.62, 62.17, 120.73, 130.29, 130.55, 130.99, 134.2, 153.46. HRMS (FAB, mNBA) m/z 367.2790. Calc'd for $C_{20}H_{38}N_2O_2Si$ (M + H^+) 367.2781.

2-((*tert*-Butyldimethylsilyl)oxy)-5-(2-((2-(dimethylamino)ethyl)(methyl)amino)ethyl)benzyl acetate (19)

Compound **18** (200 mg, 0.55 mmol) was added to a solution of excess trimethylamine (2 mL) in chloroform (10 mL). The mixture was cooled to 0 ^{o}C, and acetyl chloride (40 μL, 0.56 mmol) was added directly into the solution. The reaction was stirred for 18h, diluted with chloroform (25 mL) and washed with saturated aqueous sodium bicarbonate (50 mL). The organic layer was collected, dried over Na_2SO_4, filtered, and concentrated under reduced pressure to yield **19** as a brown oil (120 mg, 54%). ^{1}H NMR (300 MHz, $CDCl_3$) δ ppm 0.24 (s, 6 H), 0.95 (s, 9 H), 2.06 (s, 3 H), 2.27 (s, 6 H), 2.34 (s, 3 H), 2.37 - 2.76 (m, 8 H), 5.08 (s, 2 H), 6.74 (d, *J*=8.3 Hz, 1 H), 7.03 (dd, *J*=8.3, 2.3 Hz, 1 H), 7.12 (s, 1 H). ^{13}C NMR (100 MHz, CD_3OD) δ -3.94, 10.11, 19.20, 21.10, 26.35, 33.32, 37.78, 42.58, 45.59, 55.38, 57.29, 63.46, 79.60, 119.91, 127.70, 130.95, 131.97, 134.03, 153.75, 172. 65. HRMS (FAB, mNBA) m/z 409.2878. Calc'd for $C_{22}H_{41}N_2O_3Si$ ($M + H^+$) 409.2886.

***N*^{1}-(3-(Acetoxymethyl)-4-((*tert*-butyldimethylsilyl)oxy)phenethyl)-*N*^{1},*N*^{1},*N*^{2},*N*^{2},*N*^{2}-pentamethylethane-1,2-diaminium chloride (QMPDA)**

To a solution of compound **19** (200 mg, 0.29 mmol) in methanol (10 mL), excess methyl iodide (1 mL) was added and stirred at 30 ^{o}C for 2 h. The solvent was removed under reduced pressure, and the collected residue was recrystallized in ether to yield a beige solid. The crude product was dissolved in water (5 mL). Chloride-form anion exchange resin (1 g) was added to the solution, and stirred for 1 h. The resin was filtered off, and the aqueous solution was lyophilized to yield

QMPDA as a white solid (83 mg, 55%). ^{1}H NMR (400 MHz, D_2O) d ppm 0.13 (s, 6 H), 0.87 (s, 9 H), 2.02 (s, 3 H), 3.06 (t, *J*=8.8 Hz, 2 H), 3.15 (s, 9 H), 3.19 (s, 6 H), 3.55 (t, *J*=8.2 Hz, 2 H), 3.84 - 3.95 (m, 3 H), 5.05 (s, 2 H), 6.93 (d, *J*=8.4 Hz, 1 H), 7.19 (d, *J*=8.6 Hz, 1 H), 7.24 (s, 1 H). ^{13}C NMR (100 MHz, CD_3OD) δ -3.82, 8.28, 19.00, 21.61, 26.34, 29.01, 37.78, 55.14, 59.03, 64.08, 68.01, 120.90, 127.79, 129.16, 132.12, 132.95, 154.82, 174.72. FAB-MS (mNBA) m/z 455.2 for $(M + OH^-)^+$. Expected m/z 219.1633 for $C_{24}H_{46}I_2N_2O_3Si$, $(M - 2I^-)^{2+}$.

2-(4-((*tert*-Butyldimethylsilyl)oxy)-3-(((*tert*-butyldimethylsilyl)oxy)methyl)phenyl)-*N,N*-dimethylethan-1-amine (14)

Substitution of the bromine for an amine was carried out using the same procedure as that described above for **17**. Using dimethylamine in 2M THF (2.73 mL, 5.46 mmol) and **13** (500 mg, 1.09 mmol) yielded an orange oil. The residue was subjected to silica gel column chromatography (2:1, hexanes:ethyl acetate) to yield **14** as a light orange oil (670 mg, 100%). ^{1}H NMR (400 MHz, $CDCl_3$) δ ppm 0.09 (s, 6 H), 0.21 (s, 6 H), 0.95 - 1.03 (m, 18 H), 2.30 (s, 3 H), 2.47 - 2.77 (m, 2 H), 3.51 - 3.78 (m, 2 H), 4.74 (s, 2 H), 6.67 (dd, *J*=11.2, 8.1 Hz, 1 H), 6.94 (d, *J*=7.8 Hz, 1 H), 7.29 (br. s, 1 H) ^{13}C NMR (100 MHz, $CDCl_3$) δ -5.57, -4.91, -3.91, 17.94, 18.22, 25.48, 25.74, 33.56, 45.20, 60.30, 61.61, 117.39, 126.94, 131.62, 132.50, 149.86. HRMS (FAB, mNBA) m/z 422.2906. Calc'd for $C_{23}H_{44}NO_2Si_2$ (M - H) 422.2911.

(2-((*tert*-Butyldimethylsilyl)oxy)-5-(2-(dimethylamino)ethyl)phenyl)methanol (15)

Synthesis of **15** was carried out using the same procedure as that described above for **18**. Selective cleavage of TBDMS from **14** (500 mg, 1.58 mmol) using pTsOH (280 mg, 1.62 mmol) yielded **15** (280 mg, 57%) as a clear oil. ^{1}H NMR (400 MHz, $CDCl_3$) δ ppm 0.22 (s, 6 H), 0.97 (s, 9 H), 2.32 (s, 6 H), 2.52 - 2.60 (m, 2 H), 2.69 - 2.79 (m, 2 H), 4.66 (s, 2 H), 6.73 (d, *J*=8.2 Hz, 3 H), 6.99 (dd, *J*=8.1, 2.1 Hz, 3 H), 7.18 (s, 3 H) ^{13}C NMR (100 MHz, $CDCl_3$) δ -3.99, 18.37, 25.94, 33.43, 45.47, 61.77, 118.46, 128.62, 128.98, 131.74, 132.87, 151.78. HRMS (FAB, mNBA) m/z 310.2208. Calc'd for $C_{17}H_{32}NO_2Si$ ($M + H^+$) 310.2202.

2-((*tert*-Butyldimethylsilyl)oxy)-5-(2-(dimethylamino)ethyl)benzyl acetate (16)

Addition of the acetate group to **15** (280 mg, 0.905 mmol) also followed the same procedure as that describe above for **19**. Completion of the reaction yielded **16** (260 mg, 82%) as a light brown oil. ^{1}H NMR (400 MHz, $CDCl_3$) δ ppm 0.23 (s, 6 H), 0.99 (s, 9 H), 2.08 (s, 3 H), 2.37 (s, 6 H), 2.55 - 2.68 (m, 2 H), 2.71 - 2.84 (m, 2 H), 5.06 (s, 2 H), 6.73 (d, *J*=7.8 Hz, 1 H), 7.04 (d, *J*=5.9 Hz, 1 H), 7.13 (br. s., 1 H). ^{13}C NMR (100 MHz, $CDCl_3$) δ -4.29, 9.04, 18.15, 21.00, 25.60, 32.83, 44.95 45.84, 61.15, 62.23, 118.51, 126.25, 129.54, 130.50, 132.06, 152.39, 170.91. HRMS (FAB, mNBA) m/z 352.2301. Calc'd for $C_{19}H_{34}NO_3Si$ ($M + H^+$) 352.2308.

2-(3-(Acetoxymethyl)-4-((*tert*-butyldimethylsilyl)oxy)phenyl)-*N,N,N*-trimethylethan-1-aminium iodide (QMPMA)

Synthesis of **QMPMA** was carried out using **16** (210 mg, 0.60 mmol), following procedures as that described above for the methylation reaction of **QMPDA**. Using excess methyl iodide (1 mL) with **16** yielded **QMPMA** as a white solid (148 mg, 50%). The product was not subjected to anion exchange. ^{1}H NMR (400 MHz, CD_3OD) δ ppm 0.27 (s, 6 H), 1.01 (s, 9 H), 2.06 (s, 3 H), 3.06 - 3.14 (m, 2 H), 3.26 (s, 9 H), 3.57 - 3.64 (m, 2 H), 5.07 (s, 2 H), 6.87 (d, *J*=8.2 Hz, 2 H), 7.27 (d, *J*=6.8 Hz, 1 H), 7.36 (s, 2 H). ^{13}C NMR (100 MHz, CD_3OD) δ -2.74, 10.76, 20.46, 22.46, 27.54, 30.84, 55.30. 64.55, 69.80, 121.58, 129.59, 132.79, 133.67, 155.86, 174.03. HRMS (FAB, mNBA) m/z 366.2462. Calc'd for $C_{20}H_{36}NO_3Si$ ($M + H^+$) 366.2465.

Alkylation of ss and dsDNA with QMPAc, QMPDA, and QMPMA

The desired ^{32}P radiolabeled ss or dsDNA (3.0 μM, 50 nCi) was incubated with the indicated concentration of alkylating agent (0 – 960 μM) in presence of NaF (10 mM), MES (10 mM, pH 7), and 20% acetonitrile. Following incubation (0 – 48 h) under ambient temperature, samples were dried with a speedvac, and treated with 10% hot piperidine, at 90°C for 30 min. The resulting samples were dried, resuspended in formamide loading solution, and subjected to 20% denaturing polyacrylamide gel electrophoresis.

Transfer of Alkylating Agent from Donor to Acceptor Strand

The indicated donor ssDNA, **OD1** (3.0 μM), was pre-incubated with **QMPAc** (240 μM)**, QMPDA** (240 μM) or **QMPMA** (960 μM) in the presence of NaF (10 mM), MES (10 mM, pH 7.0) and 20% acetonitrile for 24 h, under ambient temperature. Following pre-incubation, the radiolabeled ^{32}P acceptor strand (**OD2**, 3.0 μM, 50 nCi) was added to the samples and incubated for 0 - 48 h under ambient temperature. DNA was then treated with hot piperidine treatment (90^{o}C, 30 min), dried on the speedvac, resuspended in formamide loading solution, and then subjected to 20% denaturing gel electrophoresis.

Migration of QMs along DNA

The donor ssDNA, **OD5** (3.0 μM), was pre-incubated with **QMPAc** or **QMPDA** (240 μM) in the presence of NaF (10 mM), MES (10 mM, pH 7.0) and 20% acetonitrile for 24 h, under ambient temperature. Following pre-incubation, a mediator strand, **OD6** (3.0 μM), was added to the reaction samples and incubated for 24 h. Finally, the radiolabeled ^{32}P acceptor strand (**OD7** or **OD8,** 3.0 μM, 50 nCi) was added to the samples and incubated for 0 – 6 days under ambient temperature. DNA was then treated with hot piperidine (90^{o}C, 30 min), dried with the speedvac, resuspended in formamide loading solution, and then subjected to 20% denaturing gel electrophoresis.

Chapter 4: Analysis of abasic site generation by mono-QMs

4.1: Introduction

Structural perturbations arising from DNA alkylation can inhibit mRNA synthesis, which can in turn impair protein synthesis, alter gene expression, or trigger apoptosis.[1] Among the numerous lesions that could arise from DNA alkylation, cleavage of the *N*-glycosidic bond is the most abundant. An estimated 10,000 abasic sites are generated in a cell per day due to spontaneous depurination.[70,71] Formation of DNA adducts at endocyclic amines of dG-N7, dA-N7, dG-N3, dA-N3, dA-N1, and dC-N3 destabilizes the nucleobases, and facilitates cleavage of the *N*-glycosidic bond to form an abasic site (Figure 4.1).[72-74]

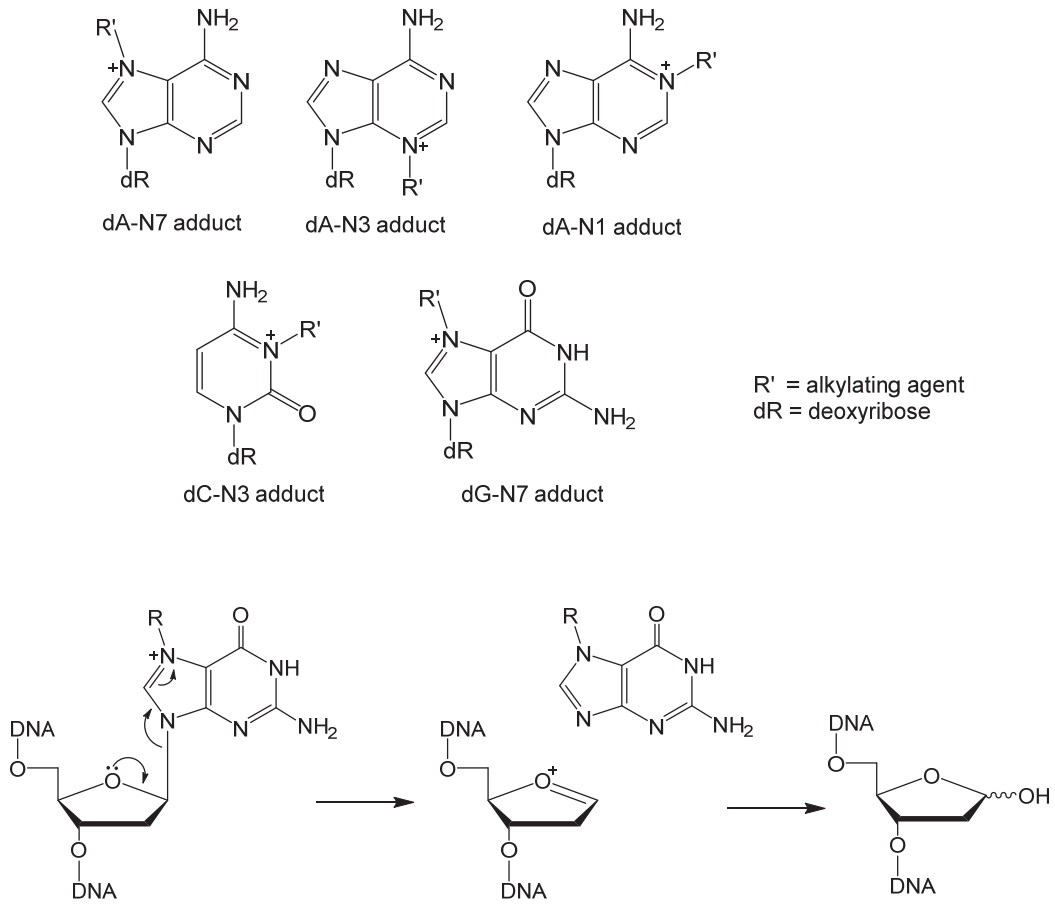

Figure 4.1: DNA adducts that facilitate cleavage of the *N*-glycosidic bond

Loss of a nucleobase is both cytotoxic and mutagenic because it leads to the non-specific incorporation of a hydrogen-bonding base pair during DNA replication, RNA synthesis, and promotes cleavage of the phosphodiester backbone.[75]

Under physiological conditions, spontaneous hydrolysis of the phosphodiester backbone occurs at a half-life of 3×10^7 years.[76] However, in the presence of an abasic site, strand cleavage of the 3'-phosphate ester occurs with a half-life of 200 h under physiological conditions.[77] The lability of the DNA backbone in the presence of apurinic/apyrimidinic (AP) sites is due to an equilibrium mixture of a ring-closed acetal and ring-opened aldehyde form of the deoxyribose. In the aldehyde form, an α-acidic proton is subject to abstraction which gives way to β-elimination of the 3'-phosphate ester to generate a single-strand break (Scheme 4.1).[78]

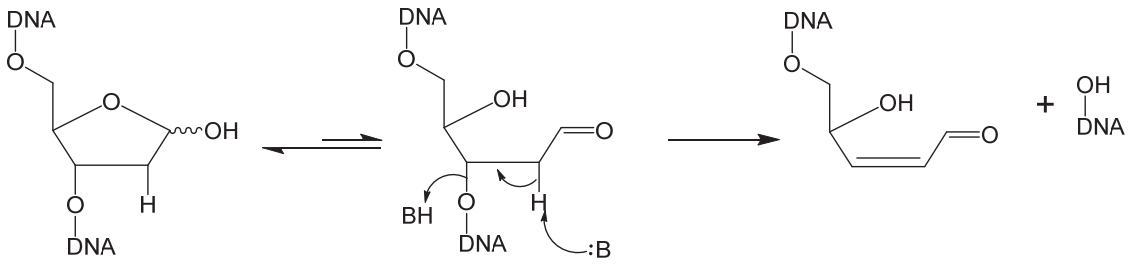

Scheme 4.1: β-elimination of 3' phosphate ester

In addition to an α-acidic proton, the aldehyde tautomer possesses an electrophilic carbon that can undergo reaction with nucleophiles such as the exocyclic N^2-amino group of deoxyguanosine to form an interstrand crosslink (Scheme 4.2).[79] Such lesions are not only mutagenic due to the loss of a gene-

encoding base, but also cytotoxic as interstrand crosslinks lead to collapse of the DNA replication fork. [10,48]

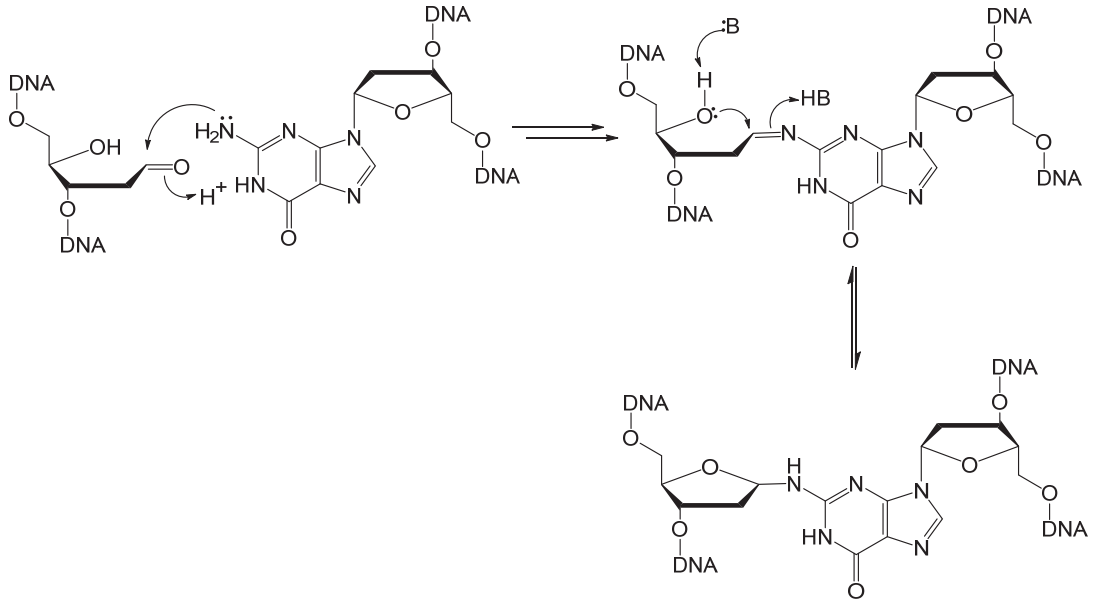

Scheme 4.2: Interstrand DNA crosslink generated via attack of C1' electrophilic carbon

In a previous chapter of this dissertation, a time-dependent alkylation of single- and double-stranded DNA by the ammonium and acridine conjugated mono-QMs showed that reaction yield was maximimum at 24 h without a decrease in fragmentation at extended time periods. This could be due to deglycosylation of dG-N7 adducts rather than DNA alkylation. Generation of G-N7 adducts reduces the overall yield of regenerated QMs that could then react on alternate sites of the duplex as G-N7 adducts are not known to form reversibly. In the preceding chapter, mono-QM acridine conjugate (**QMPAc**) was shown to migrate along duplex DNA via reversible alkylation of dG-N7. However, no evidence of migration was detected with a quaternary ammonium QM conjugate (**QMPDA**). The inability to detect migration with **QMPDA**-treated samples could be due to higher prevalence of

deglycosylated dG-N7 adducts than **QMPAc**. Abasic lesions are known to decrease the thermodynamic stability of duplex DNA structure.[48] This destabilization prevents proper hybridization of complementary strands, and could in turn reduce association of QM ligands to DNA, enhance solvent accessibility and promote quenching of regenerated electrophiles by water adducts. The sum of these factors would limit migration and reversible DNA alkylation by QMs along duplex DNA.

Reactions of QMs with nucleosides formed adducts with the endocyclic amines of dA-N1, dA-N7, dC-N3, dG-N1, and dG-N7.[32] However, deglycosylation of QM adducts has only been observed when reaction occurred at dG-N7. Covalent adducts of QMs at dG-N7 partition between regeneration of the electrophile and cleavage of the *N*-glycosidic bond at comparable rates (Scheme 4.3).[32] A time-dependent profile of a dG-N7-QM adduct has also shown that the deglycosylated product, guanine-N7 (G-N7), did not decompose over time. This suggests that the G-N7 adduct is formed irreversibly as these adducts do not possess the good leaving group ability necessary to regenerate the QM.

This chapter is directed towards determining the fraction of abasic sites generated in comparison to total dG-N7 adducts when ssDNA and dsDNA are alkylated by either **QMPDA**, **QMPAc**, or **eQMPAc** (Figure 4.2). Although deglycosylation prevents proper hybridization of dsDNA and limit migration of regenerated QMs, it is also important to note that generation of abasic sites is an alternate means through which may QMs exhibit cytotoxicity. Within the nucleosome core particles (NCP), histone proteins catalyze strand cleavage at abasic

sites.[80] High prevalence of single- and/or double-strand breaks within the NCP would be advantageous in tumor cells as it may trigger apoptosis.

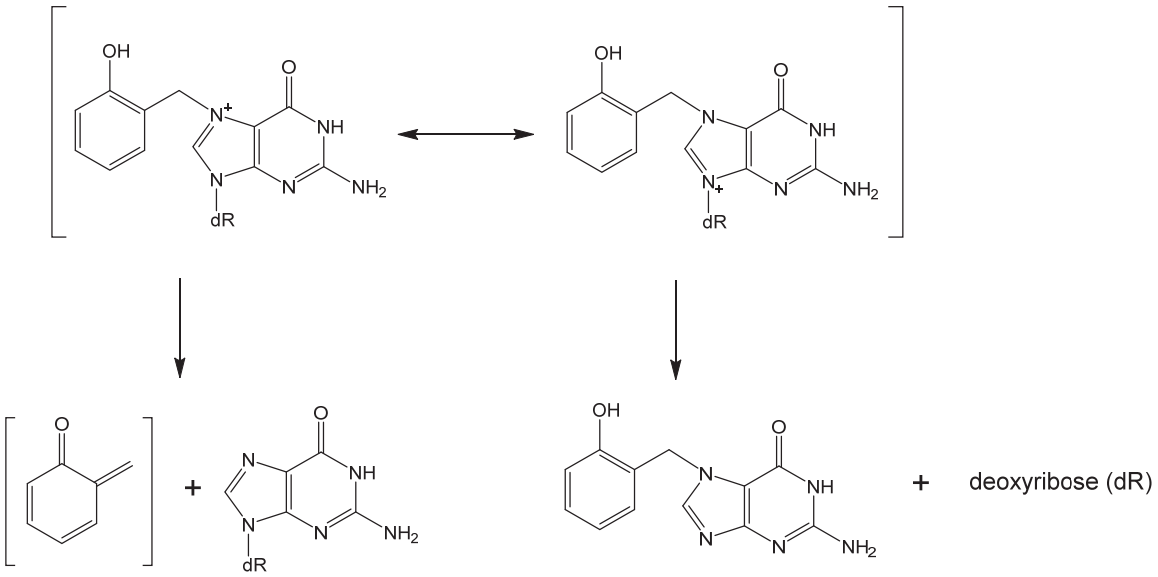

Scheme 4.3: Partitioning of QM dG-N7 adducts

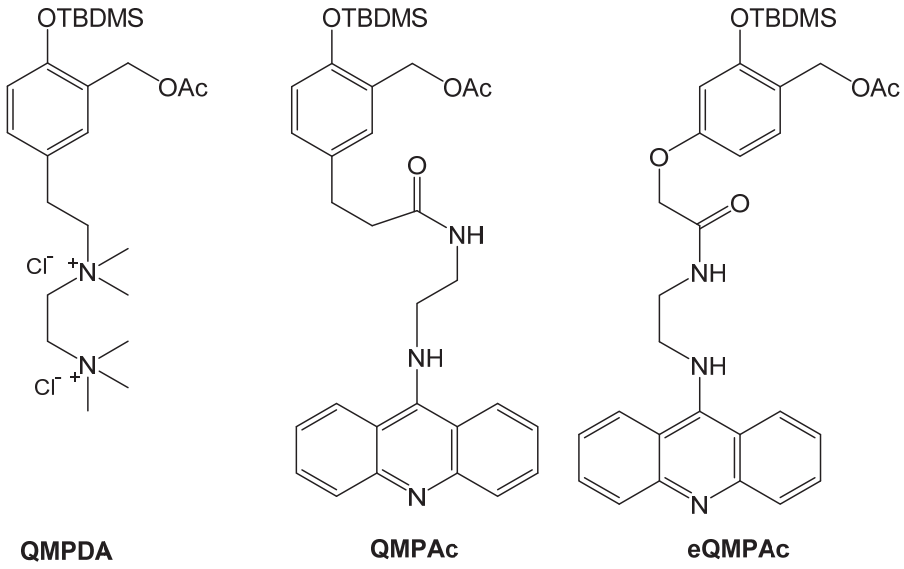

Figure 4.2: Mono-QMs for alkylation of dG-N7 and abasic site generation

4.2: Results and Discussion

Thus far, DNA alkylation by QMs was detected via treatment of DNA samples with hot piperdine. Fragments generated through this means are due to the presence of both dG-N7 and subsequent deglycosylated G-N7 adducts. In order to definitively distinguish between total DNA adducts arising from alkylation of dG-N7 and deglycosylated products, phosphodiester backbone at the 5'-end of an abasic site was cleaved using apurinic/apyrimidinic endonuclease 1 (APE1) (Scheme 4.4).[81] This allowed for direct comparison of the fraction of abasic sites generated in the presence of eith **QMPDA**, **QMPAc** or **eQMPAc**. A DNA sequence containing a single uracil (**dU**) was used as a control for strand cleavage by APE1 upon generation of an abasic site with uracil deglycosylase (UDG). To allow for direct comparison of abasic site formation in both desilylated starting material and regenerated QMs, APE1 induced cleavage experiments were conducted using the same DNA sequences utilized to test reversible DNA alkylation by **eQMPAc**, **QMPAc**, and **QMPDA**.

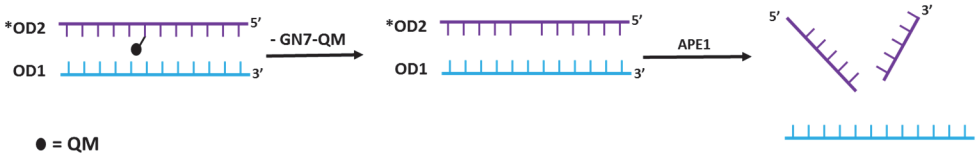

5'-[^{32}P]-OD2: 3'-GTC CAG TCA GTA CAG CAA TTA GCG CGC GTA TT -5

OD1: 5'-CAG GTC AGT CAT GTC GTT AAT CGC GCG CAT AA -3'

Scheme 4.4: Hydrolysis of phosphate esters at abasic sites by APE1

Alkylation of ssDNA incubated with **QMPDA** for 0 – 24 h followed by treatment with either hot piperidine or APE1 resulted in cleavage of ^{32}P labeled strands when adducts were formed at dG-N7 and subsequent deglycosylation to generate G-N7 occurred (Figure 4.3A). Analysis of the denaturing gel electrophoresis image showed that alkylation of ssDNA resulted in hydrolysis of phosphate esters by APE1 to generate fragments primarily at dGs. Treatment with hot piperidine resulted in a maximum yield of 33%, while samples with APE1 produced a yield of 15% (Figure 4.3B).

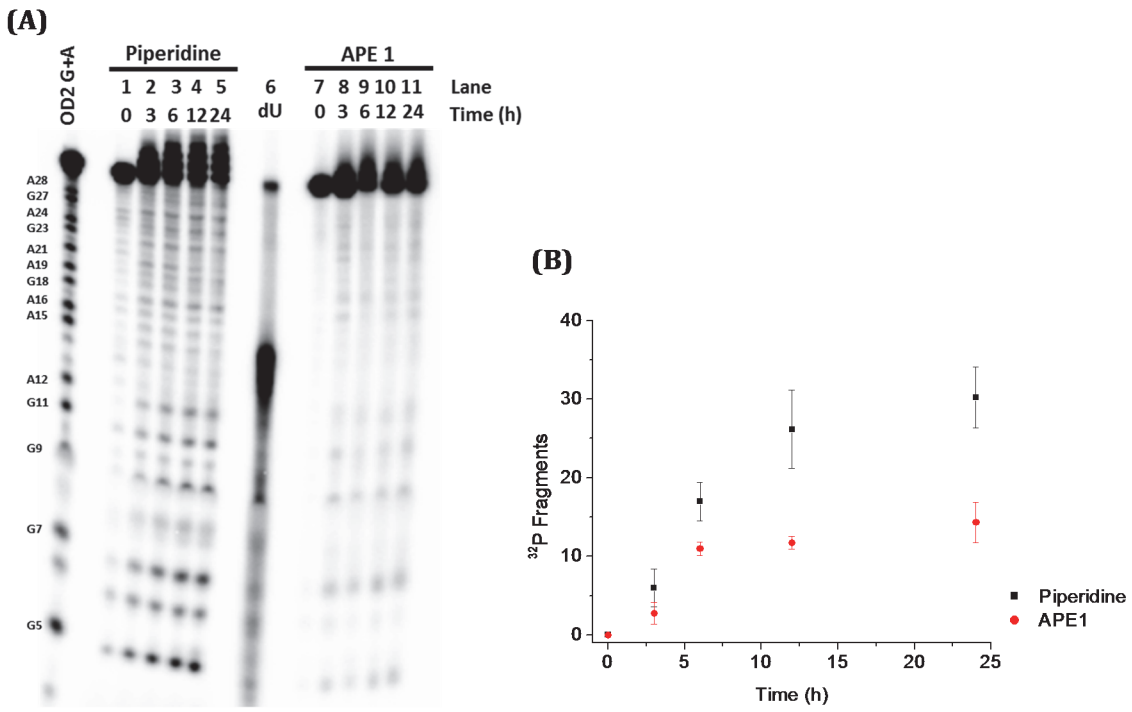

Figure 4.3: Abasic site generation as a result of ssDNA alkylation by **QMPDA.** (A) ssDNA 5'-**[^{32}P]-OD2** (3.0 μM) and QMPDA (240 μM) were incubated for 0 - 24 h, in the presence of NaF (10 mM) and MES buffer (10 mM, pH 7.0) before treating samples with either 10% hot piperidine (lanes 1 - 5) or APE1 (lanes 7 – 11). Lane 6 represents treatment of 5'-**[^{32}P]-dU** with UDG, and then strand cleavage with APE1. (B) Rate of 5'-**[^{32}P]-OD2** alkylation and abasic site generation by **QMPDA** plotted as a percentage of total lane fragments for piperidine and APE1-induced DNA strand cleavage. Reaction yield is an average of independent three trials, determined by subtracting fragment intensity from t = 0. Error is an average of the standard deviation.

Comparison of the fraction of piperidine vs. APE1-induced fragments indicated that approximately 50% of ssDNA adducts at dG-N7 had subsequently resulted in deglycosylation to form an abasic site. This is consistent with reports in which reaction of an unconjugated QM with nucleosides produced a 50:50 ratio of deglycosylated G-N7 products and regenerated electrophile.[32] The similar percentages of abasic site generated in oligonucleotides for a diammnonium-conjugate in comparison to the unconjugated QM suggest that the ligand does not have a significant influence on the deglycosylation of QM adducts.

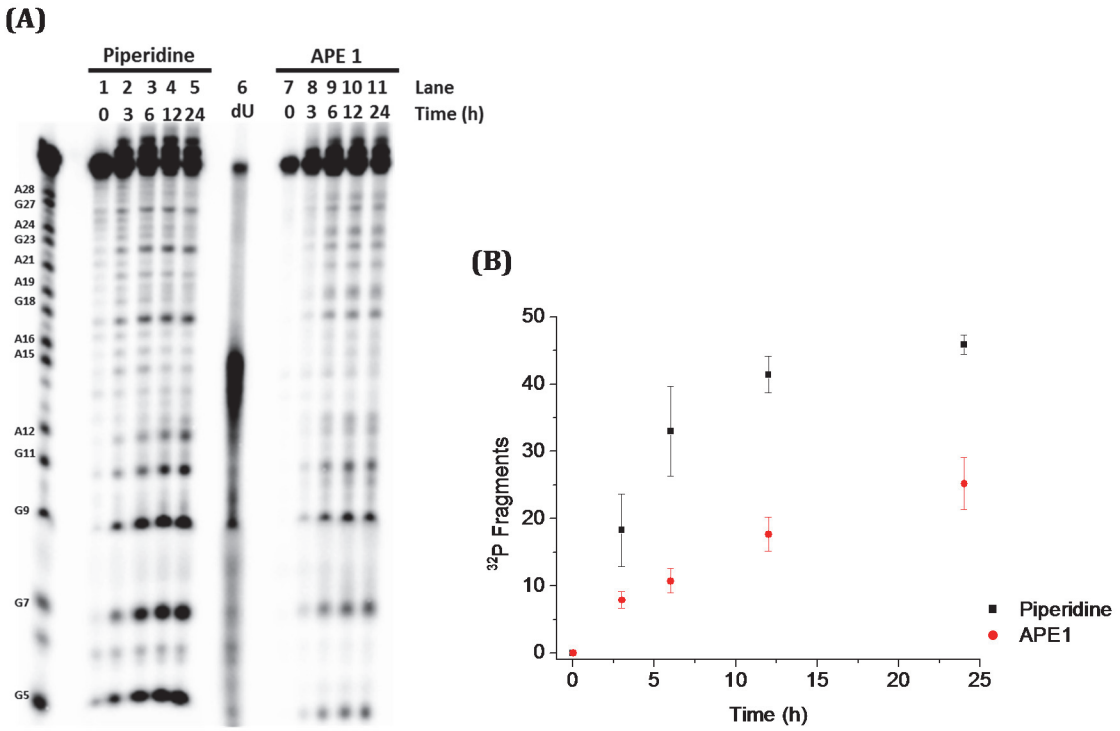

Figure 4.4: Abasic site generation as a result of dsDNA alkylation by **QMPDA.** (A) dsDNA 5'-**[^{32}P]-OD2:OD1** (3.0 μM) and QMPDA (240 μM) were incubated for 0 - 24 h, in the presence of NaF (10 mM) and MES buffer (10 mM, pH 7.0) before treating samples with either 10% hot piperidine (lanes 1 - 5) or APE 1 (lanes 7 – 11). Lane 6 represents treatment of 5'-**[^{32}P]-dU** with UDG, and then strand cleavage with APE1. (B) Rate of 5'-**[^{32}P]-OD2:OD1** alkylation and abasic site generation by **QMPDA** plotted as a percentage of total lane fragments for piperidine- and APE1-induced DNA strand cleavage. Reaction yield is an average of independent three trials, determined by subtracting fragment intensity from t = 0. Error is an average of the standard deviation.

Similarly, incubation of dsDNA with **QMPDA** for 0 – 24 h, followed by treatment with either hot piperidine or APE1, resulted in strand cleavage (Figure 4.4A). Alkylation of dsDNA by **QMPDA** produced fragments primarily at dGs, with minor fragments at dAs. Analysis of the DNA fragments on the gel image as a function of total lane intensity showed that fragments produced from APE1- and piperidine-induced strand cleavage were 25% and 45%, respectively (Figure 4.4B). Based on these results, approximately 55% of dG-N7 adducts deglycosylated to form G-N7. In addition, the percentage of dG-N7 adducts that resulted in deglycosylation of single- versus double-stranded DNA were equivalent for **QMPDA** treated samples. Previous reports indicate that abasic sites are generated at a faster rate in ssDNA than dsDNA.[82] However, a similar percentages of depurinated bases were obtained in ssDNA versus dsDNA in these studies.

To evaluate the contribution of **QMPAc** to the formation of abasic sites, time-dependent alkylation of ssDNA and dsDNA were conducted using the same reaction conditions as above, for **QMPDA**. **QMPAc** was first incubated with ssDNA for 0-24 h. Subsequent treatment of alkylated bases with either hot piperidine or APE1 resulted in strand cleavage with dG-N7 adducts or abasic sites (Figure 4.5A). Reaction of **QMPAc** with ssDNA also resulted in fragments at both dGs and dAs for piperidine- and APE1-treated samples. However, ^{32}P-DNA fragments formed in higher yields when cleavage occurred at dGs than dAs. Analysis of ^{32}P-DNA bands from gel image as a percentage of the total lane intensity showed that piperidine and APE1 strand cleavage produced a maximum yield of 32% and 15% total DNA fragments, respectively (Figure 4.5B). Similar to **QMPDA**, approximately half of the

dG-N7 adducts formed by **QMPAc** resulted in deglycosylation to generate abasic sites.

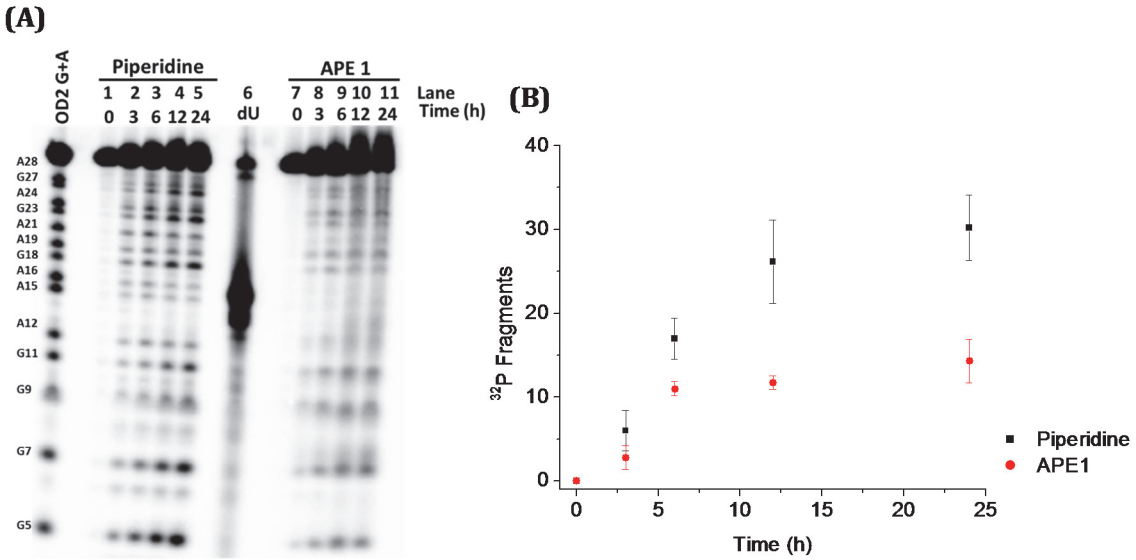

Figure 4.5: Abasic site generation as a result of ssDNA alkylation by **QMPAc.** (A) ssDNA 5'-**[^{32}P]-OD2** (3.0 μM) and QMPDA (240 μM) were incubated for 0 - 24 h, in the presence of NaF (10 mM) and MES buffer (10 mM, pH 7.0) before treating samples with either 10% hot piperidine (lanes 1 - 5) or APE 1 (lanes 7 – 11). Lane 6 represents treatment of 5'-**[^{32}P]-dU** with UDG, and then strand cleavage with APE1. (B) Rate of 5'-**[^{32}P]-OD2** alkylation and abasic site generation by **QMPAc** plotted as a percentage of total lane fragments for piperidine- and APE1-induced DNA strand cleavage. Reaction yield is an average of independent three trials, determined by subtracting fragment intensity from t = 0. Error is an average of the standard deviation.

Similarly incubation of **QMPAc** with dsDNA for 0-24 h produced major DNA fragments at dGs as well as minor fragments at dAs (Figure 4.6A). Analysis of ^{32}P-DNA fragments as a percentage of total lane intensity from gel image indicated that piperidine- and APE1-induced DNA cleavage produced a maximum of 54% and 34% at the end of the 24 h incubation period, respectively (Figure 4.6B). Based on the ratio of APE1 and piperidine generated fragments, this suggests that 63% of dG-N7 fragments were deglycosylated to form abasic sites. This percentage is slightly higher than the yield of abasic sites generated in the presence of **QMPDA** and

conflicts with the initial hypothesis that the inability to detect migration of **QMPDA** along duplex DNA was due to higher prevalence of abasic sites than **QMPAc**. Since abasic site formation is known to destabilize duplex DNA,[48,83] present data suggests that DNA alkylation by **QMPAc** is thermodynamically more destabilizing to duplexes than **QMPDA**. The average decrease in the melting temperature of a 13-mer containing a single apurinic site is 15 ^{o}C.[83] Although, studies have shown that acridines bind to abasic sites and stabilize duplex DNA, cationic charges can also stabilize a duplex.[84,85] Therefore, based on these results, the ability of abasic site generation to impede migration of **QMPDA** over **QMPAc** cannot be determined from these data.

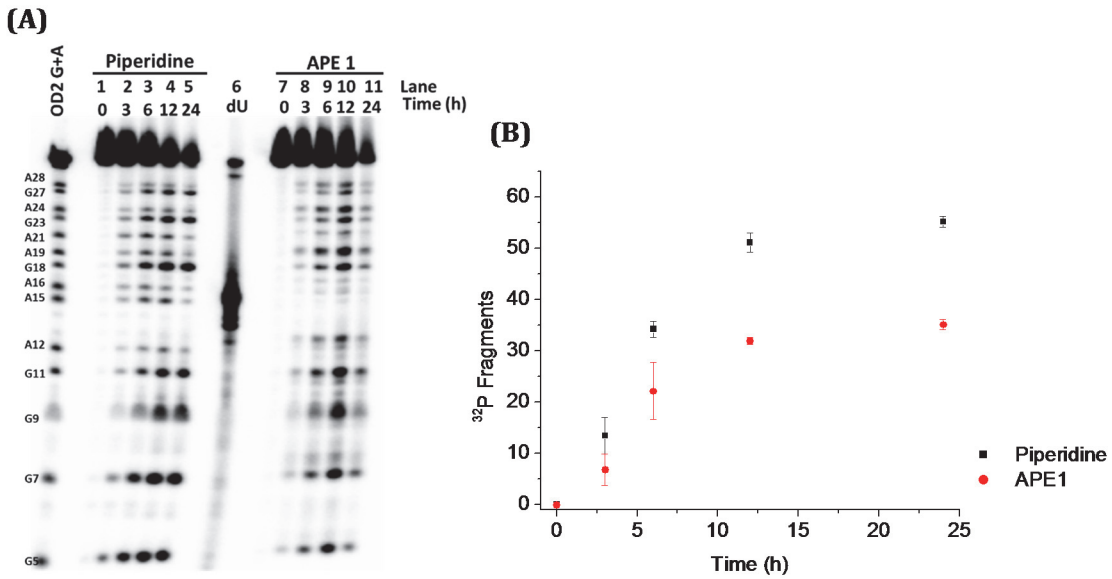

Figure 4.6: Abasic site generation as a result of dsDNA alkylation by **QMPAc.** (A) dsDNA 5'-**[^{32}P]-OD2:OD1** (3.0 μM) and **QMPDA** (240 μM) were incubated for 0 - 24 h, in the presence of NaF (10 mM) and MES buffer (10 mM, pH 7.0) before treating samples with either 10% hot piperidine (lanes 1 - 5) or APE 1 (lanes 7 – 11). Lane 6 represents treatment of 5'-**[^{32}P]-dU** with UDG, and then strand cleavage with APE1. (B) Rate of 5'-**[^{32}P]-OD2:OD1** alkylation and abasic site generation by **QMPAc** plotted as a percentage of total lane fragments for piperidine and APE1 induced DNA strand cleavage. Reaction yield is an average of independent three trials, determined by subtracting fragment intensity from t = 0. Error is an average of the standard deviation.

Since reaction of the methylene-bridged acridine conjugate, **QMPAc,** produced abasic sites, analysis of the consequences of DNA alkylation by an ether-substituted electron-rich QM-acridine conjugate (**eQMPAc**) was also investigated. Both **eQMPAc** and **QMPAc** are conjugated to acridine ligands, but initial alkylation studies showed that **eQMPAc** formed DNA adducts more rapidly than **QMPAc** following elimination of the TBDMS protecting group (Figure 2.5). However, yields of transferred QM adducts at dG-N7 were lower with the electron-rich conjugate (Figure 2.8). This could be due to increased generation of G-N7 adducts in the presence of **eQMPAc** over **QMPAc** that reduced the total availability of regenerated QMs. In order to determine the fraction of dG-N7 adducts that undergo deglycosylation when reacted with an electron-rich QM, DNA was incubated with **eQMPAc** under similar conditions as stated above for that of **QMPAc**, followed by treatment with either hot piperidine or APE1.

Time-dependent alkylation of ssDNA by **eQMPAc** followed by strand cleavage due to either formation of dG-N7 adducts or abasic site generation resulted in DNA fragments at primarily dGs when treated with either hot piperidine or APE1 (Figure 4.7A). Formation of abasic sites resulting in DNA cleavage by APE1 reached completion within 2 h of incubation, as determined from a plot of the yield of total ^{32}P fragments as a function of time (Figure 4.7B). Piperidine- and APE1-induced DNA cleavage produced a total yield of 6% and 4% ^{32}P fragments at the end of the 8 h incubation period, respectively. Comparison of the ratio of APE1 to piperidine induced fragments suggests that 67% of dG-N7 adducts had resulted in the deglycosylated product, G-N7. The percentage of deglycosylated products were

relatively high for reactions of **eQMPAc** with ssDNA in comparison to **QMPAc** and **QMPDA,** which produced approximately a 50:50 mix of regenerated QMs and G-N7 adducts. Such high yields of deglycosylated products could explain why yields of reversible DNA adducts were lower for **eQMPAc** than **QMPAc**.

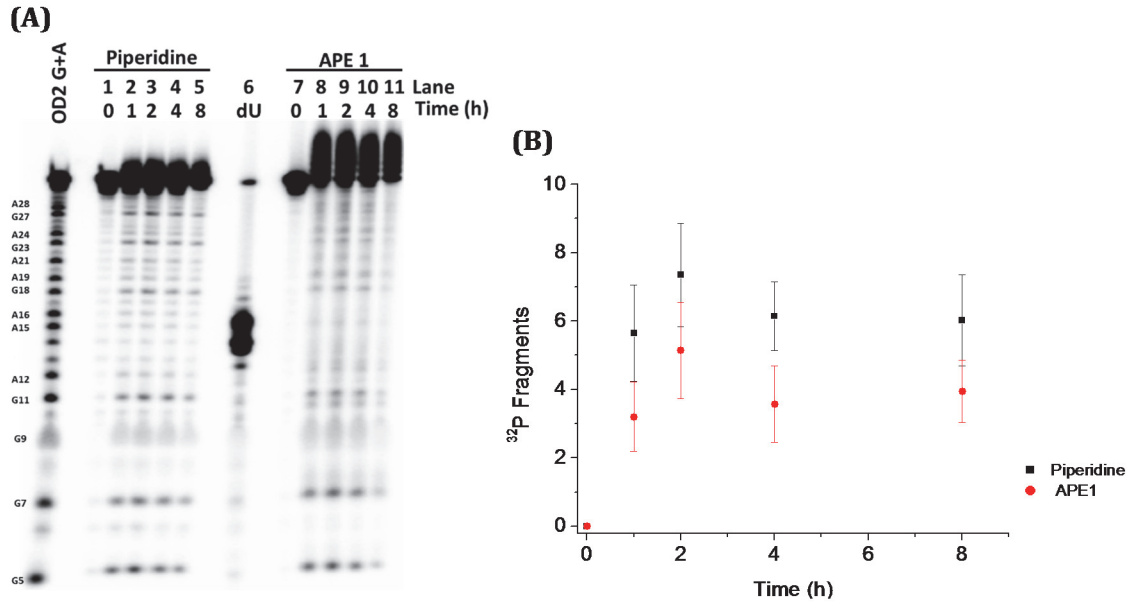

Figure 4.7: Abasic site generation as a result of ssDNA alkylation by **eQMPAc.** (A) ssDNA 5'-**[^{32}P]-OD2** (3.0 μM) and **eQMPAc** (240 μM) were incubated for 0 - 8 h, in the presence of NaF (10 mM) and MES buffer (10 mM, pH 7.0) before treating samples with either 10% hot piperidine (lanes 1 - 5) or APE 1 (lanes 7 – 11). Lane 6 represents treatment of 5'-**[^{32}P]-dU** with UDG, and then strand cleavage with APE1. (B) Rate of 5'-**[^{32}P]-OD2** alkylation and abasic site generation by **eQMPAc** plotted as a percentage of total lane fragments for piperidine- and APE1-induced DNA strand cleavage. Reaction yield is an average of independent three trials, determined by subtracting fragment intensity from t = 0. Error is an average of the standard deviation.

Previous studies of QM transfer between complementary strands via regeneration of the electrophile were conducted by incubating the alkylating agent with a donor ssDNA for 24 h before the subsequent addition of a complementary acceptor strand. If two-thirds of dG-N7 adducts on the donor strand undergo deglycosylation when

alkylated by **eQMPAc**, the concentration of regenerated electrophiles for reversible DNA alkylation is significantly reduced. In addition, high yields of abasic sites may prevent the proper hybridization of the donor and acceptor strands.

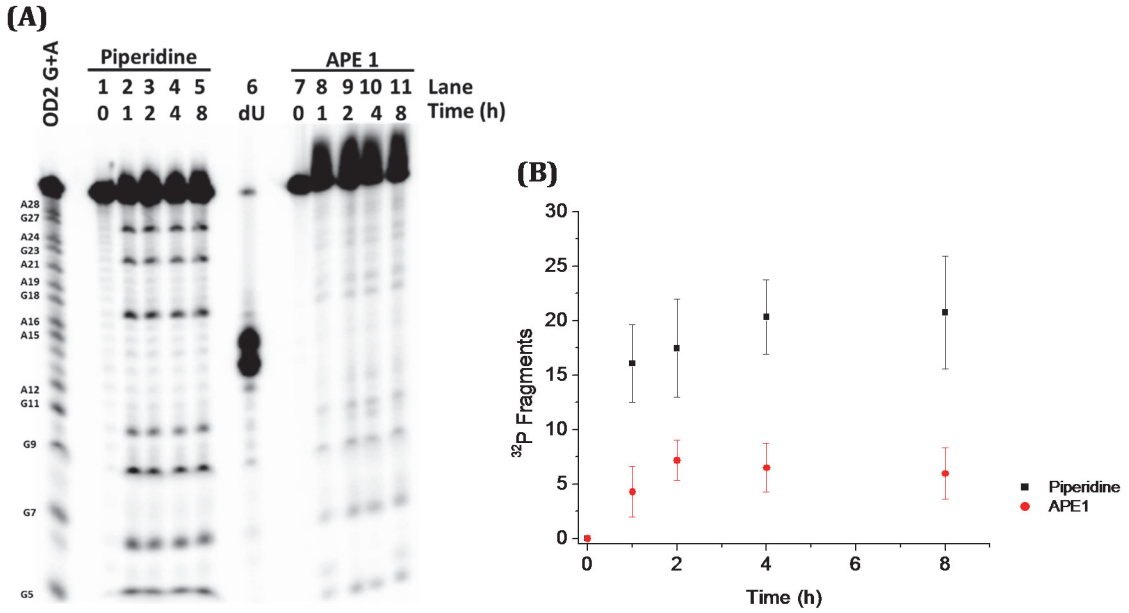

Figure 4.8: Abasic site generation as a result of dsDNA alkylation by **eQMPAc.** (A) dsDNA 5'-**[^{32}P]-OD2:OD1** (3.0 μM) and **eQMPAc** (240 μM) were incubated for 0 - 24 h, in the presence of NaF (10 mM) and MES buffer (10 mM, pH 7.0) before treating samples with either 10% hot piperidine or APE1. (B) Rate of 5'-**[^{32}P]-OD2:OD1** alkylation and abasic site generation by **eQMPAc** plotted as a percentage of total lane fragments for piperidine- and APE1-induced DNA strand cleavage. Reaction yield is an average of independent three trials, determined by subtracting fragment intensity from t = 0. Error is an average of the standard deviation.

Alkylation of dsDNA by **eQMPAc** also produced DNA fragments primarily at dGs following treatment with either hot piperidine or APE1 (Figure 4.8A). Similar to alkylation of ssDNA by **eQMPAc**, generation of abasic sites in dsDNA reach completion within 2 h, as determined from the plot of total ^{32}P fragments as a function of time (Figure 4.8B). Piperidine- and APE1-induced DNA cleavage produced a yield of 22% and 7% ^{32}P fragments at the end of the 8 h incubation

period, respectively. As a result, approximately a third of dG-N7 adducts generated abasic sites via deglycosylation to produce G-N7. Unlike reactions of **eQMPAc** with ssDNA, it appears that abasic sites are generated less frequently in dsDNA. This is consistent with literature reports that have shown evidence of higher yields of abasic site generation in ssDNA than dsDNA. [82]

4.4: Conclusion

Studies in this chapter have established that mono-QMs conjugated to ammonium and acridine ligands alkylate both ssDNA and dsDNA, and subsequently generate abasic sites. Analysis of DNA fragments produced by APE1- and piperidine-induced strand cleavage have now shown that neither **QMPAc** nor **QMPDA** show a strong preference for abasic site generation. Therefore, efforts to determine if a higher prevalence of abasic sites by the acridine or ammonium conjugated QM facilitated or inhibited migration of the intermediate along duplex DNA have provided inconclusive results. Since both **QMPAc** and **QMPDA** produce similar yields of abasic sites, it is difficult to deduce if the destabilization of DNA induced solely by abasic site generation impaired migration of one conjugate over the other.

As anticipated, **eQMPAc** produced low yields of piperidine- and APE1-induced fragments. However, the rate of abasic site generation reached a maximum within 2 h and the percentage of abasic sites generated where significantly higher (~33%) in ssDNA than dsDNA. Such high prevalence of abasic sites in ssDNA may

impair proper hybridization of complementary strands and limit transfer of **eQMPAc** within duplex DNA.

4.5: Materials and Methods

Alkylation of ss and dsDNA with QMPDA, QMPAc and eQMPAc

ssDNA **5'-[^{32}P]-OD2** (3.0 μM, 50 nCi) or dsDNA **5'-[^{32}P]-OD2**:**OD1** (3.0 μM, 50 nCi) was incubated in the presence of NaF (10 mM), MES (10 mM, pH 7), followed by the addition of alkylating agent (240 μM), dissolved in HPLC grade acetonitrile and diluted to 20% of the reaction volume. DNA samples were incubated at ambient temperature for 0 - 24 h incubation. Reaction was stopped at the indicated times by drying samples on the speedvac. Samples were prepared in duplicates, half were treated with hot piperidine and the other half was subject to APE1 digestion. The first set of DNA samples were then suspended in 10% piperidine (10 μL), and heated at 90^{o}C for 30 min. The resulting samples were dried, resuspended in formamide loading solution, and subjected to 20% denaturing polyacrylamide gel electrophoresis.

Ethanol precipitation of alkylated DNA

Following alkylation of single- or double-stranded DNA as described in the previous section, the second set of samples dried on speedvac were resuspended in water (10 μL), NaOAc (10 μL) and cold ethanol (50 μL). DNA was incubated at -80 ^{o}C for 1 h, and then centrifuged (16,000 rpm, 4 ^{o}C) for 16 min. The supernatant was gently

decanted and DNA pellets were resupended in 80% ethanol (50 μL), and centrifuged (16,000 rpm, 4 ^{o}C) for 6 min. After decanting the supernatant, DNA was dried on the speed vac. The resulting sample was subject to APE1 digestion.

Generation of an abasic site in a deoxyuridine-containing sequence

A sequence analog of **OD2** containing a single deoxyuracil, **dU,** was radiolabeled with γ-^{32}P-ATP (30 nCi) and diluted to a final concentration of 3.0 uM. Deglycosylation of deoxyuracil was initiated by incubating 5'-**[^{32}P]-dU** in water with UDG buffer (1X), and UDG (3 U) at 37^{o}C for 10 min. The reaction was quenched by heating samples at 95^{o}C for 10 min. DNA was then purified via phenol-chloroform extraction and then ethanol precipitation.

dU: 5'-TTA TGC GCG CGA T<u>U</u>A ACG ACA TGA CTG ACC TG-3'

Hydrolysis of abasic sites with APE1

To the previously alkylated and ethanol precipitated DNA samples, NEB buffer (1X) and APE1 (3 U) were added and diluted to a final volume of 10 uL. Samples were incubated at 37^{o}C for 1 h and enzyme was inactivated by heating at 65^{o}C for 20 min. The resulting samples were dried, resuspended in an equal volume of formamide loading solution, and subjected to 20% denaturing polyacrylamide gel electrophoresis.

Chapter 5: Conclusions

This dissertation investigated reversible DNA alkylation by mono-functional quinone methide (mono-QM) intermediates for future applications as anticancer therapeutic agents. In an effort to promote diffusion of mono-QMs along dsDNA via reversibly alkylation, an ether and methylene substituted mono-QM were conjugated to an acridine intercalator. The electron-donating effect of the ether substituent was anticipated would stabilize the electrophile of the mono-QM acridine conjugate, and facilitate its rapid regeneration. Through intercalation and de-intercalation of the acridine ligands, regenerated QMs would be able to migrate along dsDNA while forming multiple reversible adducts.

Present studies have now shown that although the ether-bridged quinone methide acridine conjugate (**eQMPAc**) reacted rapidly with DNA via alkylation of dG-N7, yields of transferred adducts were 10% and 6% for the methylene and ether bridged acridine conjugate, respectively. Reasons for the low yields of dG-N7 adducts with **eQMPAc** are uncertain. However, it is possible that the **eQMPAc** electrophile is more susceptible to reaction with water or other nucleophilic sites of DNA in comparison to the methylene substituted acridine conjugate (**QMPAc**). Under similar reaction conditions, **eQMPAc** showed a preference for transfer of regenerated QMs at GC-rich sequences, while the methylene-bridged conjugate, **QMPAc**, had no sequence preference when adducts were detected solely at dG-N7. Based on high yields of QM-dC-N3 adducts when reacted with equimolar concentrations of all four deoxynucleosides,[32] this preference of **eQMPAc** for GC-rich sequences is attributed to probable high yields of dC adducts which would then

facilitate transfer of regenerated QMs to dG-N7. In the future, HPLC analysis of the yield of **eQMPAc** and **QMPAc** adducts via digestion of alkylated oligonucleotides would provide conclusive evidence of high yields of dC-N3 adducts.

In the presence of the strong thiol nucleophile of β-mercaptoethanol (BME), neither **eQMPAc** nor **QMPAc** transferred regenerated QMs from one complementary strand to another. This demonstrated the ability of endogenous nucleophiles to impede migration of mono-QMs. Based on yields of transferred adducts, these studies have demonstrated that **QMPAc** is a better candidate for promoting reversible alkylation and migration of QMs along dsDNA. Although electron-donating substituent improved the rate of DNA alkylation by mono-QMs, they may also make the electrophile for susceptible to quenching by endogenous nucleophiles. Perhaps modification of the positions of the aromatic substituent from the *meta* to *para* position may provide faster reaction and higher yields of reversible adducts for migration along dsDNA.

Since the ether substituted **eQMPAc** provided low yields of transfer, interest in promoting reversible alkylation and migration of QMs focused on enhancing the lability of the methylene substituted mono-QM. Conjugation of mono-QMs to an acridine intercalator enabled the electrophile to alkylate duplex strands reversibly however these ligands are known to localize preferentially at nicks and bulges.[69,84] Previous studies showed that although bis-QM acridine conjugate, **bis-QMPAc,** migrated along dsDNA, adducts stalled at nicks, encountered kinetic barriers that prevented migration past a TT-bulge.[47] High yields of **bis-QMPAc** adducts at nicks

was attributed to the strong association of the acridine intercalator at these sites. In order to overcome kinetic barriers that may limit migration of QMs, a mono and di-ammonium ligand was conjugated to a methylene substituted mono-QM. It was anticipated that the association of the cationic ligands to the negatively charged phosphate backbone would enable regenerated QMs freely migrate past diverse secondary DNA structures without kinetic limitations. Studies have now shown that although di-cationic **QMPDA** alkylated DNA more efficiently than mono-cationic **QMPMA**, neither provided evidence of migration along dsDNA. Even though both **QMPDA** and **QMPAc** were able to alkylate complementary strands reversibly, only the acridine conjugate migrated along duplex DNA, with minimal preference for nicks and bulges.

Finally, to gain an understanding of why migration was detected with **QMPAc** but not **QMPDA**, abasic site generation by each mono-QM conjugate was tested. It was anticipated that the ammonium conjugate might be generating a higher fraction of abasic sites than **QMPAc** via deglycosylation of dG-N7 adducts. Abasic sites are known to destabilize hybridization of dsDNA[48,83] and this may impede association of the ammonium ligand to the phosphate backbone and limit migration of regenerated QMs between complementary strands. Studies have now shown that **QMPAc** and **QMPDA** generate equivalent fractions of abasic sites via deglycosylation of dG-N7 adducts in ssDNA. Treatment of alkylated DNA with apurinic/apyrimidinic endonuclease 1 (APE1) produced fragments of ^{32}P radiolabeled DNA primarily at deoxyguanosines (dG), with slight fragments at deoxyadenosines (dA) within a 32-mer oligonucleotide.

Reaction of **QMPAc** and **QMPDA** with dsDNA also produced fragments induced by APE1 at dGs. However, the acridine conjugate produced a slightly higher fraction of abasic sites than the ammonium conjugate. Reasons for the higher percentage of abasic sites with **QMPAc** than **QMPDA** are still unknown. In addition, it is still uncertain if the destabilization produced by deglycosylation of QM adducts promotes or hinders association of the acridine and ammonium ligands to duplex DNA, thereby facilitating migration of regenerated electrophiles along duplex DNA. Further investigation of the thermodynamic contribution of DNA ligands to the stabilization of abasic sites will aid in the development of QMs for improved migration via reversible DNA alkylation along a duplex.

This dissertation studied the ability of aromatic substituents and DNA ligands to promote reversible alkylation and migration of mono-QMs along dsDNA. Results presented in this dissertation have established that mono-QMs conjugated to acridine and di-ammonium ligands alkylate DNA reversibly. The ability of **QMPAc** to migrate along dsDNA and bypass nicks and bulges presents a new opportunity to explore migration of QMs along other diverse secondary and tertiary structures found in DNA and RNA. In the future, mono-QMs may also be conjugated to other non-sequence specific ligands such as minor groove binders that would promote faster migration of the electrophile along a duplex.

Appendix A

Supporting Information for Chapter 2

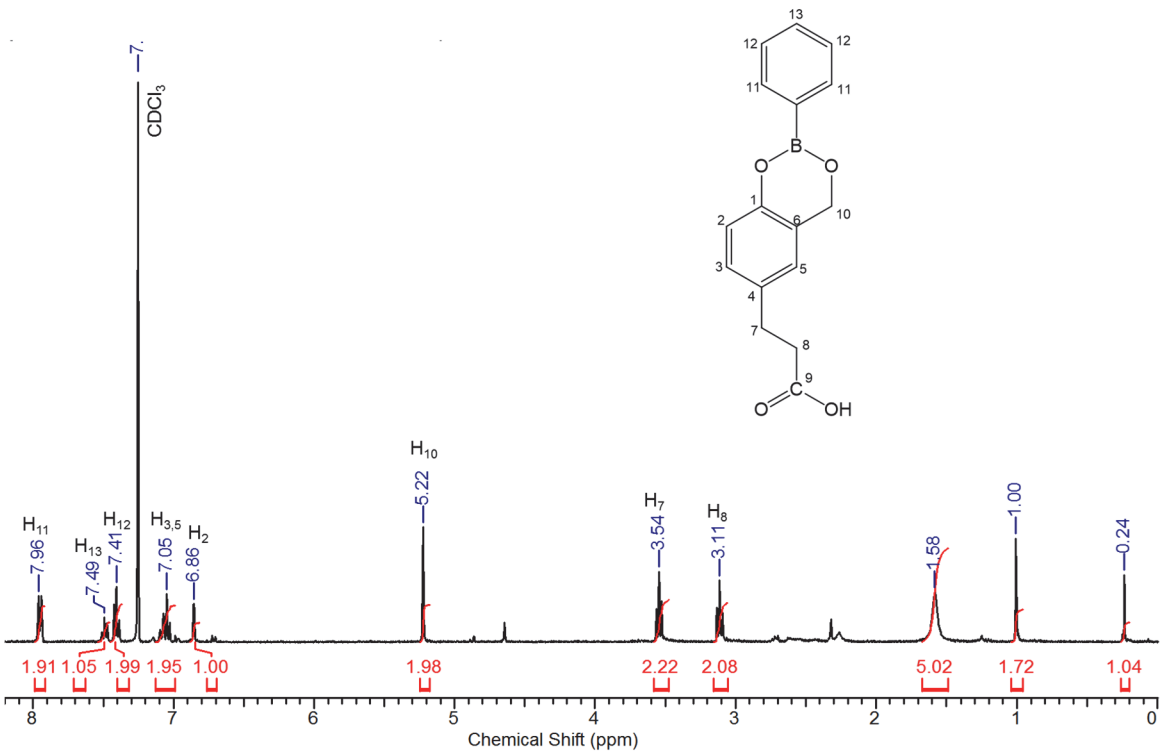
CDCl3
H11
7.96
H13
7.49
H12
7.41
H3,5
7.05
H2
6.86
H10
5.22
H7
3.54
H8
3.11
1.58
1.00
0.24
1.91 1.05 1.99 1.95 1.00
1.98
2.22 2.08
5.02
1.72
1.04
Chemical Shift (ppm)

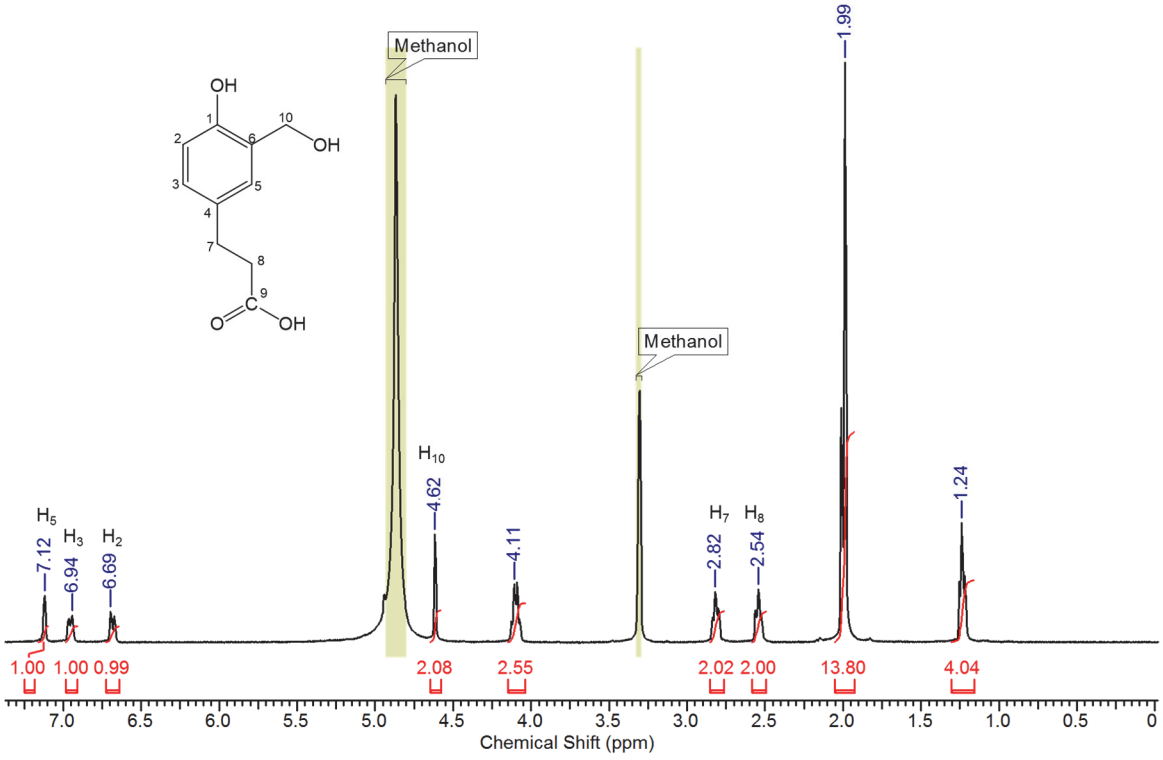
Methanol
Methanol
1.99
H5
7.12
H3
6.94
H2
6.69
H10
4.62
4.11
H7
2.82
H8
2.54
1.24
1.00 1.00 0.99
2.08
2.55
2.02 2.00
13.80
4.04
Chemical Shift (ppm)

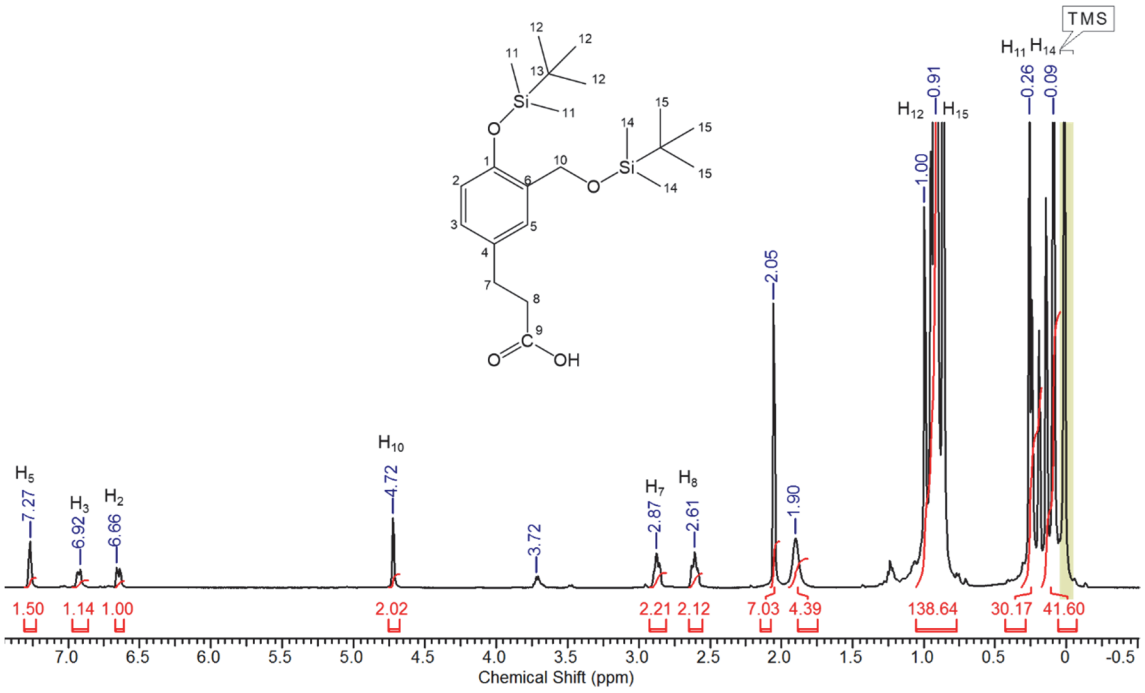
TMS
H5
H3
H2
H10
H7
H8
H12
H15
H11 H14
7.27
6.92
6.66
4.72
3.72
2.87
2.61
2.05
1.90
1.00
0.91
0.26
0.09
1.50
1.14
1.00
2.02
2.21
2.12
7.03
4.39
138.64
30.17
41.60
Chemical Shift (ppm)

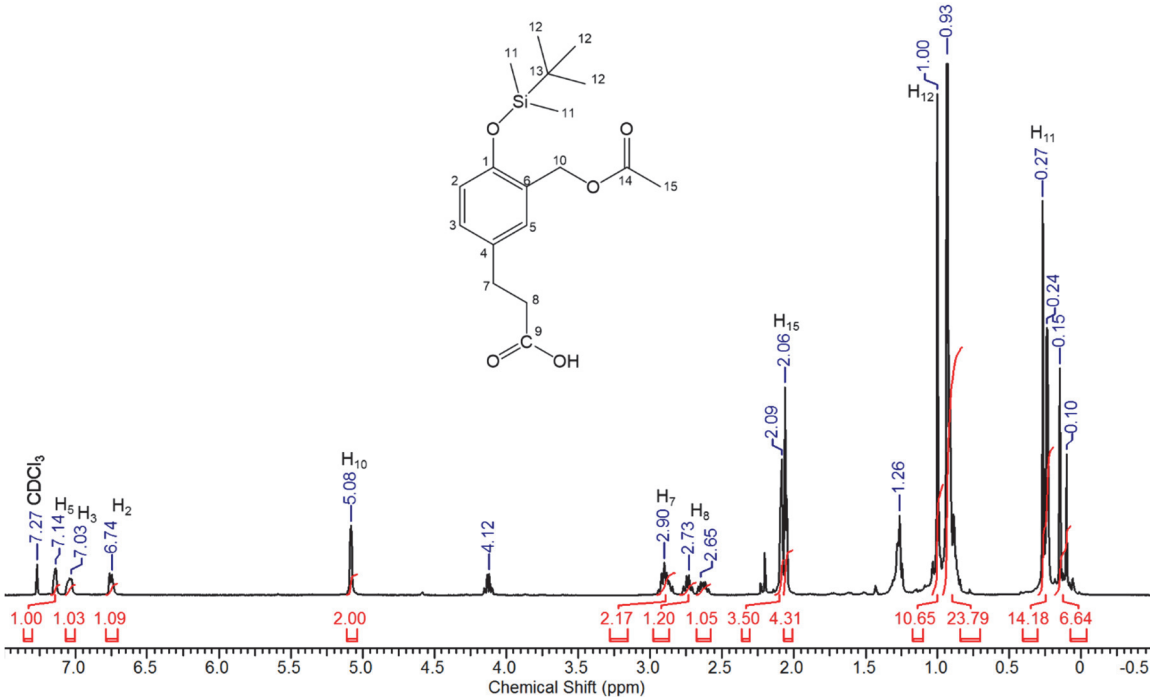
CDCl3
H5
H3
H2
H10
H7
H8
H15
H12
H11
7.27
7.14
7.03
6.74
5.08
4.12
2.90
2.73
2.65
2.09
2.06
1.26
1.00
0.93
0.27
0.24
0.15
0.10
1.00
1.03
1.09
2.00
2.17
1.20
1.05
3.50
4.31
10.65
23.79
14.18
6.64
Chemical Shift (ppm)

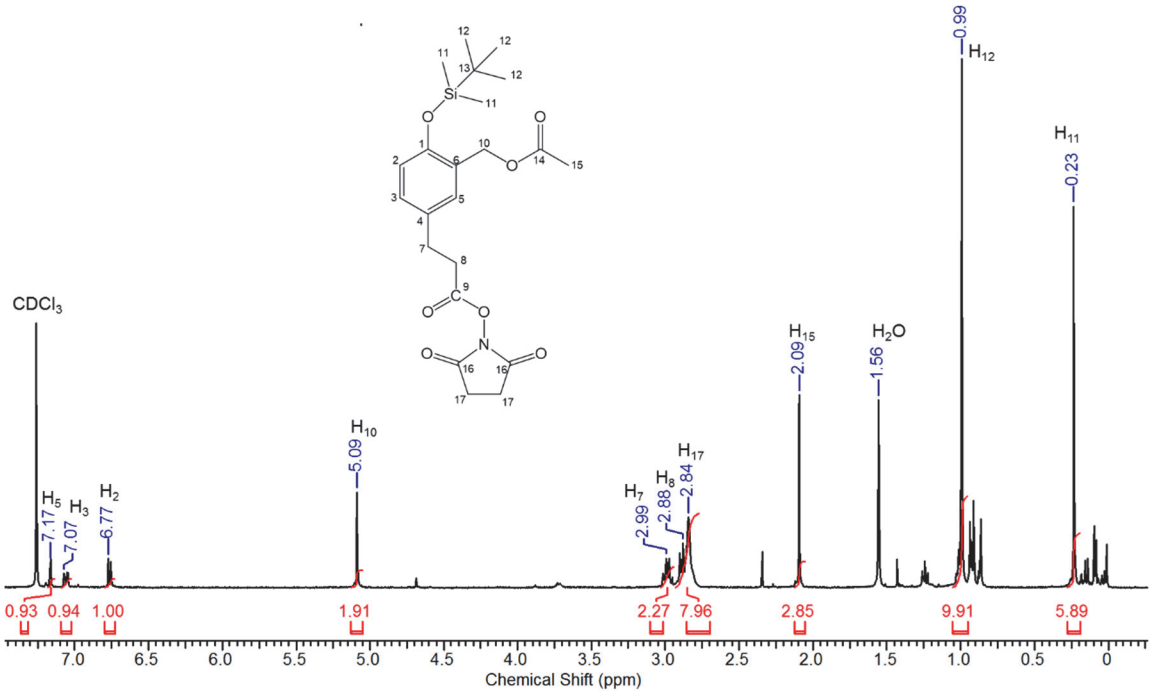
CDCl3
H5
H3
H2
H10
H7
H8
H17
H15
H2O
H12
H11
7.17
7.07
6.77
5.09
2.99
2.88
2.84
2.09
1.56
0.99
0.23
0.93
0.94
1.00
1.91
2.27
7.96
2.85
9.91
5.89
Chemical Shift (ppm)

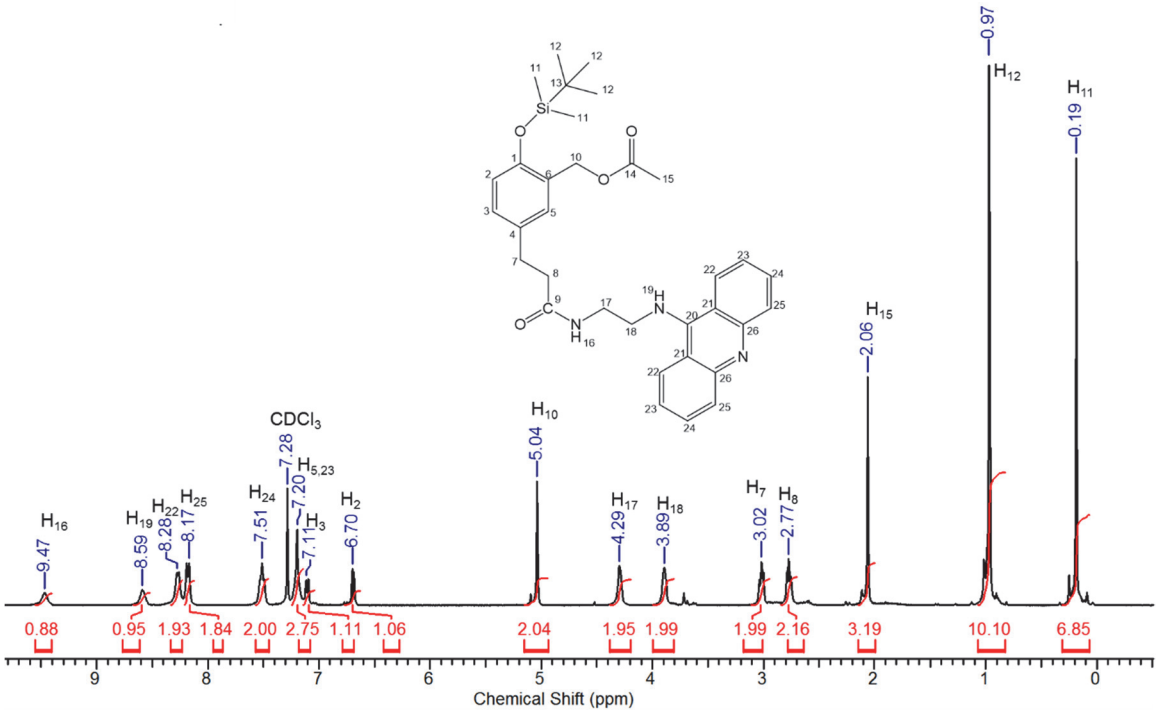
H16
H19
H22
H25
H24
CDCl3
H5,23
H3
H2
H10
H17
H18
H7
H8
H15
H12
H11
9.47
8.59
8.28
8.17
7.51
7.28
7.20
7.11
6.70
5.04
4.29
3.89
3.02
2.77
2.06
0.97
0.19
0.88
0.95
1.93
1.84
2.00
2.75
1.11
1.06
2.04
1.95
1.99
1.99
2.16
3.19
10.10
6.85
Chemical Shift (ppm)

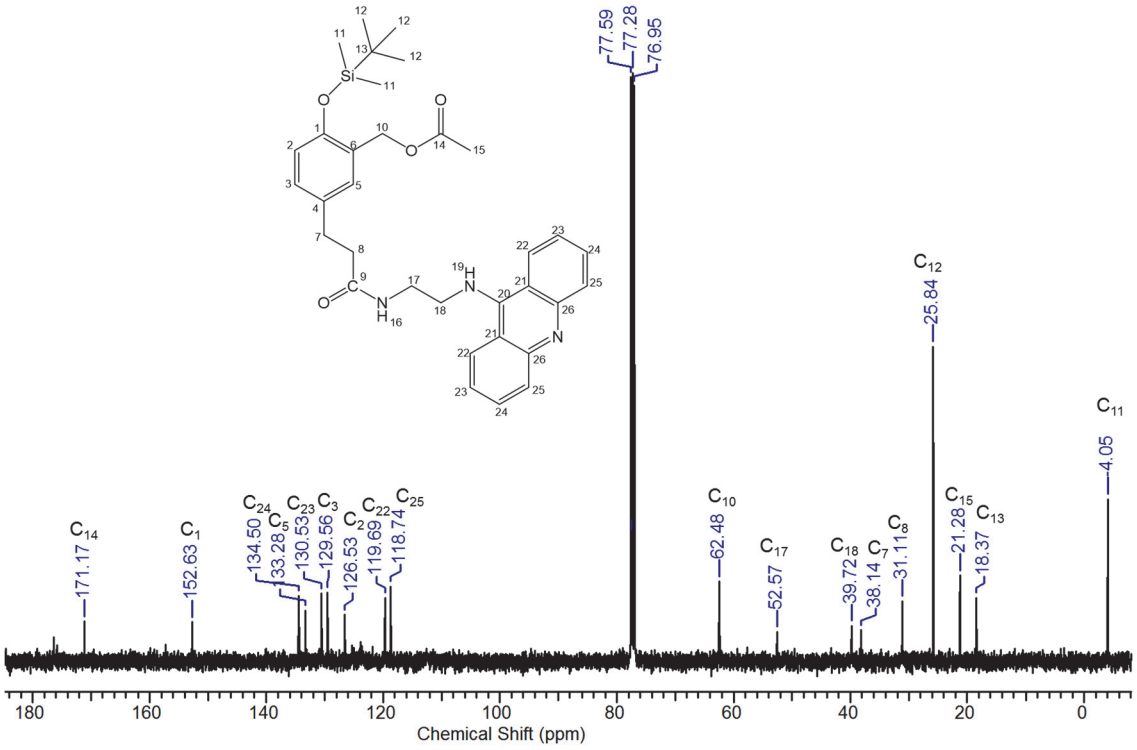
77.59
77.28
76.95
C12
25.84
C11
4.05
C14
171.17
C1
152.63
C24
134.50
C5
133.28
C23
130.53
C3
129.56
C2
126.53
C22
119.69
C25
118.74
C10
62.48
C17
52.57
C18
39.72
C7
38.14
C8
31.11
C15
21.28
C13
18.37
180
160
140
120
100
80
60
40
20
0
Chemical Shift (ppm)

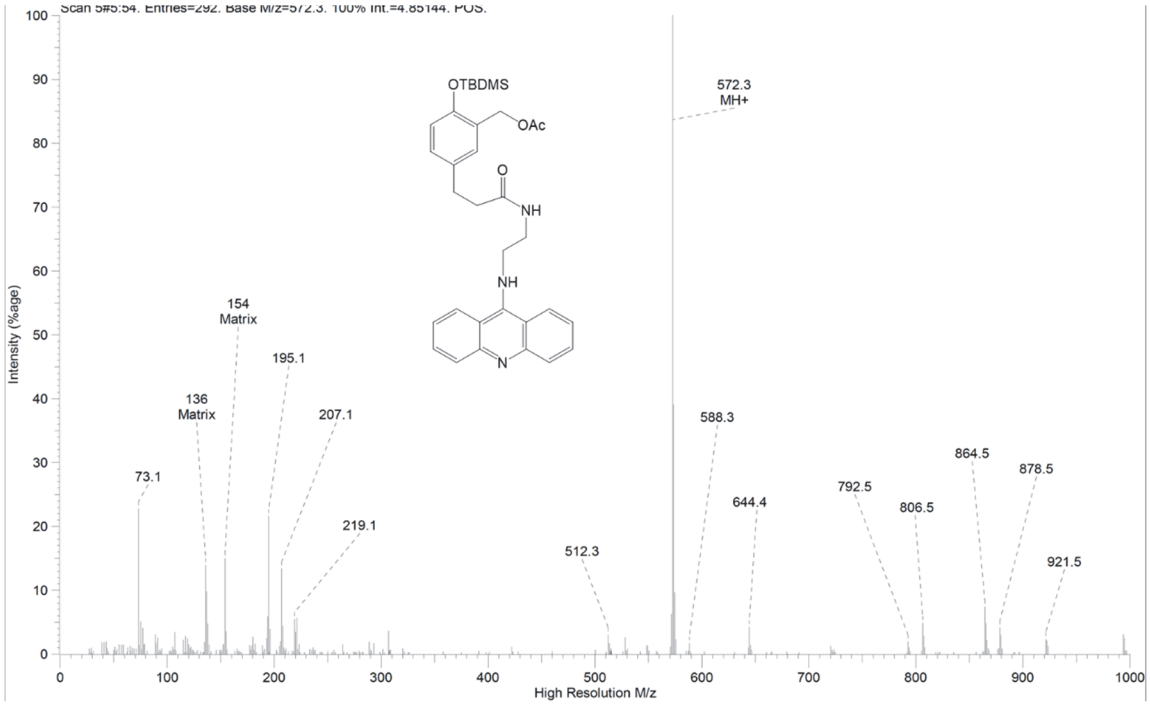
OTBDMS
OAc
NH
NH
N
572.3
MH+
154
Matrix
195.1
136
Matrix
207.1
73.1
219.1
512.3
588.3
644.4
792.5
806.5
864.5
878.5
921.5
Intensity (%age)
High Resolution M/z
0
100
200
300
400
500
600
700
800
900
1000

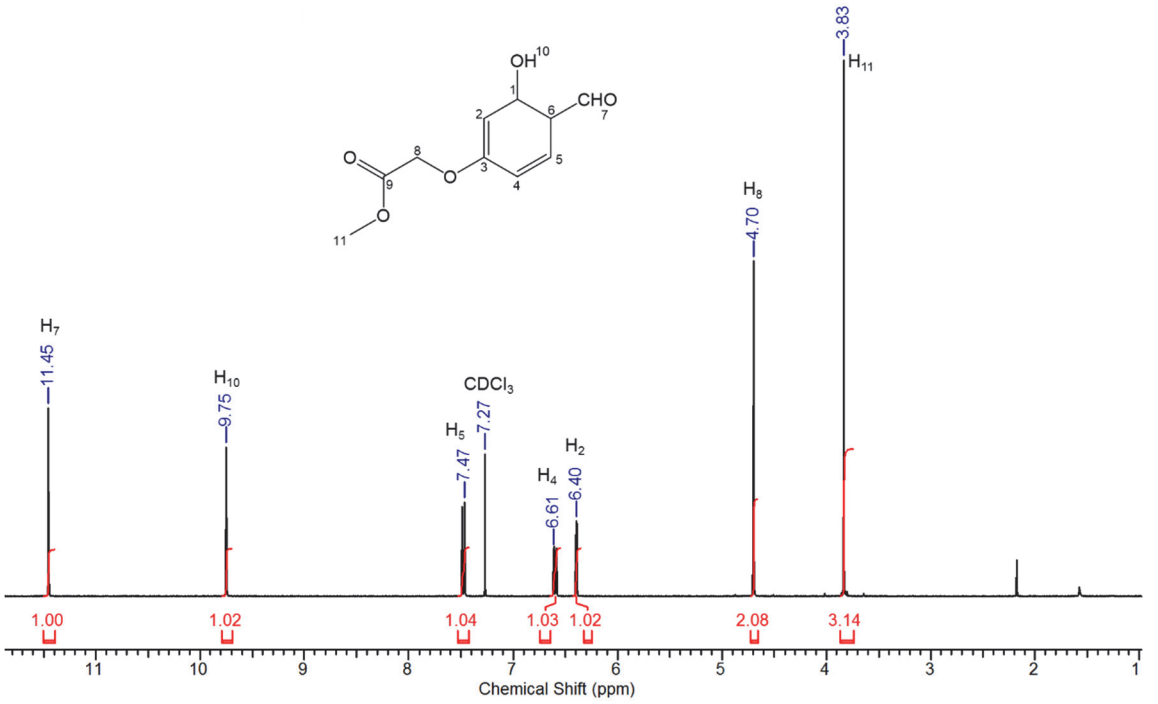
OH10
CHO7
O
O
O
11
H7
11.45
H10
9.75
CDCl3
H5
7.47
7.27
H2
H4
6.61
6.40
H8
4.70
3.83
H11
1.00
1.02
1.04
1.03
1.02
2.08
3.14
Chemical Shift (ppm)

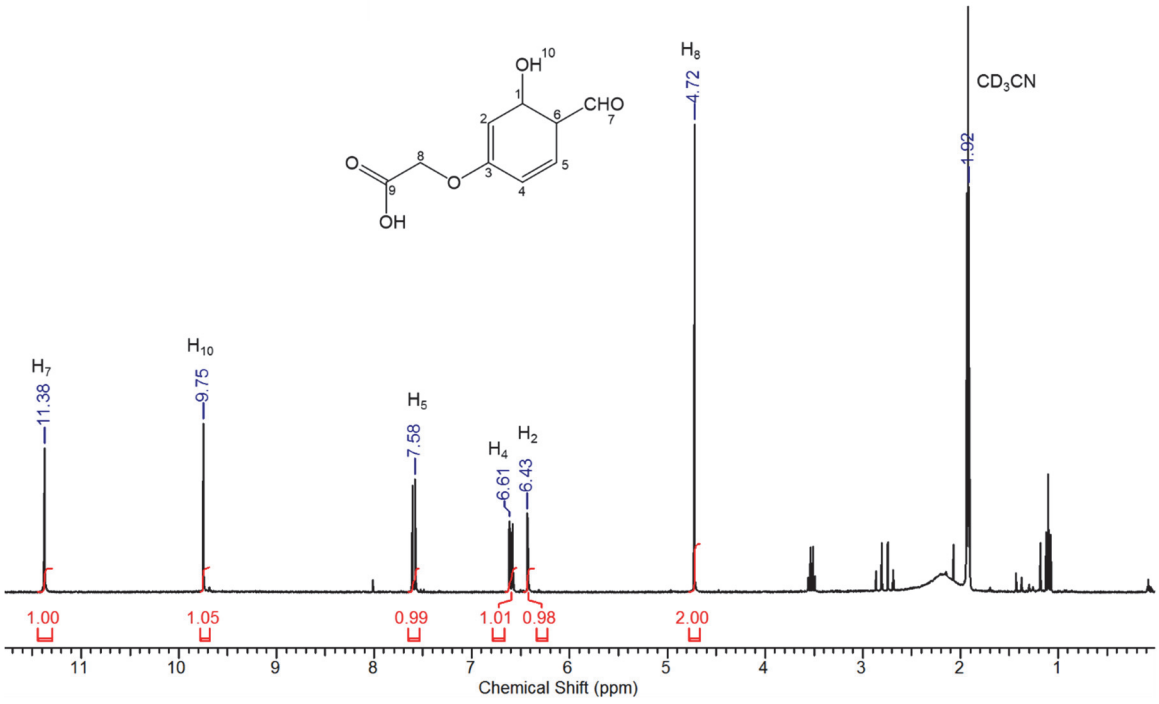
OH10
CHO7
O
O
OH
H8
4.72
CD3CN
1.92
H7
11.38
H10
9.75
H5
7.58
H4
6.61
H2
6.43
1.00
1.05
0.99
1.01
0.98
2.00
Chemical Shift (ppm)

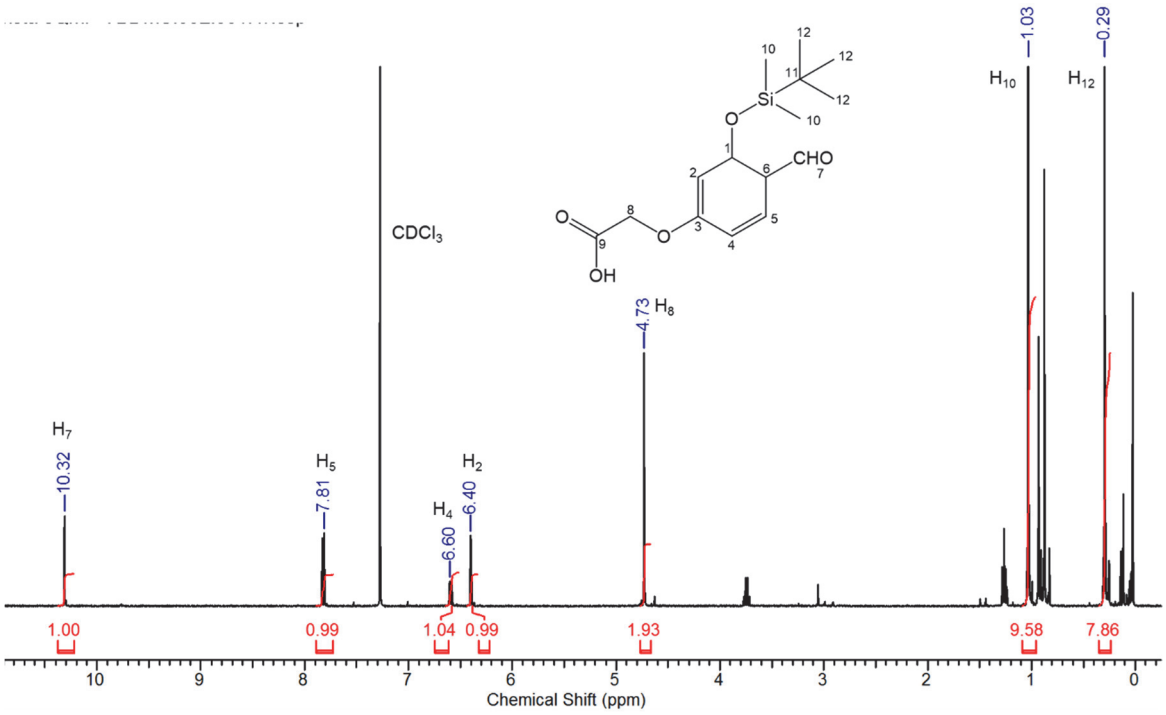
CDCl3
H7
10.32
H5
7.81
H4
6.60
H2
6.40
4.73 H8
1.03
H10
0.29
H12
1.00
0.99
1.04
0.99
1.93
9.58
7.86
Chemical Shift (ppm)

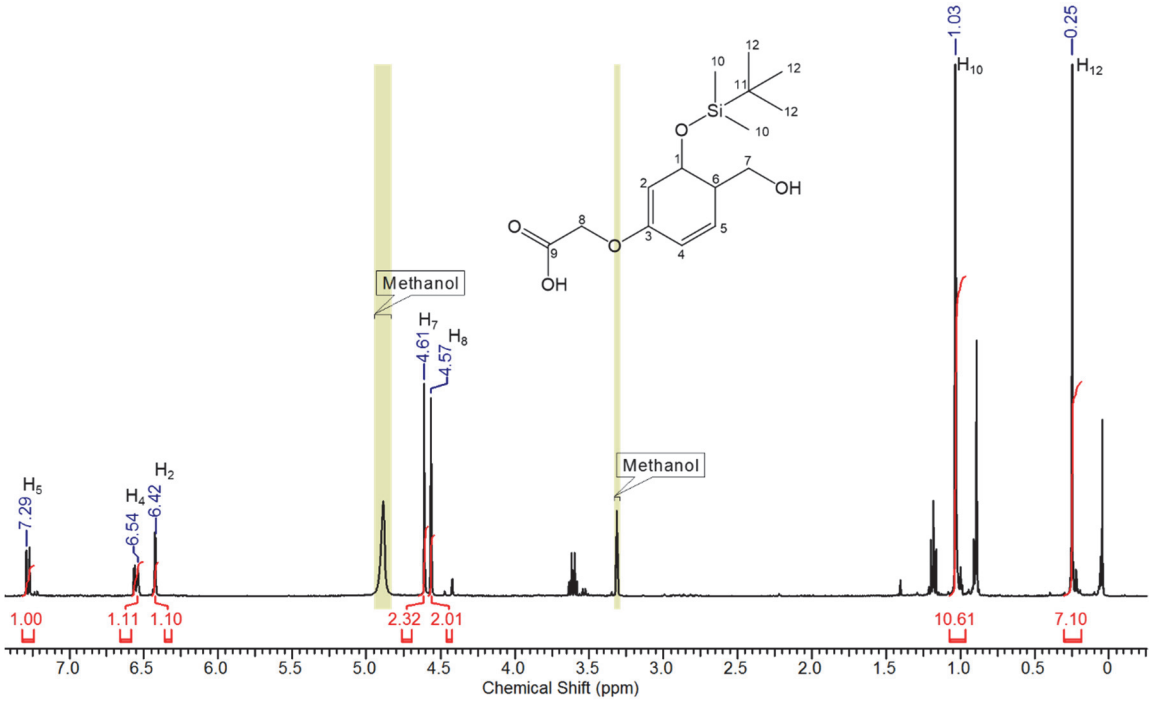
Methanol
H7
4.61
H8
4.57
H5
7.29
H4
6.54
H2
6.42
Methanol
1.03
H10
0.25
H12
1.00
1.11
1.10
2.32
2.01
10.61
7.10
Chemical Shift (ppm)

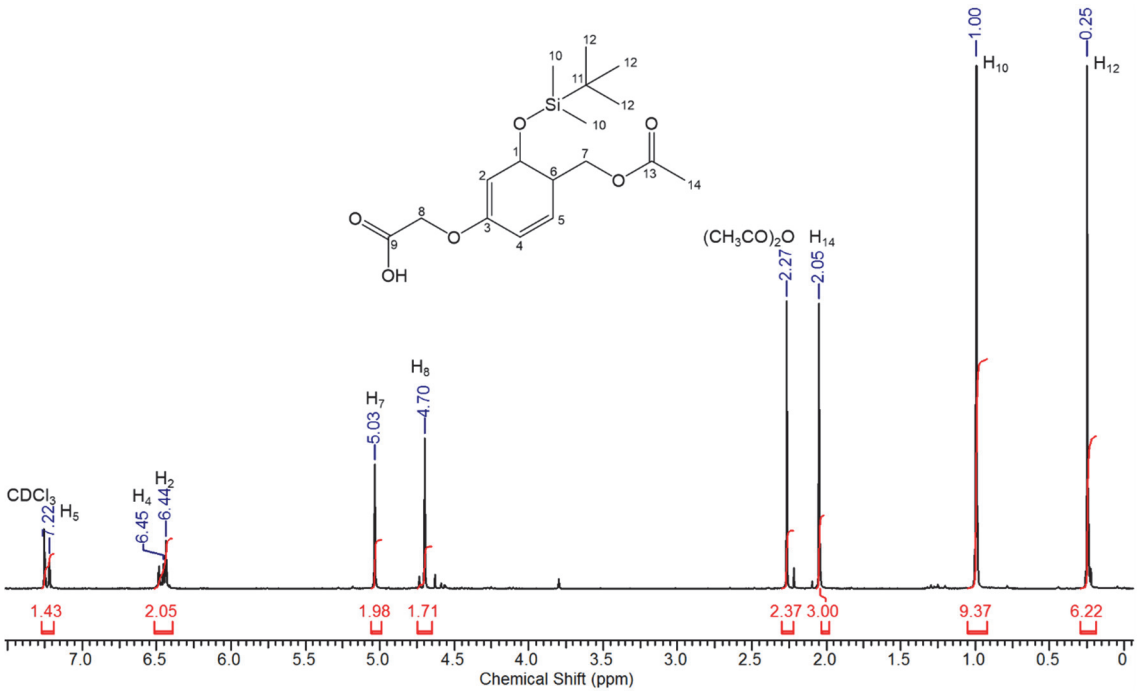
CDCl3
H5
H4
H2
H7
H8
(CH3CO)2O
H14
H10
H12
1.43
2.05
1.98
1.71
2.37
3.00
9.37
6.22
Chemical Shift (ppm)

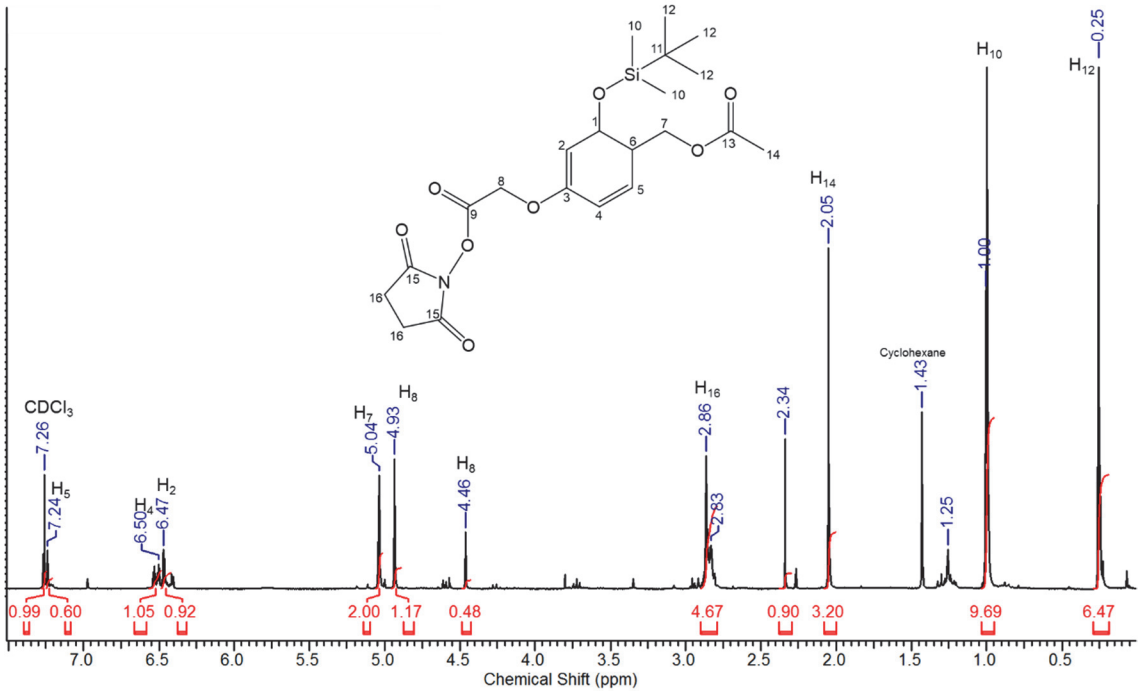
CDCl3
H5
H4
H2
H7
H8
H16
H14
H10
H12
Cyclohexane
0.99
0.60
1.05
0.92
2.00
1.17
0.48
4.67
0.90
3.20
9.69
6.47
Chemical Shift (ppm)

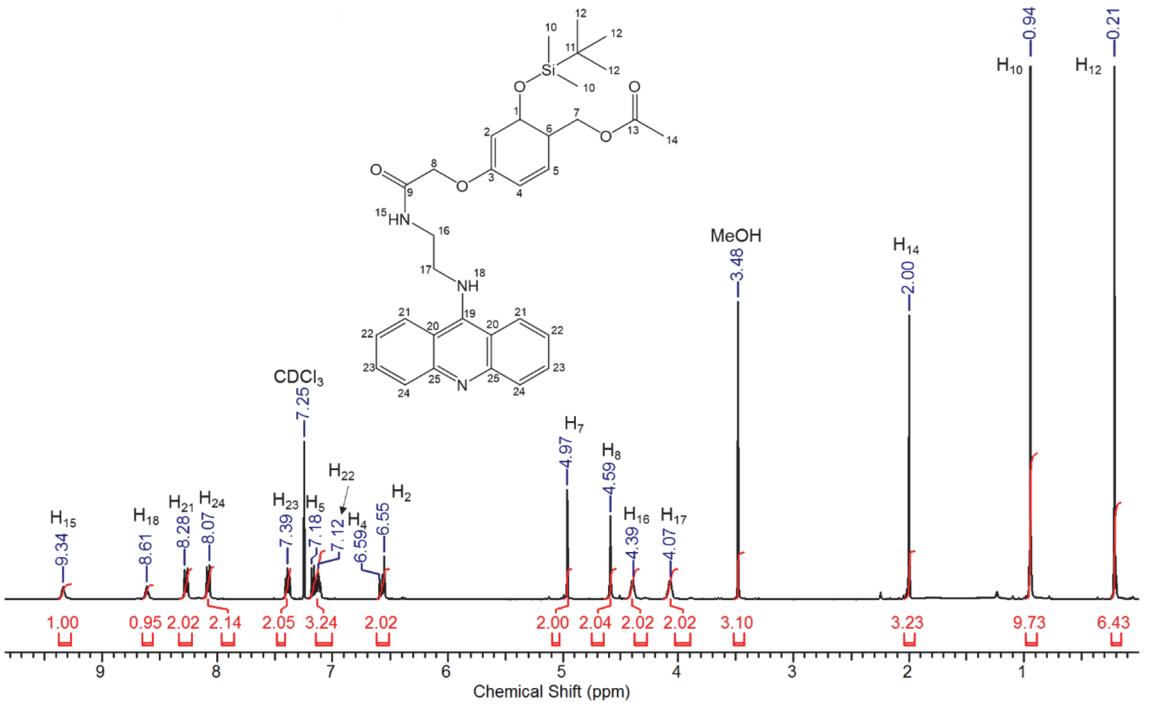
H10 0.94
H12 0.21
MeOH 3.48
H14 2.00
CDCl3 7.25
H15 9.34
H18 8.61
H21 8.28
H24 8.07
H23 7.39
H5 7.18
H22 7.12
H4 6.59
H2 6.55
H7 4.97
H8 4.59
H16 4.39
H17 4.07
1.00 0.95 2.02 2.14 2.05 3.24 2.02 2.00 2.04 2.02 2.02 3.10 3.23 9.73 6.43
Chemical Shift (ppm)

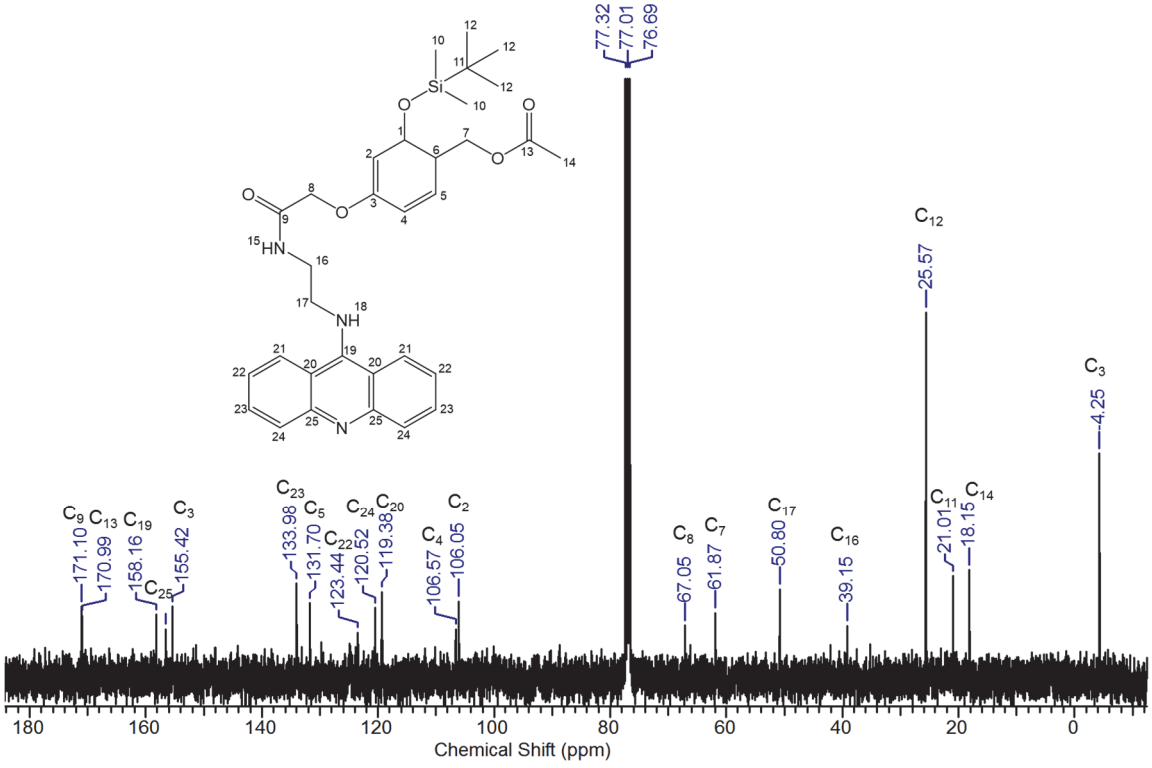
77.32
77.01
76.69
C12 25.57
C3 4.25
C9 171.10
C13 170.99
C19 158.16
C25
C3 155.42
C23 133.98
C5 131.70
C22 123.44
C24 120.52
C20 119.38
C4 106.57
C2 106.05
C8 67.05
C7 61.87
C17 50.80
C16 39.15
C11 21.01
C14 18.15
Chemical Shift (ppm)

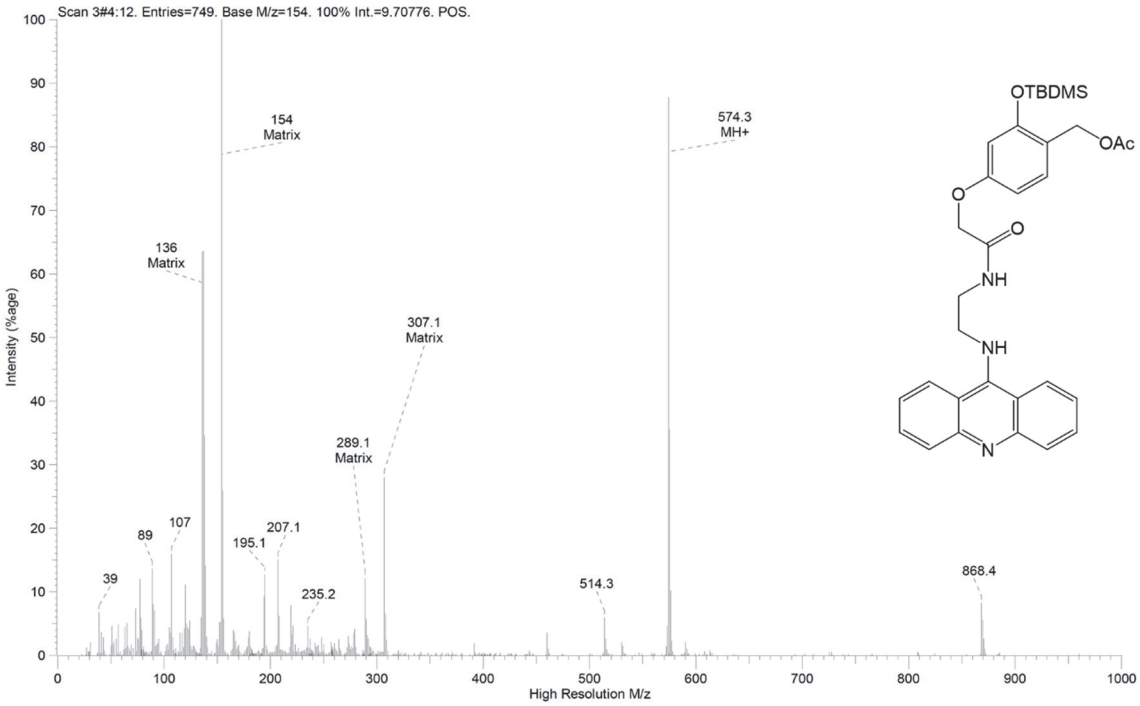
Scan 3#4:12. Entries=749. Base M/z=154. 100% Int.=9.70776. POS.
Intensity (%age)
High Resolution M/z
154
Matrix
574.3
MH+
136
Matrix
307.1
Matrix
289.1
Matrix
207.1
195.1
107
89
39
235.2
514.3
868.4
OTBDMS
OAc
O
O
NH
NH
N

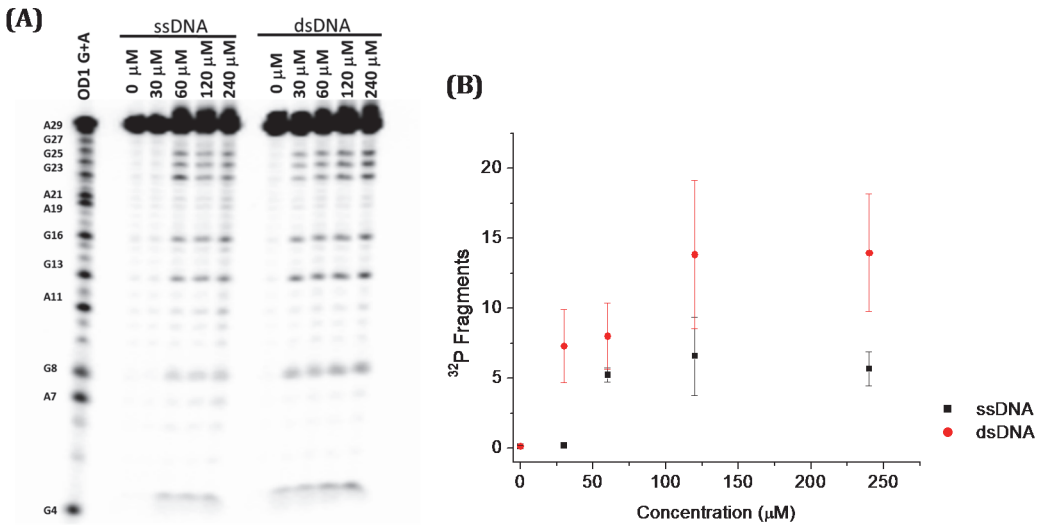

Figure A1: Alkylation of ssDNA and dsDNA by eQMPAc. (A) Reaction at dG-N7 of dsDNA 5'-**[^{32}P]-OD1:OD2** (3.0 μM) and ssDNA 5'-**[^{32}P]-OD1** (3.0 μM) with **eQMPAc** (0 - 120 μM), in the presence of NaF (10 mM) and MES buffer (10 mM, pH 7.0) for 24 h, followed by 10 % hot piperidine. (B) Yield of 5'-**[^{32}P]-OD1** fragments as total percentage of lane intensity for ssDNA and dsDNA alkylation by **eQMPAc**. Reaction yield is an average of independent three trials, determined by subtracting fragment intensity from t = 0. Error is an average of the standard deviation.

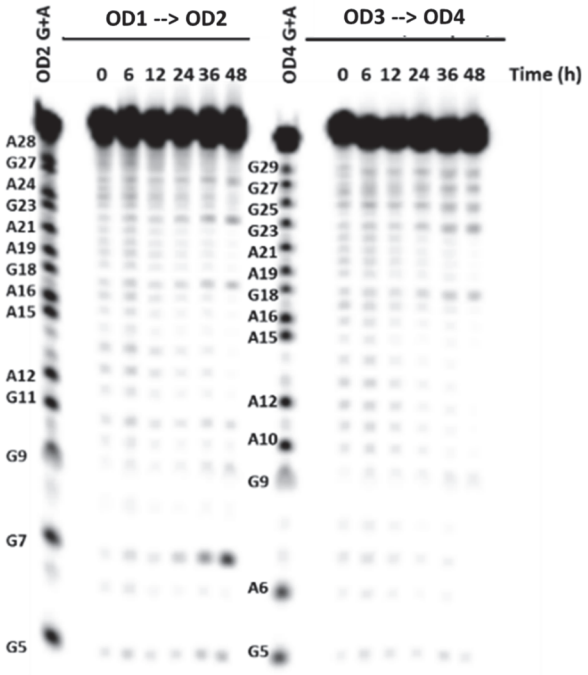

Figure S4: Transfer of **eQMPAc** at GC-rich sequences. Single strand DNA, **OD1** or **OD3** (3.0 μM was incubated with either **eQMPAc** (240 μM) in the presence of NaF (10 mM) and MES buffer (10 mM, pH 7.0) for 24 h, followed the addition of its complement, **5'-[^{32}P]-OD2 or 5'-[^{32}P]-OD4,** (3.3 μM) for 0 - 48 h**.** Subsequently, samples were treated with 10 % hot piperidine. DNA sequences are illustrated on Figure 2.9.

Appendix B

Supporting Information for Chapter 3

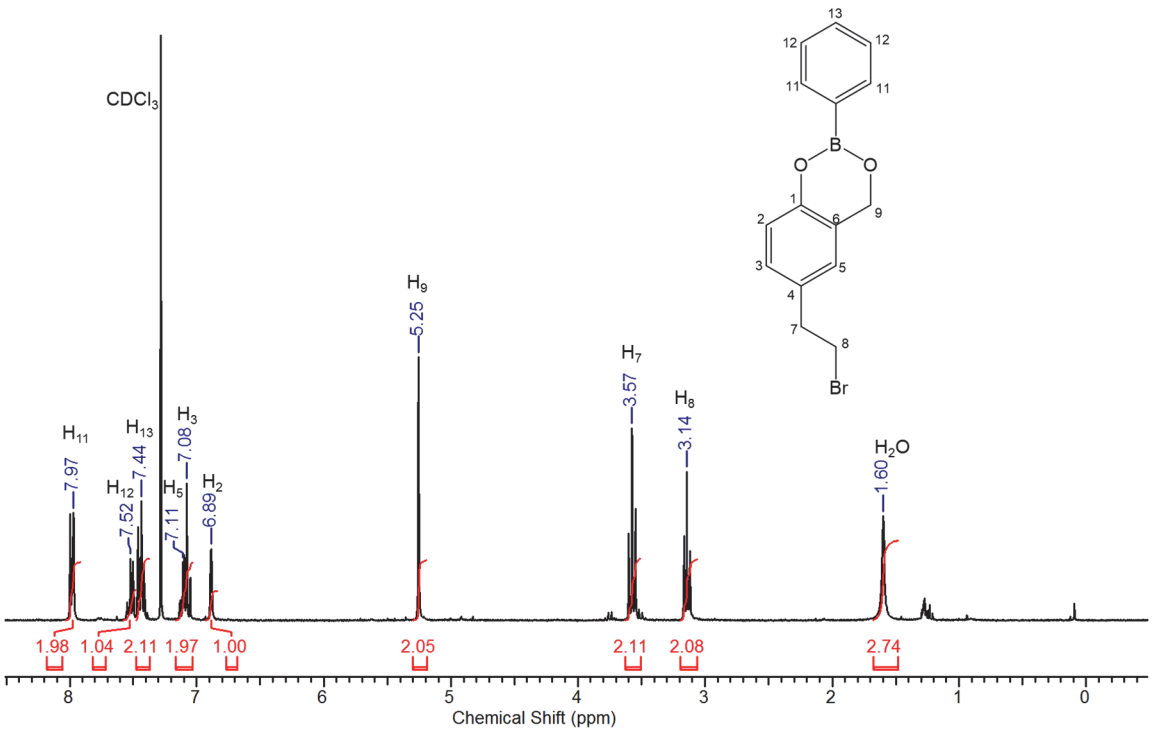
CDCl3
H11
7.97
H13
7.44
H12
7.52
H5
7.11
H3
7.08
H2
6.89
H9
5.25
H7
3.57
H8
3.14
H2O
1.60
1.98 1.04 2.11 1.97 1.00
2.05
2.11 2.08
2.74
Chemical Shift (ppm)

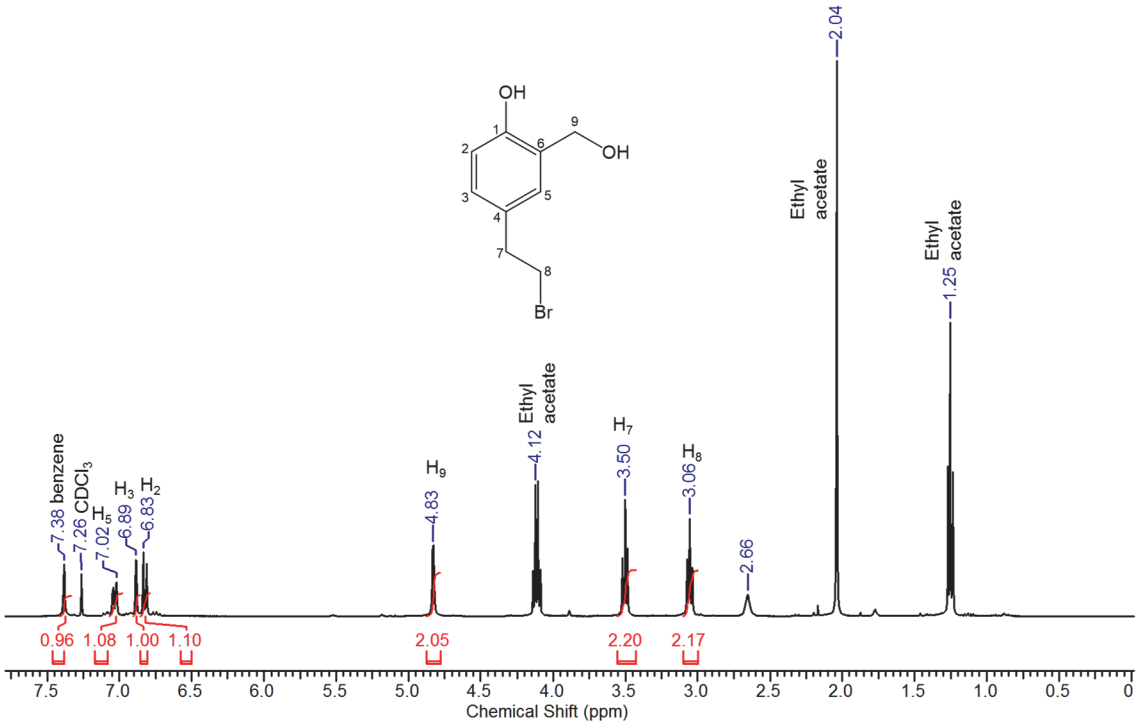
OH
OH
Br
7.38 benzene
7.26 CDCl3
H5
7.02
H3
6.89
H2
6.83
H9
4.83
Ethyl acetate
4.12
H7
3.50
H8
3.06
2.66
Ethyl acetate
2.04
Ethyl acetate
1.25
0.96 1.08 1.00 1.10
2.05
2.20 2.17
Chemical Shift (ppm)

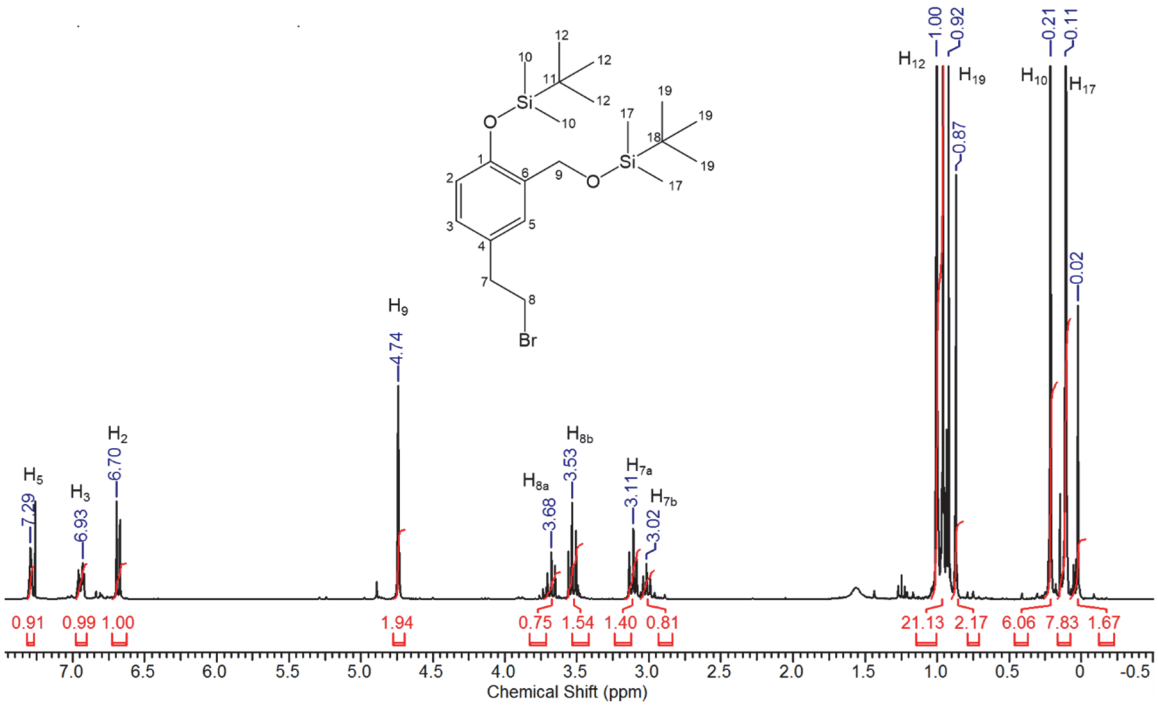
H5
7.29
H3
6.93
H2
6.70
H9
4.74
H8a
3.68
H8b
3.53
H7a
3.11
H7b
3.02
H12
1.00
H19
0.92
0.87
H10
0.21
H17
0.11
0.02
0.91 0.99 1.00 1.94 0.75 1.54 1.40 0.81 21.13 2.17 6.06 7.83 1.67
Chemical Shift (ppm)

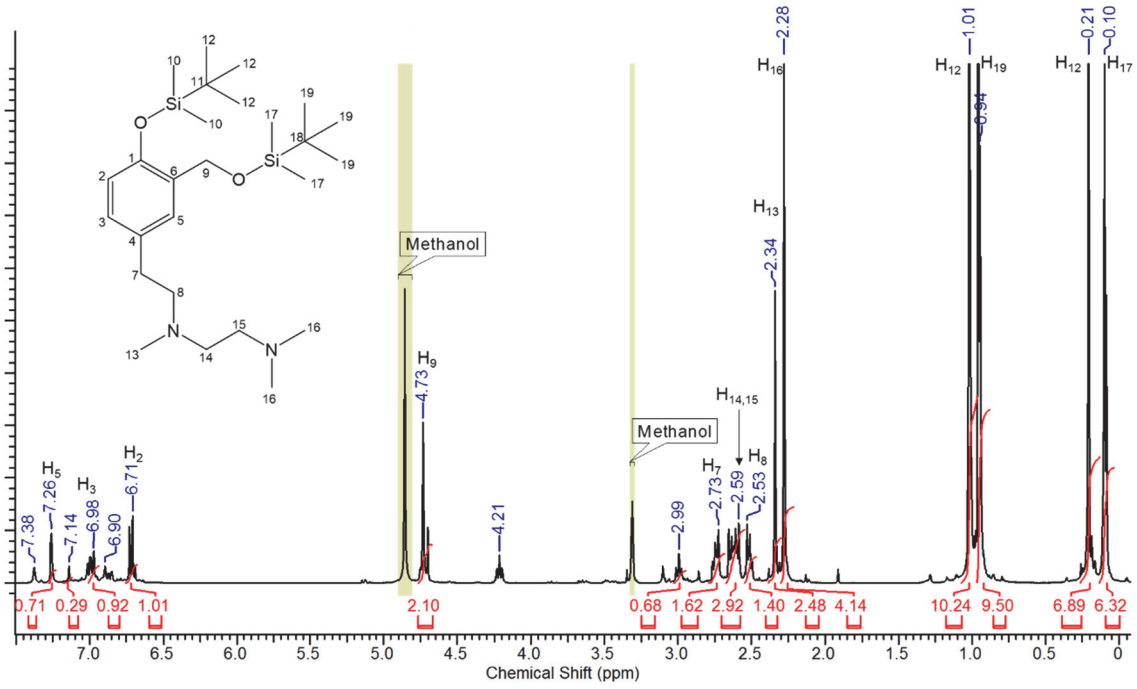
Methanol
Methanol
H16
2.28
H13
2.34
H12
1.01
H19
0.94
H12
0.21
H17
0.10
H9
4.73
H14,15
H8
H7
2.73
2.59
2.53
2.99
4.21
H5
7.26
H3
6.98
H2
6.71
7.38
7.14
6.90
0.71 0.29 0.92 1.01 2.10 0.68 1.62 2.92 1.40 2.48 4.14 10.24 9.50 6.89 6.32
Chemical Shift (ppm)

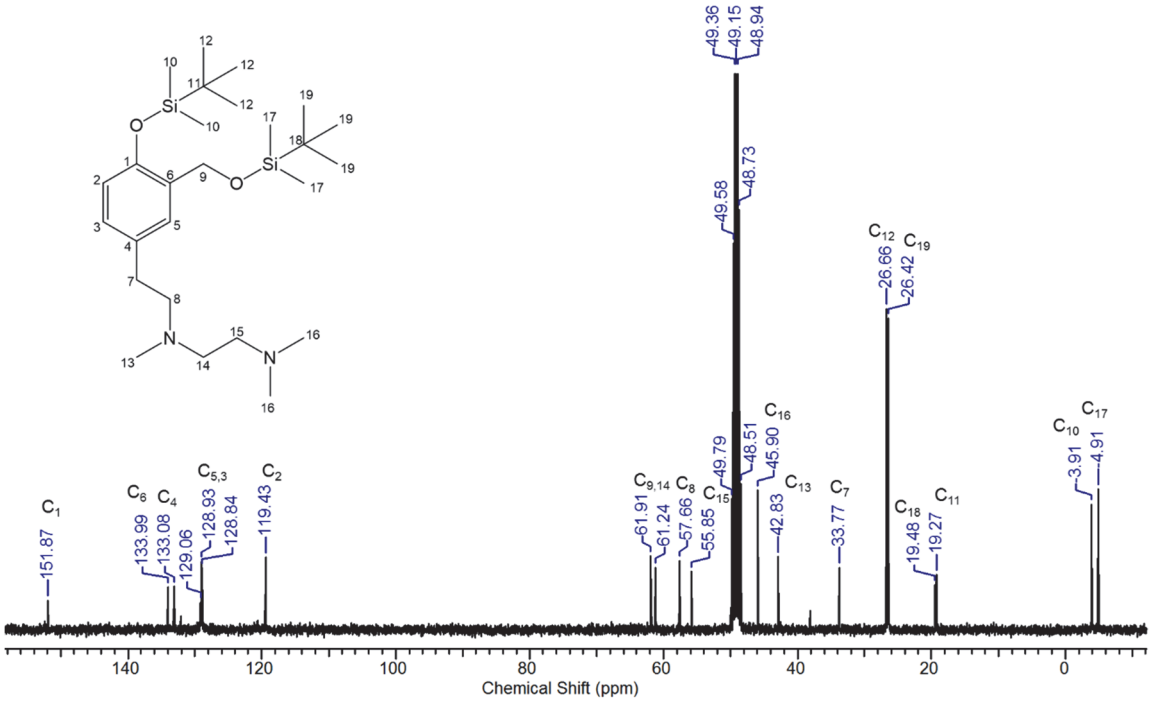
C1 151.87
C6 133.99
C4 133.08
129.06
C5,3 128.93
128.84
C2 119.43
C9,14 61.91
61.24
C8 57.66
C15 55.85
49.79
49.58
48.73
48.51
C16 45.90
C13 42.83
C7 33.77
C12 C19 26.66
26.42
C18 19.48
C11 19.27
C10 3.91
C17 4.91
Chemical Shift (ppm)

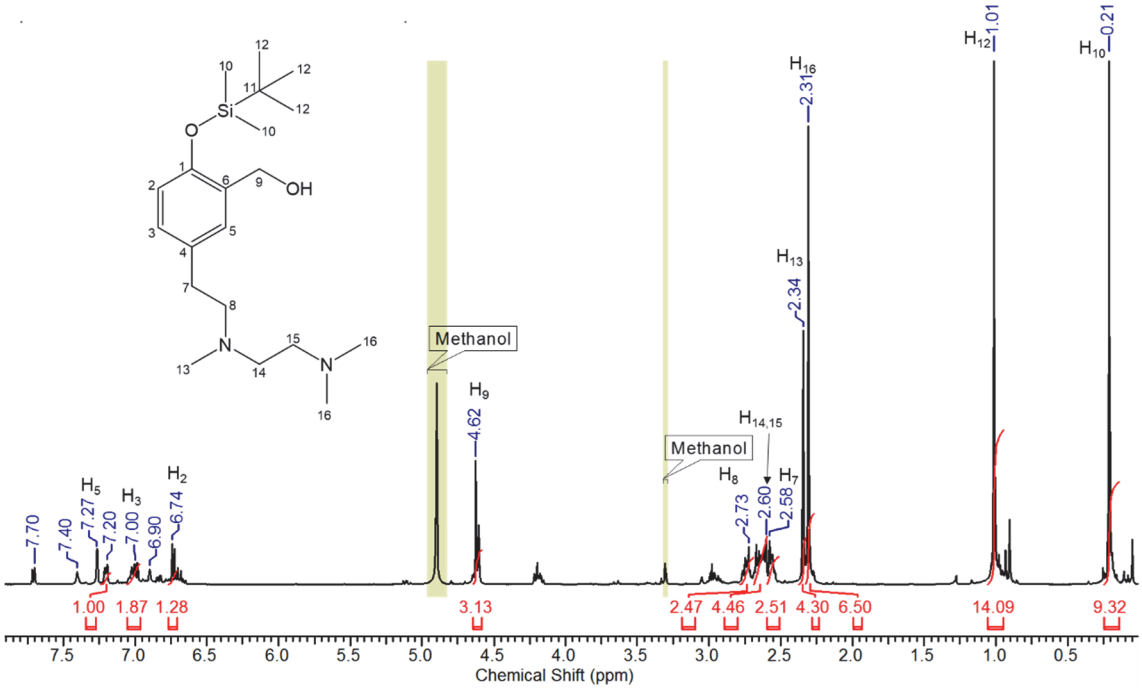
H12 1.01
H10 0.21
H16 2.31
H13 2.34
Methanol
H9 4.62
Methanol
H14,15
H8
H7
H5
H3
H2
7.70
7.40
7.27
7.20
7.00
6.90
6.74
2.73
2.60
2.58
1.00 1.87 1.28
3.13
2.47 4.46 2.51 4.30 6.50
14.09
9.32
Chemical Shift (ppm)

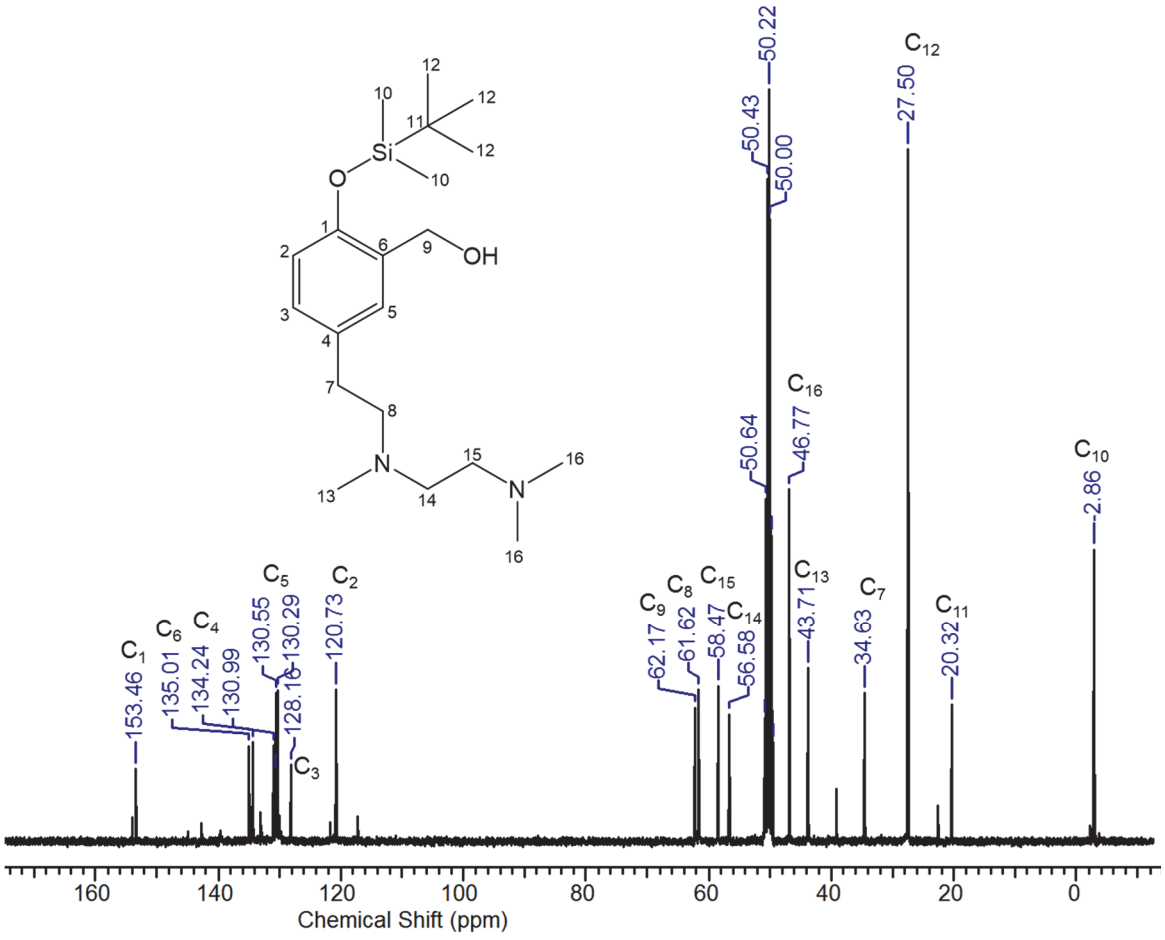
C1 153.46
C6 135.01
C4 134.24
130.99
C5 130.55
130.29
128.18
C3
C2 120.73
C9 62.17
C8 61.62
C15 58.47
C14 56.58
50.64
50.43
50.22
50.00
C16 46.77
C13 43.71
C7 34.63
C12 27.50
C11 20.32
C10 2.86
Chemical Shift (ppm)

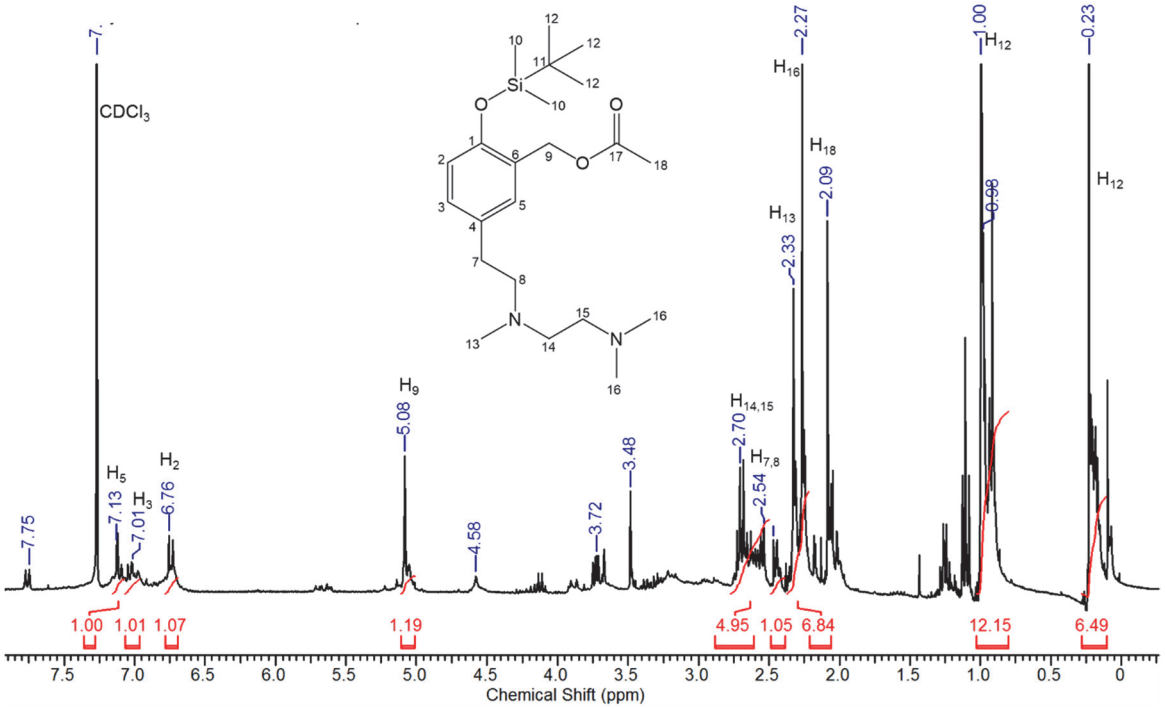
CDCl3
H5 7.13
H3 7.01
H2 6.76
7.75
H9 5.08
4.58
3.72
3.48
H14,15 2.70
H7,8 2.54
H16 2.27
H13 2.33
H18 2.09
1.00 H12
0.98
0.23
H12
1.00 1.01 1.07
1.19
4.95 1.05 6.84
12.15
6.49
Chemical Shift (ppm)

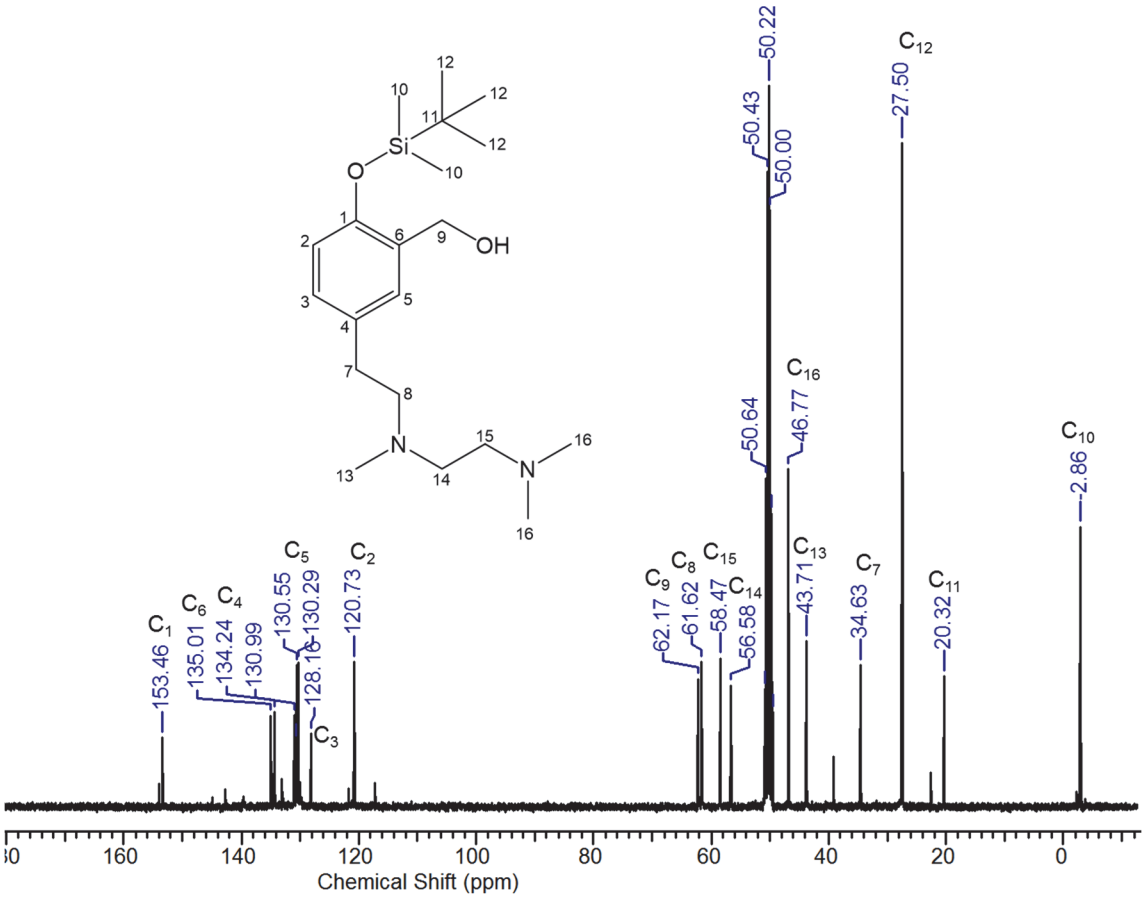
C12
27.50
50.22
50.43
50.00
C16
46.77
50.64
C10
2.86
C13
43.71
C7
34.63
C11
20.32
C15
58.47
C14
56.58
C8
61.62
C9
62.17
C5
130.55
C2
120.73
C6
135.01
C4
134.24
130.99
130.29
128.16
C1
153.46
C3
Chemical Shift (ppm)

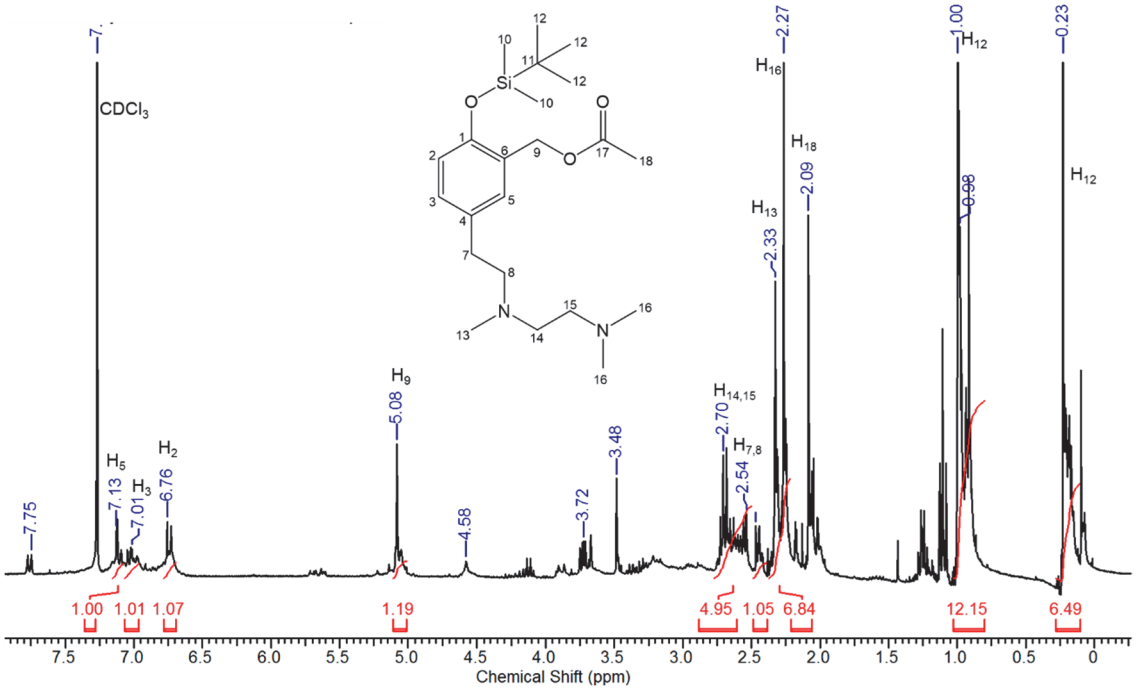
CDCl3
H16
2.27
H18
2.09
H13
2.33
H12
1.00
0.98
0.23
H9
5.08
H14,15
2.70
H7,8
2.54
3.48
3.72
4.58
H5
7.13
H3
7.01
H2
6.76
7.75
1.00
1.01
1.07
1.19
4.95
1.05
6.84
12.15
6.49
Chemical Shift (ppm)

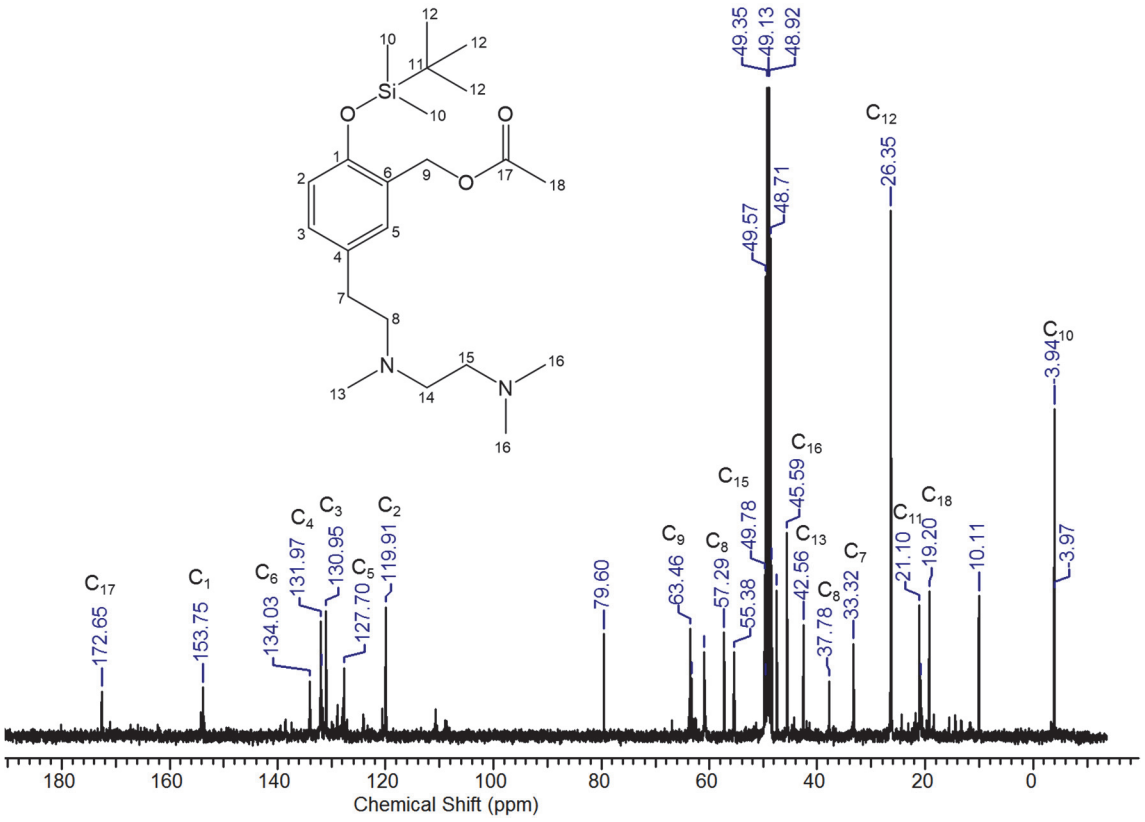
C17 172.65
C1 153.75
C6 134.03
C4 131.97
C3 130.95
C5 127.70
C2 119.91
79.60
C9 63.46
C8 57.29
C15 49.78
55.38
49.57
49.35
49.13
48.92
48.71
C16 45.59
C13 42.56
C8 37.78
C7 33.32
C12 26.35
C11 21.10
C18 19.20
10.11
C10 3.94
3.97
Chemical Shift (ppm)

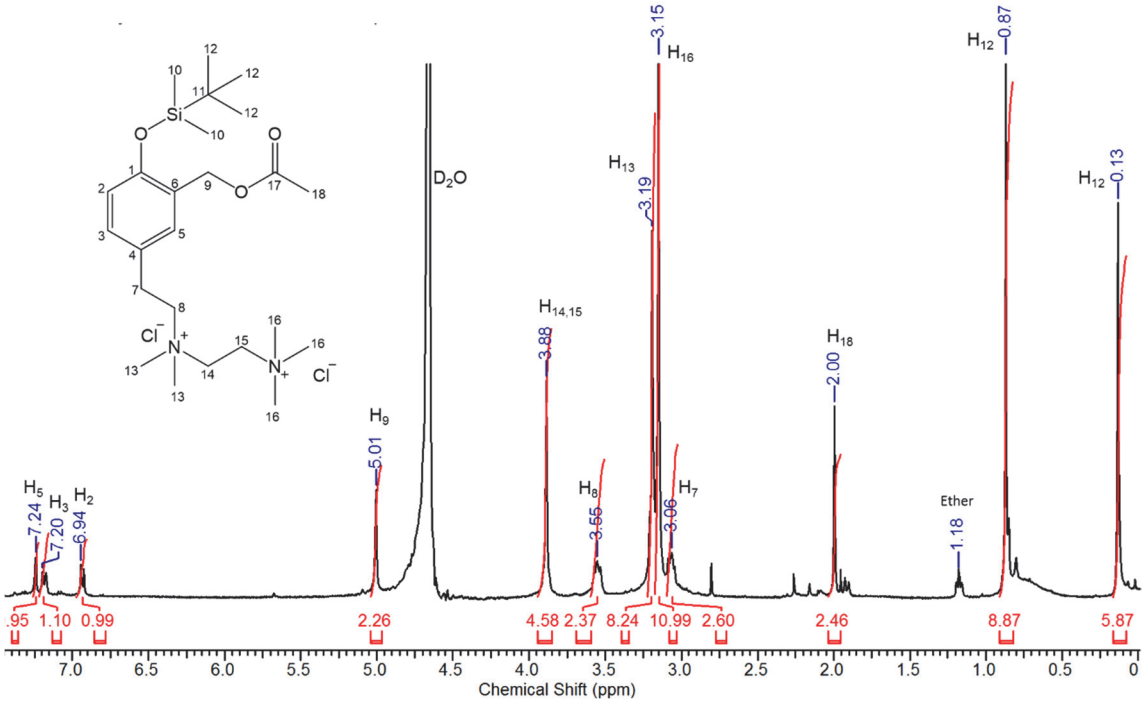
H5 7.24
H3 7.20
H2 6.94
H9 5.01
D2O
H14,15 3.88
H8 3.55
H13 3.19
3.15 H16
H7 3.06
H18 2.00
Ether 1.18
H12 0.87
H12 0.13
.95 1.10 0.99
2.26
4.58 2.37 8.24 10.99 2.60
2.46
8.87
5.87
Chemical Shift (ppm)

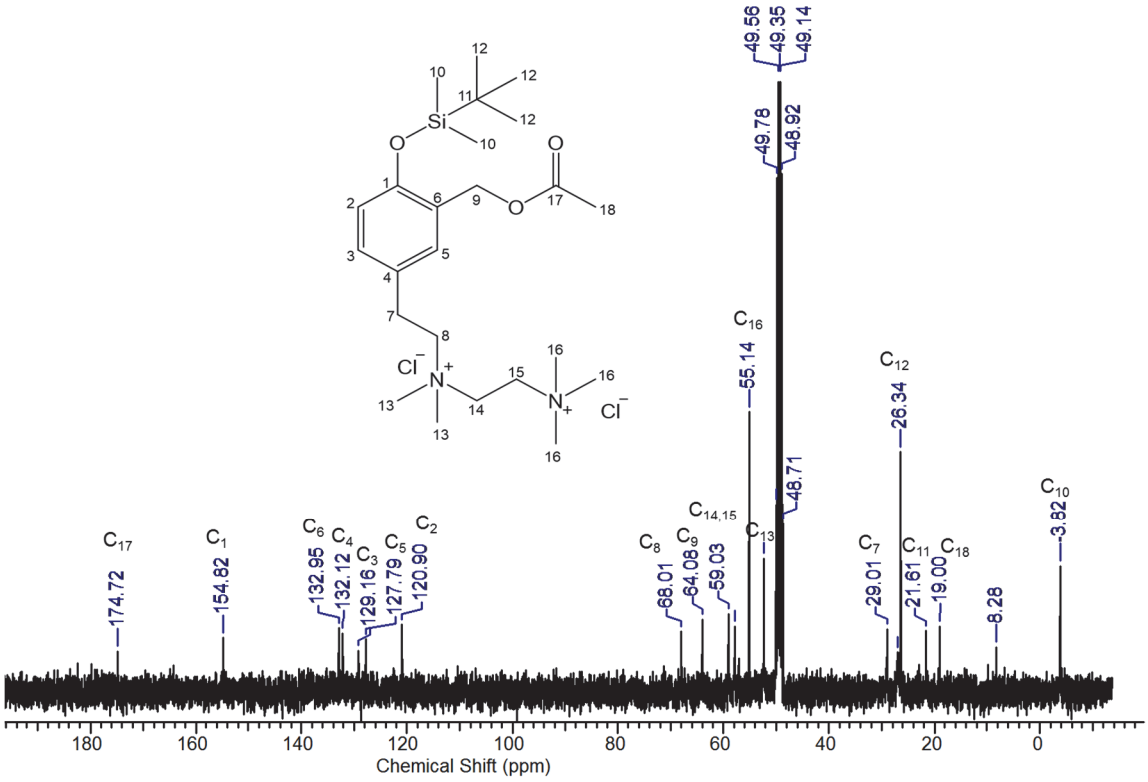
49.56
49.35
49.14
49.78
48.92
48.71
C16
55.14
C12
26.34
C10
3.82
C14,15
C13
C17
174.72
C1
154.82
C6
132.95
C4
132.12
C3
129.16
C5
127.79
C2
120.90
C8
68.01
C9
64.08
59.03
C7
29.01
C11
21.61
C18
19.00
8.28
Cl⁻
Cl⁻
Chemical Shift (ppm)

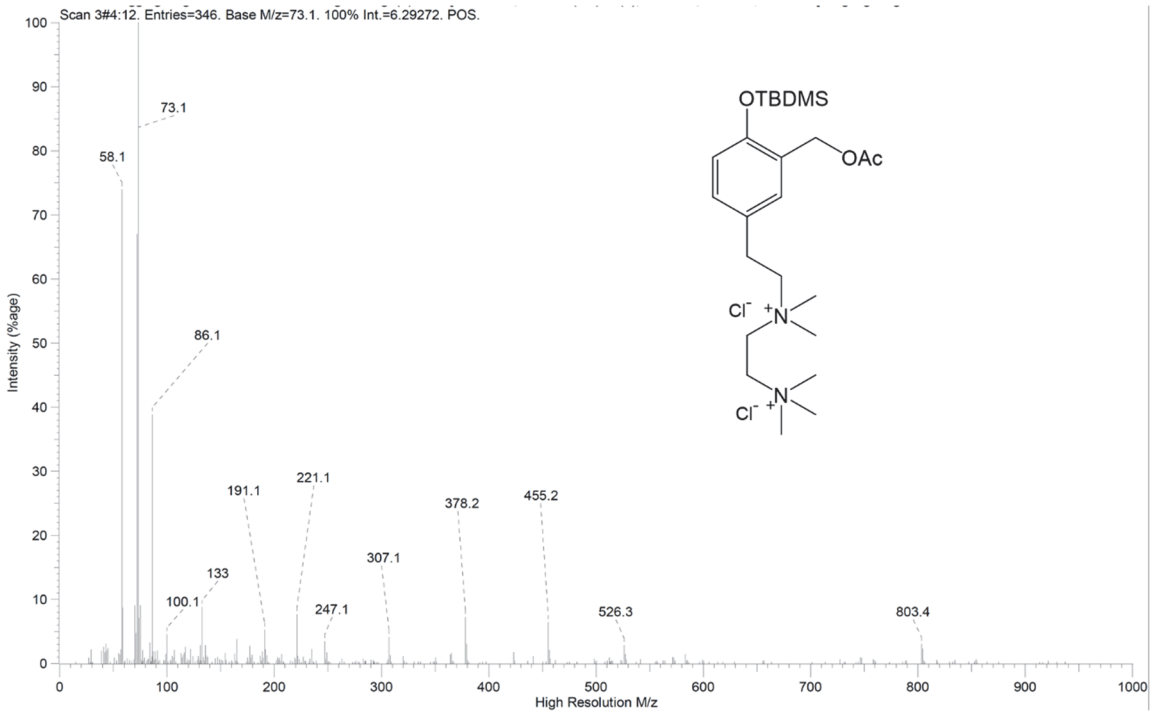
Scan 3#4:12. Entries=346. Base M/z=73.1. 100% Int.=6.29272. POS.
Intensity (%age)
High Resolution M/z
73.1
58.1
86.1
191.1
221.1
378.2
455.2
307.1
133
100.1
247.1
526.3
803.4
OTBDMS
OAc
Cl⁻
Cl⁻

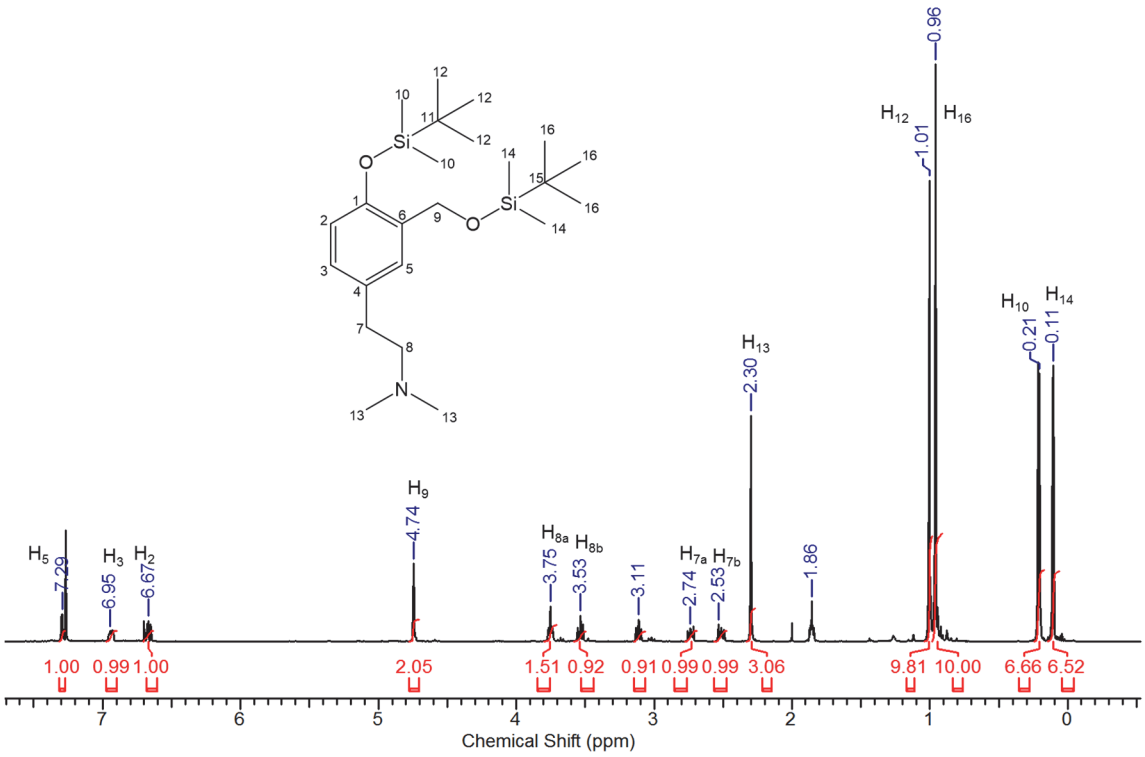
H5
7.29
H3
6.95
H2
6.67
H9
4.74
H8a
3.75
H8b
3.53
3.11
H7a
2.74
H7b
2.53
H13
2.30
1.86
H12
H16
1.01
0.96
H10
0.21
H14
0.11
1.00 0.99 1.00 2.05 1.51 0.92 0.91 0.99 0.99 3.06 9.81 10.00 6.66 6.52
7 6 5 4 3 2 1 0
Chemical Shift (ppm)

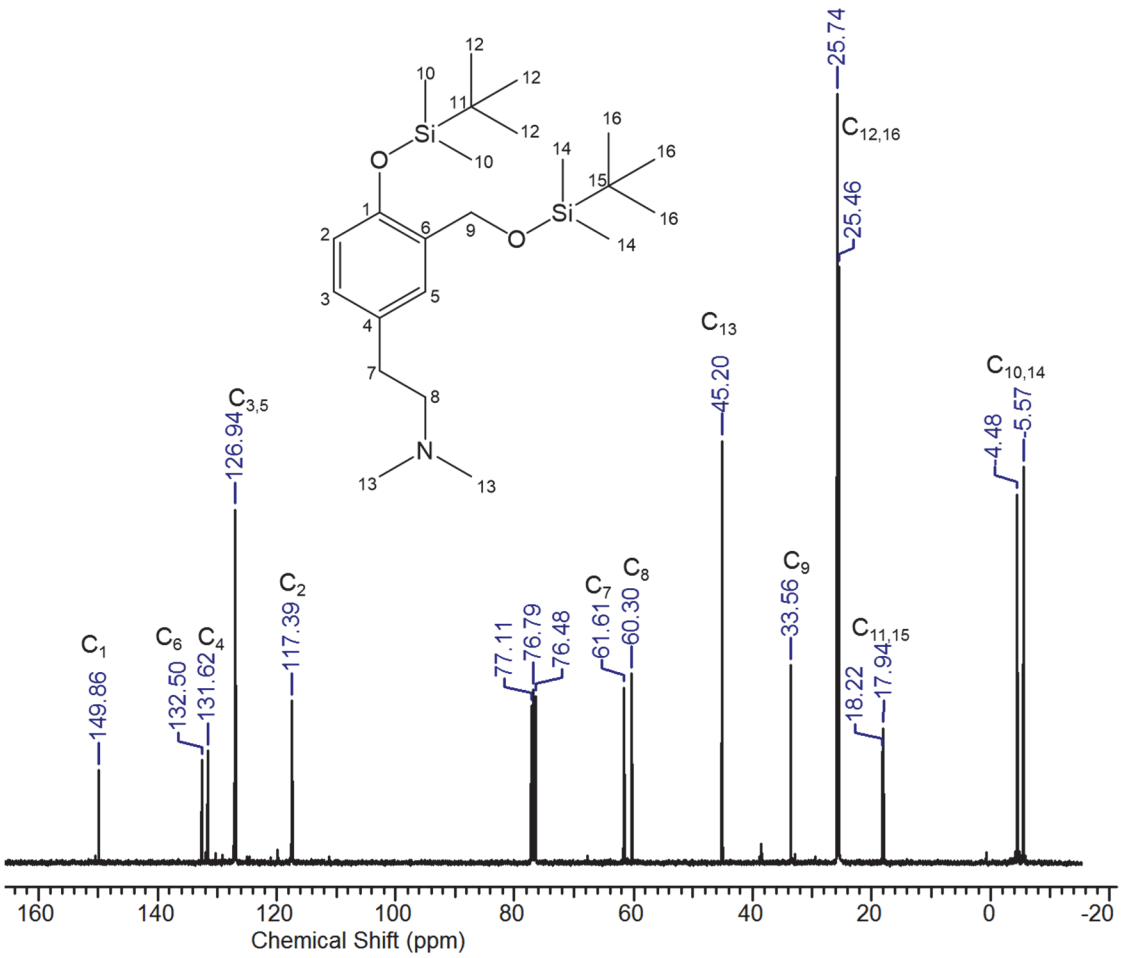
C1
149.86
C6
132.50
C4
131.62
C3,5
126.94
C2
117.39
77.11
76.79
76.48
C7
61.61
C8
60.30
C13
45.20
C9
33.56
25.74
C12,16
25.46
C11,15
18.22
17.94
C10,14
4.48
5.57
160
140
120
100
80
60
40
20
0
-20
Chemical Shift (ppm)

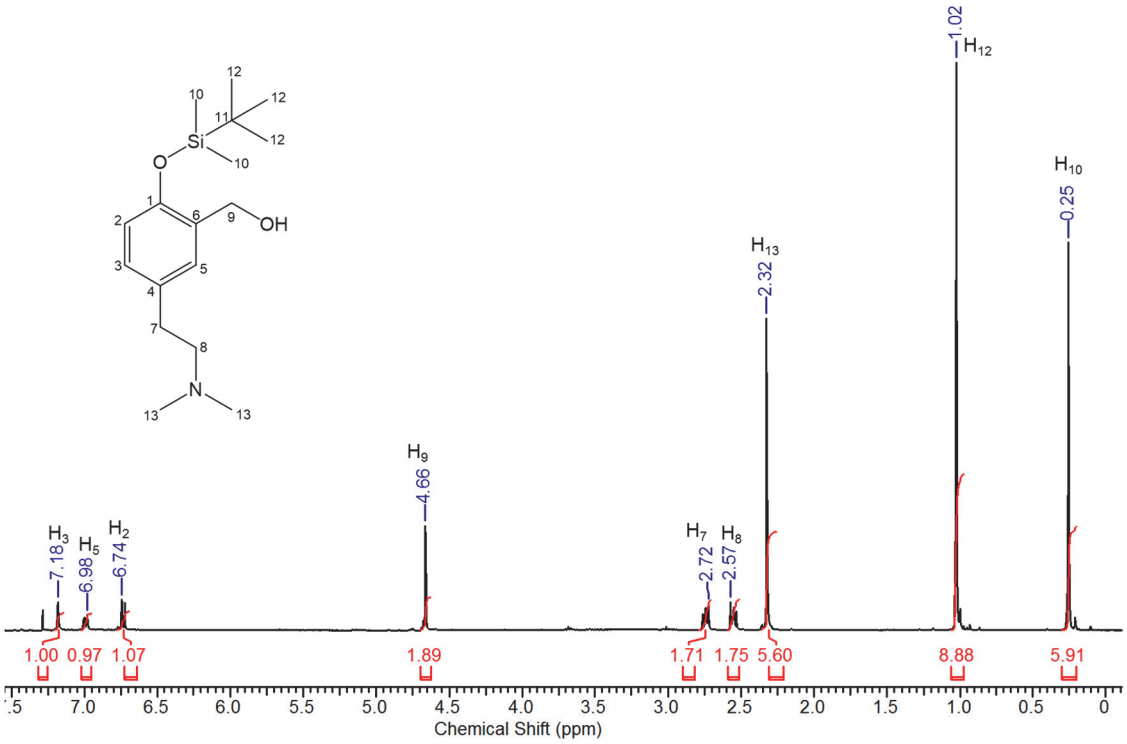
H12
1.02
H10
0.25
H13
2.32
H9
4.66
H3
7.18
H5
6.98
H2
6.74
H7
2.72
H8
2.57
1.00 0.97 1.07 1.89 1.71 1.75 5.60 8.88 5.91
Chemical Shift (ppm)

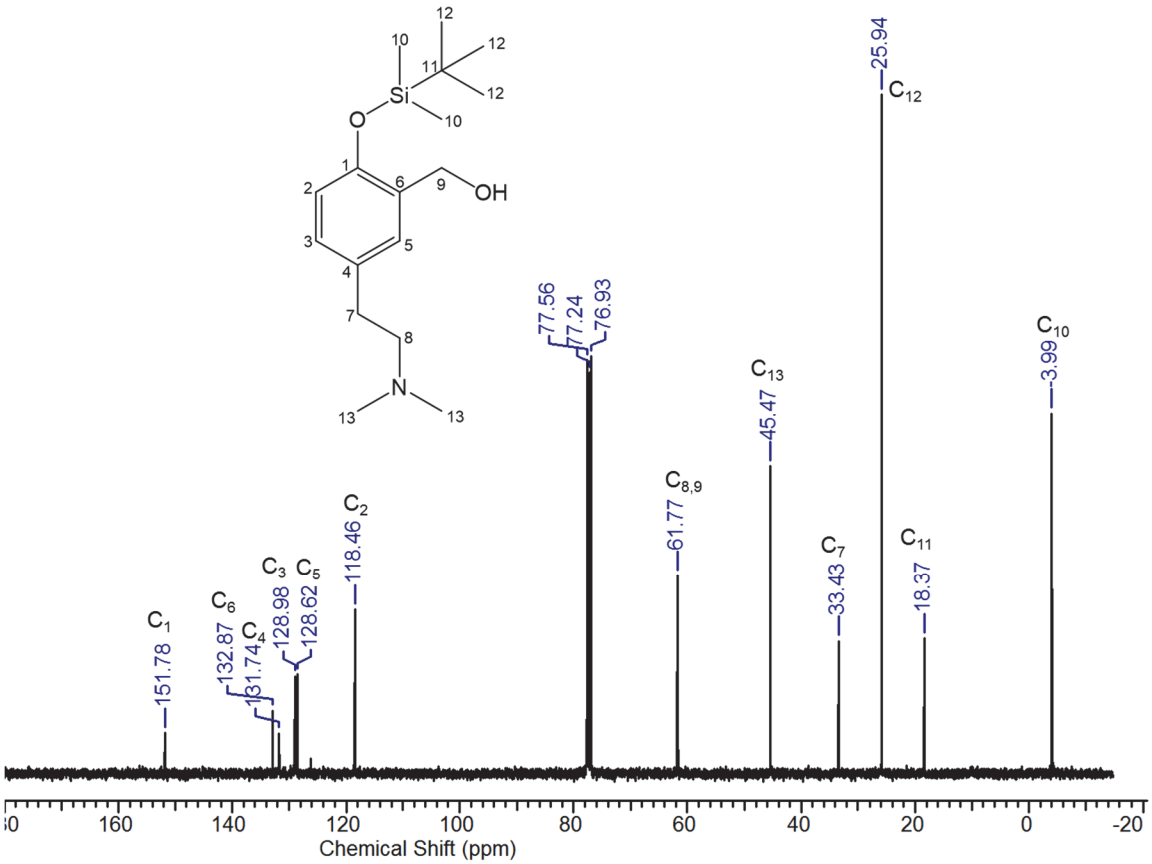
C12
25.94
C10
3.99
C13
45.47
C8,9
61.77
C7
33.43
C11
18.37
C2
118.46
C3
128.98
C5
128.62
C6
132.87
C4
131.74
C1
151.78
77.56
77.24
76.93
Chemical Shift (ppm)

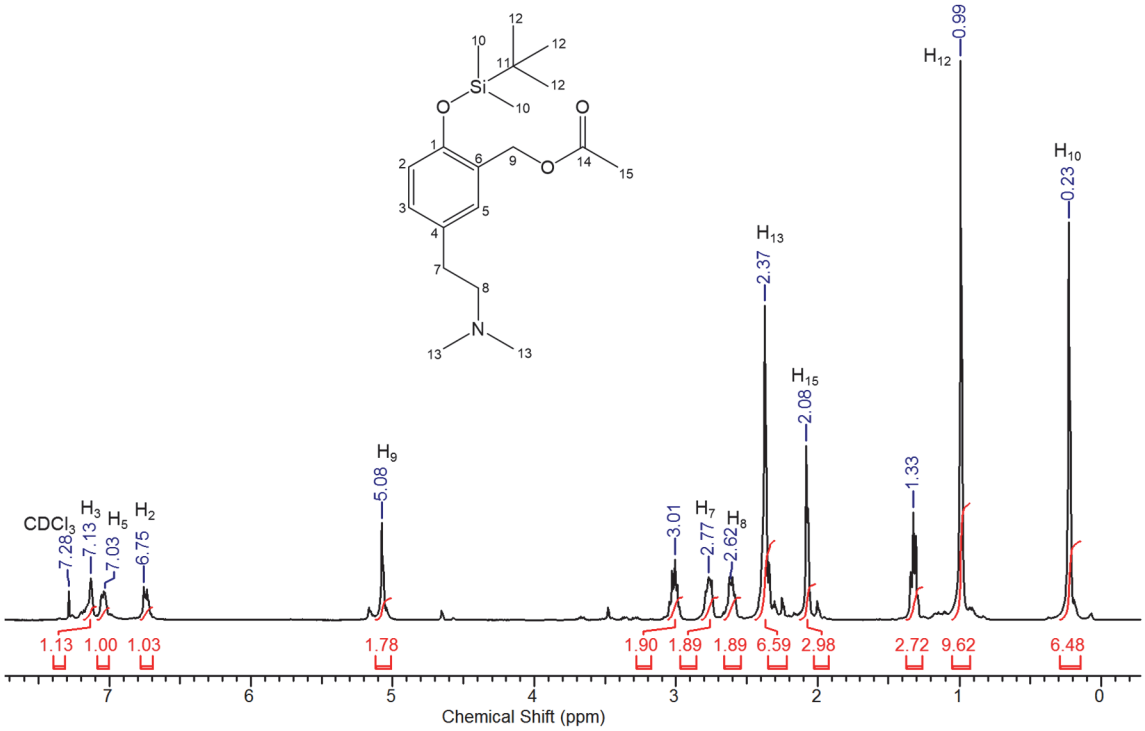
CDCl3
H3
H5
H2
H9
H7
H8
H13
H15
H12
H10
7.28
7.13
7.03
6.75
5.08
3.01
2.77
2.62
2.37
2.08
1.33
0.99
0.23
1.13
1.00
1.03
1.78
1.90
1.89
1.89
6.59
2.98
2.72
9.62
6.48
Chemical Shift (ppm)

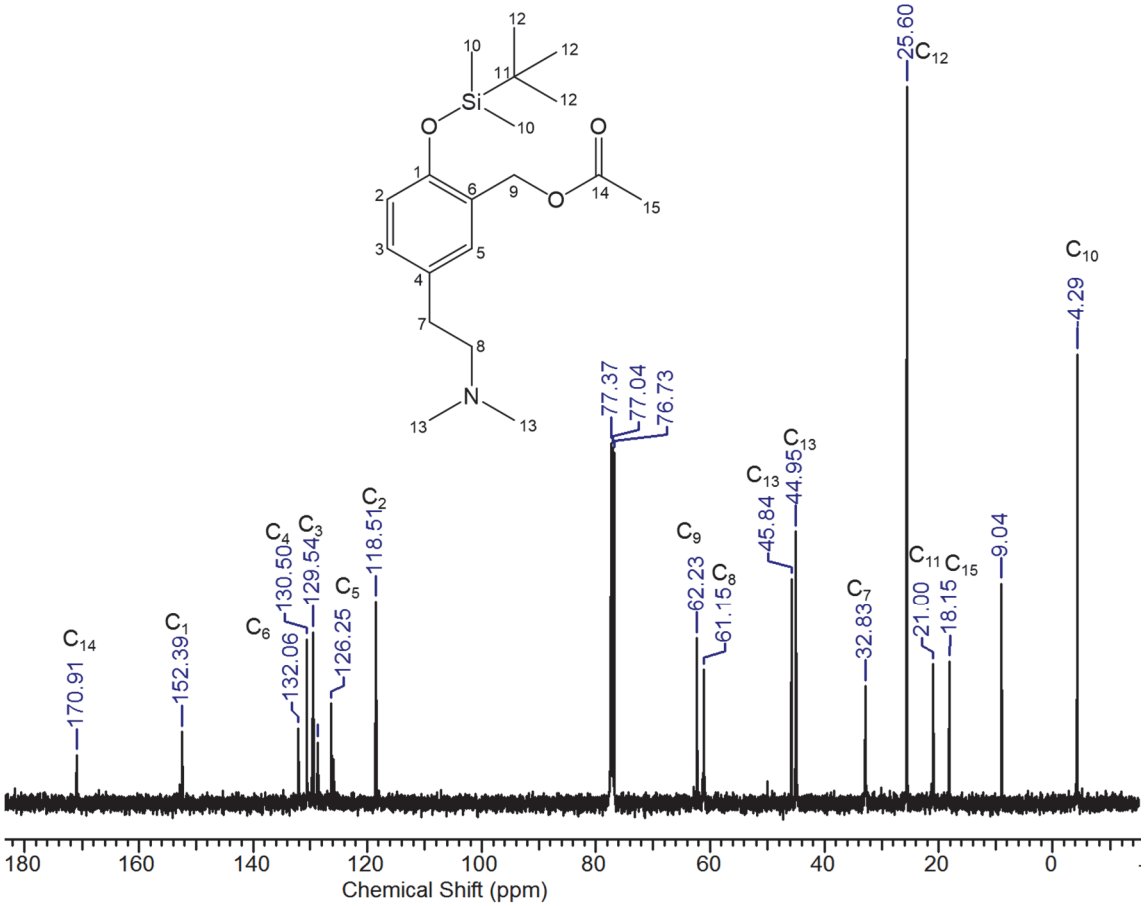
C14
C1
C6
C4
C3
C5
C2
C9
C8
C13
C13
C7
C11
C15
C12
C10
170.91
152.39
132.06
130.50
129.54
126.25
118.51
77.37
77.04
76.73
62.23
61.15
45.84
44.95
32.83
21.00
18.15
25.60
9.04
4.29
Chemical Shift (ppm)

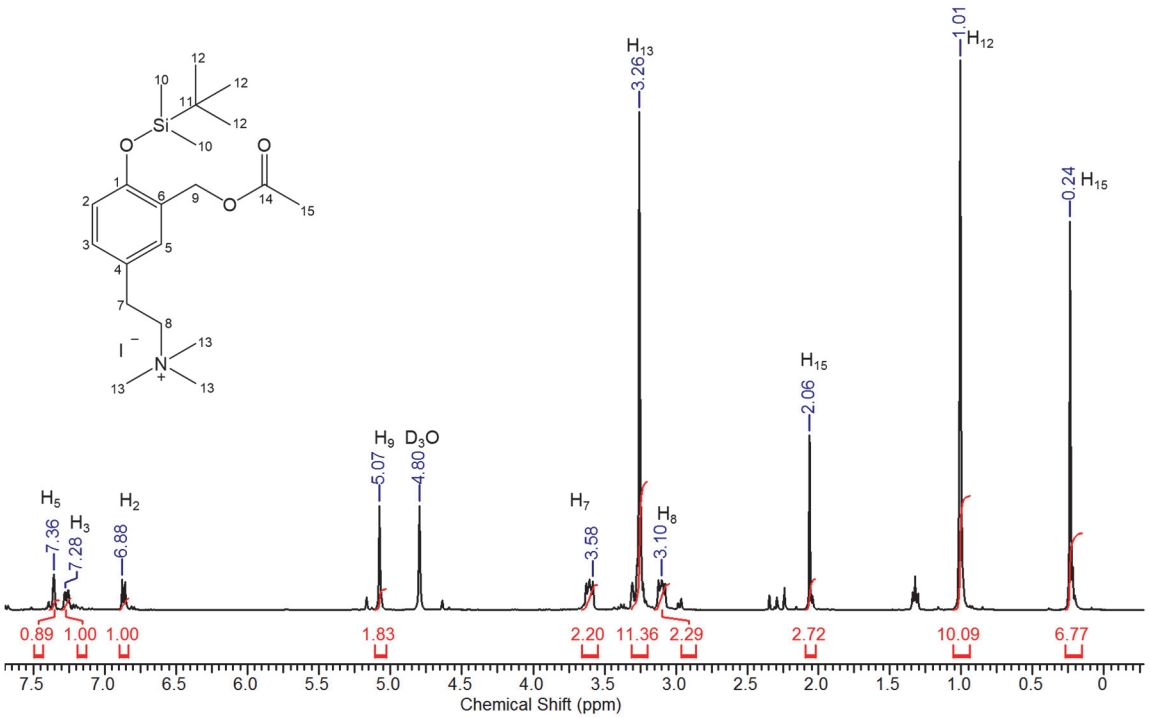
H13
3.26
1.01
H12
0.24
H15
H15
2.06
H9
D3O
5.07
4.80
H5
7.36
H3
7.28
H2
6.88
H7
3.58
H8
3.10
0.89
1.00
1.00
1.83
2.20
11.36
2.29
2.72
10.09
6.77
Chemical Shift (ppm)

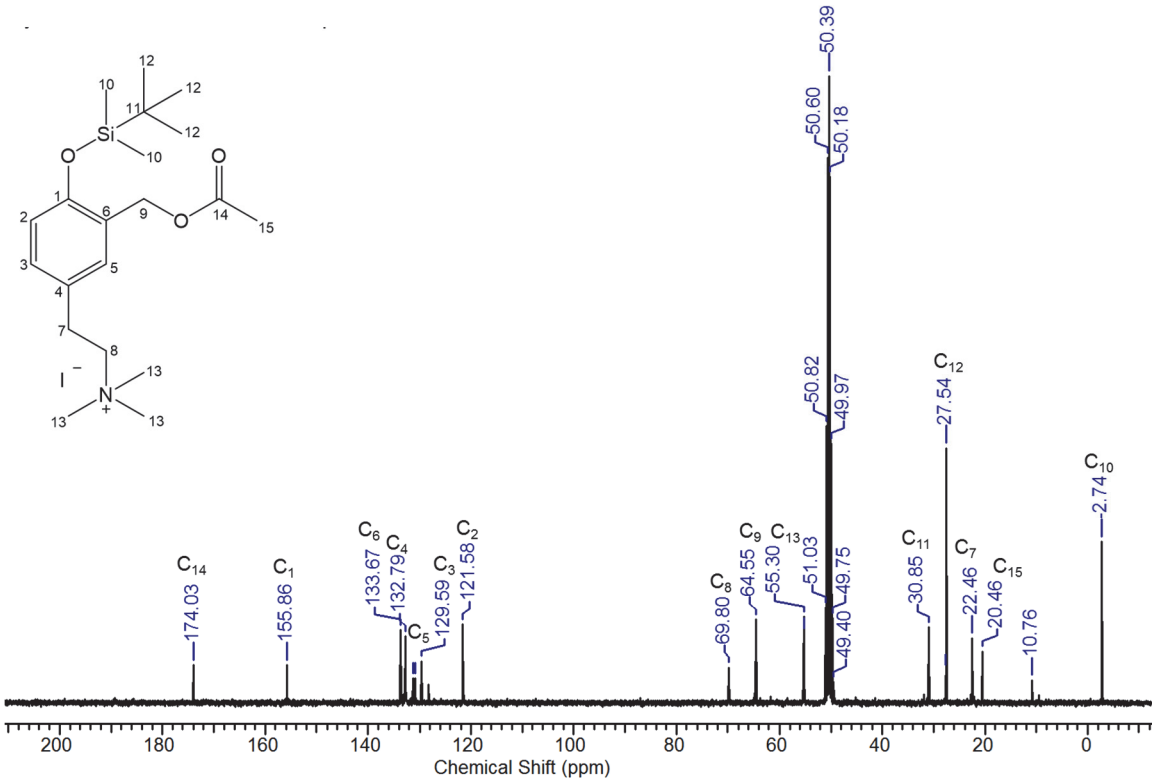
50.39
50.60
50.18
50.82
49.97
C12
27.54
C10
2.74
C14
174.03
C1
155.86
C6
133.67
C4
132.79
C5
C3
129.59
C2
121.58
C8
69.80
C9
64.55
C13
55.30
51.03
49.75
49.40
C11
30.85
C7
22.46
C15
20.46
10.76
Chemical Shift (ppm)

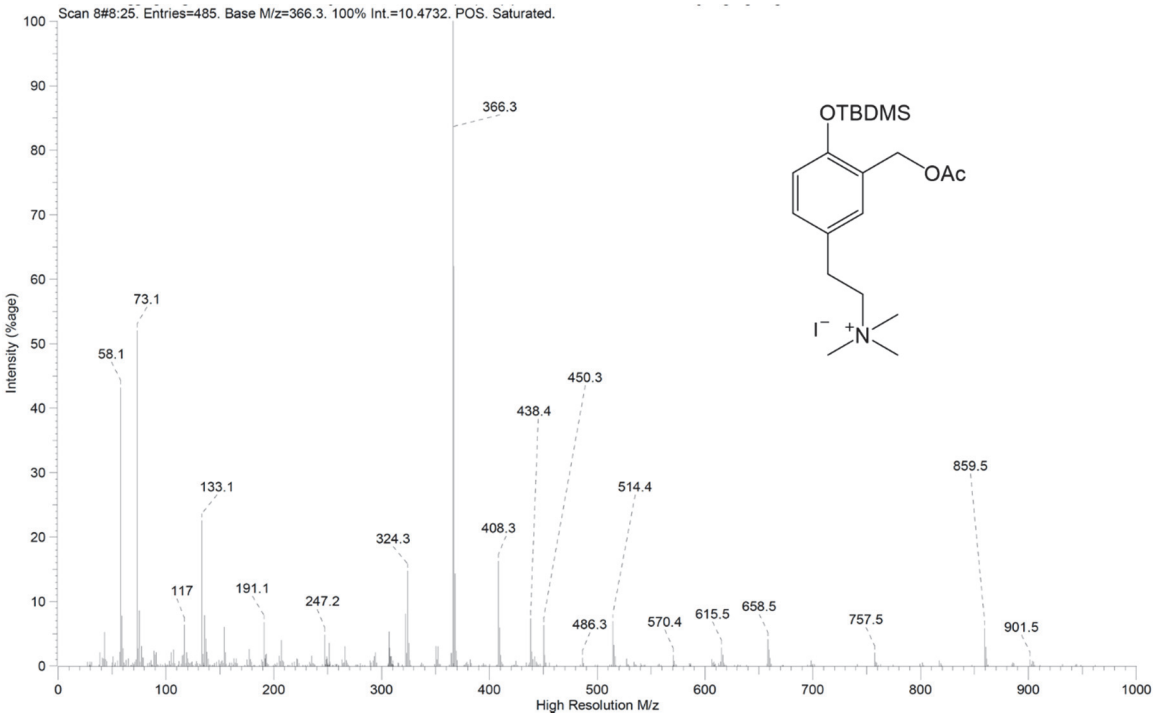
Scan 8#8:25. Entries=485. Base M/z=366.3. 100% Int.=10.4732. POS. Saturated.
Intensity (%age)
High Resolution M/z
366.3
73.1
58.1
450.3
438.4
133.1
514.4
859.5
408.3
324.3
117
191.1
247.2
486.3
570.4
615.5
658.5
757.5
901.5
OTBDMS
OAc
I⁻
+N

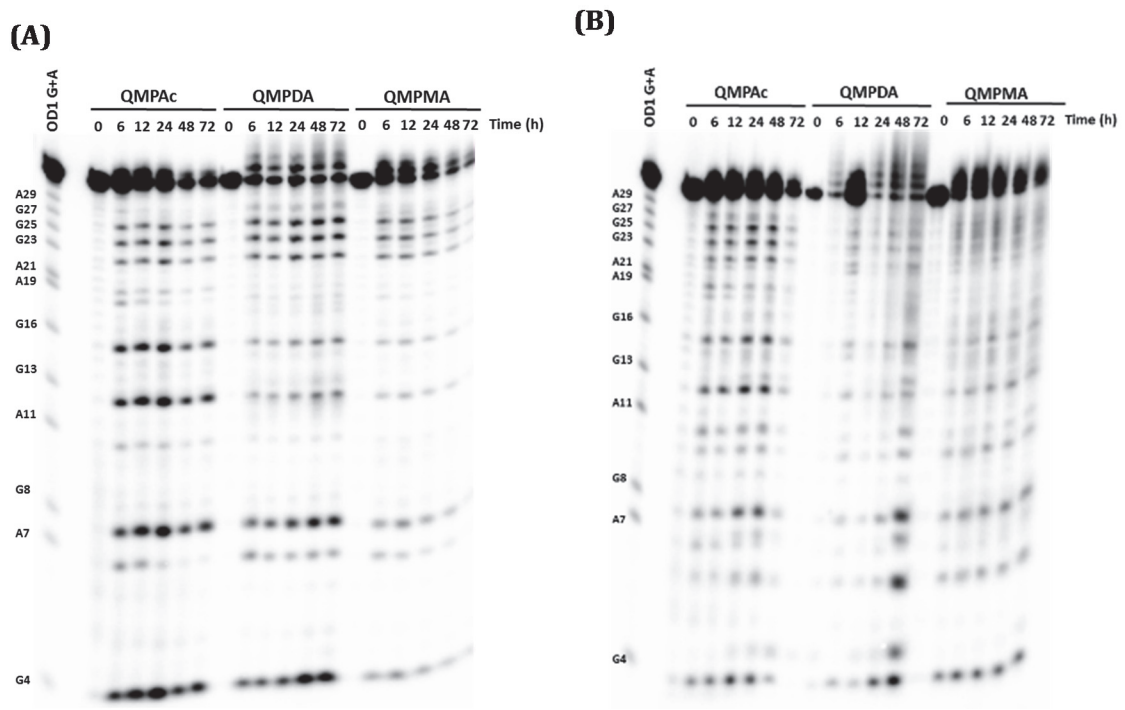

Figure B1: Time-dependent alkylation of ssDNA and dsDNA by either **QMPAc**, **QMPDA** or **QMPMA** at dG-N7. (A) dsDNA 5'-**[^{32}P]-OD1:OD2** (3.0 μM) and (B.) ssDNA 5'-**[^{32}P]-OD1** (3.0 μM) alkylation with **QMPAc** (120 μM), **QMPDA** (240 μM), and **QMPMA** (960 μM), in the presence of NaF (10 mM) and MES buffer (10 mM, pH 7.0) from 0 – 72 h, followed by 10 % hot piperidine treatment.

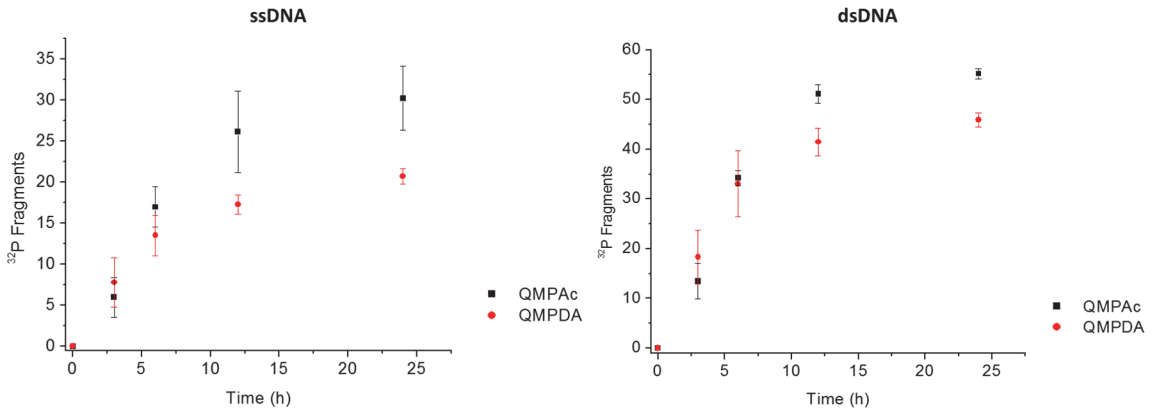

Figure B2: Time-dependent alkylation of ssDNA and dsDNA by either **QMPAc**, or **QMPDA** at dG-N7. ssDNA 5'-**[^{32}P]-OD1** (3.0 μM) and dsDNA 5'-**[^{32}P]-OD1:OD2** (3.0 μM) alkylation with either **QMPAc** or **QMPDA** (240 μM), in the presence of NaF (10 mM) and MES buffer (10 mM, pH 7.0) from 0 – 24 h, followed by 10 % hot piperidine treatment. Reaction yield is an average of independent three trials, determined by subtracting fragment intensity from t = 0. Error is an average of the standard deviation.

References

1 Drabløs, F.; Feyzi, E.; Aas, P. A.; Vaagbø, C. B.; Kavli, B.; Bratlie, M. S.; Peña-Diaz, J.; Otterlei, M.; Slupphaug, G.; Krokan, H. E. Alkylation damage in DNA and RNA—repair mechanisms and medical significance. *DNA Repair* **3**, 1389-1407, 2004.

2 Sancar, A., Lindsey-Boltz, L. A., Ünsal-Kaçmaz, K. & Linn, S. Molecular mechanisms of mammalian dna repair and the dna damage checkpoints. *Annu. Rev. Biochem.* **73**, 39-85, 2004.

3 Blackburn, G. M. & Gait, M. J. *Nucleic Acids in Chemistry and Biology*. 3 edn, 285-370, Oxford, 2007.

4 Hurley, L. H. DNA and its associated processes as targets for cancer therapy. *Nat. Rev. Cancer* **2**, 188-200, 2002.

5 Ferguson, L. R. & Denny, W. A. Genotoxicity of non-covalent interactions: DNA intercalators. *Mut. Res.-Fund. Mol. M.* **623**, 14-23, 2007.

6 Kohn, K. W. Beyond DNA Cross-Linking: History and Prospects of DNA-targeted Cancer Treatment—Fifteenth Bruce F. Cain Memorial Award Lecture. *Cancer Res.* **56**, 5533-5546, 1996.

7 Strekowski, L. & Wilson, B. Noncovalent interactions with DNA: An overview. *Mutat. Res., Fundam. Mol. Mech. Mutagen.* **623**, 3-13, 2007.

8 Rajski, S. R. & Williams, R. M. DNA cross-linking agents as antitumor drugs. *Chem. Rev.* **98**, 2723-2796, 1998.

9 Denny, W. A. DNA minor groove alkylating agents. *Expert Opin. Ther. Pat.* **10**, 459-474, 2000.

10 Noll, D. M., Mason, T. M. & Miller, P. S. Formation and repair of interstrand cross-links in DNA. *Chem. Rev.* **106**, 277-301, 2006.

11 Goodman, L. S.; Wintrobe, M. M.; Dameshek, W.; Goodman, M. J.; Gilman, A.; Mc, L. M. Nitrogen mustard therapy: Use of methyl-bis(beta-chloroethyl)amine hydrochloride and tris(beta-chloroethyl)amine hydrochloride for hodgkins disease, lymphosarcoma, leukemia and certain allied and miscellaneous disorders. *JAMA* **132**, 126-132, 1946.

12 Povirk, L. F. & Shuker, D. E. DNA damage and mutagenesis induced by nitrogen mustards. *Mut. Res.-Rev Genet.* **318**, 205-226, 1994.

13 Rink, S. M.; Solomon, M. S.; Taylor, M. J.; Rajur, S. B.; McLaughlin, L. W.; Hopkins, P. B. Covalent structure of a nitrogen mustard-induced DNA interstrand cross-link: an N7-to-N7 linkage of deoxyguanosine residues at the duplex sequence 5'-d(GNC). *J. Am. Chem. Soc.* **115**, 2551-2557, 1993.

14 Mattes, W. B., Hartley, J. A. & Kohn, K. W. DNA sequence selectivity of guanine–N7 alkylation by nitrogen mustards. *Nucleic Acids Res.* **14**, 2971-2987, 1986.

15 Rink, S. M. & Hopkins, P. B. A mechlorethamine-induced DNA interstrand cross-link bends duplex DNA. *Biochemistry..* **34**, 1439-1445, 1995.

16 Puyo, S., Montaudon, D. & Pourquier, P. From old alkylating agents to new minor groove binders. *Crit. Rev. Oncol./Hematol.* **89**, 43-61, 2014.

17 Tomasz, M. Mitomycin C: small, fast and deadly (but very selective). *Chem. Biol.* **2**, 575-579, 1995.

18 Weidner, M. F., Sigurdsson, S. T. & Hopkins, P. B. Sequence preferences of DNA interstrand cross-linking agents: dG-to-dG cross-linking at 5'-CG by structurally simplified analogs of mitomycin C. *Biochemistry.* **29**, 9225-9233, 1990.

19 Gnewuch, C. T. & Sosnovsky, G. A Critical Appraisal of the Evolution of N-Nitrosoureas as Anticancer Drugs. *Chem. Rev.* **97**, 829-1014, 1997.

20 Kohn, K. W. Interstrand Cross-linking of DNA by 1,3-Bis(2-chloroethyl)-1-nitrosourea and Other 1-(2-haloethyl)-1-nitrosoureas. *Cancer Res.* **37**, 1450-1454, 1977.

21 Sariban, E., Erickson, L. C. & Kohn, K. W. Effects of carbamoylation on cell survival and DNA repair in normal human embryo cells (IMR-90) treated with various 1-(2-chloroethyl)-1-nitrosoureas. *Cancer Res.* **44**, 1352-1357, 1984.

22 Rokita, S. E. Reversible alkylation of DNA by quinone methides. *Quinone Methides. John Wiley & Sons, Inc, New York*, 297-327, 2009.

23 Asai, A., Nagamura, S., Saito, H., Takahashi, I. & Nakano, H. The reversible DNA-alkylating activity of duocarmycin and its analogues. *Nucleic Acids Res.* **22**, 88-93, 1994.

24 Warpehoski, M. A., Harper, D. E., Mitchell, M. A. & Monroe, T. J. Reversibility of the covalent reaction of CC-1065 and analogs with DNA. *Biochemistry.* **31**, 2502-2508, 1992.

25 Boger, D. L. & Yun, W. Reversibility of the duocarmycin A and SA DNA alkylation reaction. *J. Am. Chem. Soc.* **115**, 9872-9873, 1993.

26 Pommier, Y.; Kohlhagen, G.; Bailly, C.; Waring, M.; Mazumder, A.; Kohn, K. W. DNA sequence- and structure-selective alkylation of guanine N2 in the DNA minor groove by Ecteinascidin 743, a potent antitumor compound from the caribbean tunicate ecteinascidia turbinata. *Biochemistry.* **35**, 13303-13309, 1996.

27 Zewail-Foote, M. & Hurley, L. H. Differential rates of reversibility of ecteinascidin 743-DNA covalent adducts from different sequences lead to migration to favored bonding sites. *J. Am. Chem. Soc.* **123**, 6485-6495, 2001.

28 Wang, H. Quinone Methides and Their Biopolymer Conjugates as Reversible DNA Alkylating Agents. *Curr. Org. Chem.* **18**, 44-60, 2014.

29 Freccero, M. Quinone methides as alkylating and cross-linking agents. *Mini-Rev. Org. Chem.* **1**, 403-415, 2004.

30 Thompson, D. C., Thompson, J. A., Sugumaran, M. & Moldéus, P. Biological and toxicological consequences of quinone methide formation. *Chem.-Biol. Interact.* **86**, 129-162, 1993.

31 Veldhuyzen, W. F., Shallop, A. J., Jones, R. A. & Rokita, S. E. Thermodynamic versus kinetic products of DNA alkylation as modeled by reaction of deoxyadenosine. *J. Am. Chem. Soc.* **123**, 11126-11132, 2001.

32 Weinert, E. E., Frankenfield, K. N. & Rokita, S. E. Time-dependent evolution of adducts formed between deoxynucleosides and a model quinone methide. *Chem. Res. Toxicol.* **18**, 1364-1370, 2005.

33 Weinert, E. E.; Dondi, R.; Colloredo-Melz, S.; Frankenfield, K. N.; Mitchell, C. H.; Freccero, M.; Rokita, S. E. Substituents on quinone methides strongly

modulate formation and stability of their nucleophilic adducts. *J. Am. Chem. Soc.* **128**, 11940-11947, 2006.

34 Zeng, Q. & Rokita, S. E. Tandem quinone methide generation for cross-linking DNA. *J. Org. Chem.* **61**, 9080-9081, 1996.

35 Verdolino, V., Cammi, R., Munk, B. H. & Schlegel, H. B. Calculation of pKa Values of Nucleobases and the Guanine Oxidation Products Guanidinohydantoin and Spiroiminodihydantoin using Density Functional Theory and a Polarizable Continuum Model. *J. Phys. Chem. B* **112**, 2008.

36 Li, T., Zeng, Q. & Rokita, S. E. Target-promoted alkylation of DNA. *Bioconjug. Chem.* **5**, 497-500, 1994.

37 Zhou, Q. & Rokita, S. E. A general strategy for target-promoted alkylation in biological systems. *Proc. Natl. Acad. Sci. U. S. A.* **100**, 15452-15457, 2003.

38 Zhou, Q., Pande, P., Johnson, A. E. & Rokita, S. E. Sequence-specific delivery of a quinone methide intermediate to the major groove of DNA. *Bioorg. Med. Chem.* **9**, 2347-2354, 2001.

39 Huang, C. & Rokita, S. E. DNA alkylation promoted by an electron-rich quinone methide intermediate. *Front. Sci. Ser.* **10**, 213-221, 2016.

40 Huang, C., Liu, Y. & Rokita, S. E. Targeting duplex DNA with the reversible reactivity of quinone methides. *Signal Transduct. Targeted Ther.* **1**, 16009, 2016.

41 Liu, Y. & Rokita, S. E. Inducible Alkylation of DNA by a quinone methide–peptide nucleic acid conjugate. *Biochemistry* **51**, 1020-1027, 2012.

42 Gleave, M. E. & Monia, B. P. Antisense therapy for cancer. *Nat Rev Cancer* **5**, 468-479, 2005.

43 Nielsen, P. E. Peptide Nucleic Acids (PNA) in Chemical Biology and Drug Discovery. *Chem. Biodivers.* **7**, 786-804, 2010.

44 Veldhuyzen, W. F., Pande, P. & Rokita, S. E. A transient product of DNA alkylation can be stabilized by binding localization. *J. Am. Chem. Soc.* **125**, 14005-14013, 2003.

45 Kumar, D., Veldhuyzen, W. F., Zhou, Q. & Rokita, S. E. Conjugation of a hairpin pyrrole-imidazole polyamide to a quinone methide for control of DNA cross-linking. *Bioconjug. Chem.* **15**, 915-922, 2004.

46 Wang, H. & Rokita, S. E. Dynamic cross-linking is retained in duplex DNA after multiple exchange of strands. *Angew. Chem. Int. Ed. Engl.* **49**, 5957-5960, 2010.

47 Fakhari, F. & Rokita, S. E. A walk along DNA using bipedal migration of a dynamic and covalent crosslinker. *Nat. Comm.* **5,** 2014.

48 Sági, J., Guliaev, A. B. & Singer, B. 15-mer DNA Duplexes Containing an Abasic Site Are Thermodynamically More Stable with Adjacent Purines Than with Pyrimidines. *Biochemistry .* **40**, 3859-3868, 2001.

49 Bolton, J. L., Valerio, L. G. & Thompson, J. A. The enzymic formation and chemical reactivity of quinone methides correlate with alkylphenol-induced toxicity in rat hepatocytes. *Chem. Res. Toxicol.* **5**, 816-822, 1992.

50 Bolton, J. L., Comeau, E. & Vukomanovic, V. The influence of 4-alkyl substituents on the formation and reactivity of 2-methoxy-quinone methides:

evidence that extended π-conjugation dramatically stabilizes the quinone methide formed from eugenol. *Chem.-Biol. Interact.* **95**, 279-290, 1995.

51 Loubinoux, B., Miazimbakana, J. & Gerardin, P. Reactivity of new precursors of quinone methides. *Tetrahedron Lett.* **30**, 1939-1942, 1989.

52 Nagata, W., Okada, K. & Aoki, T. ortho-Specific α-Hydroxyalkylation of Phenols with Aldehydes. An Efficient Synthesis of Saligenol Derivatives. *Synthesis* **1979**, 365-368, 1979.

53 Lönnberg, T., Hutchinson, M. & Rokita, S. Selective Alkylation of C-Rich Bulge Motifs in Nucleic Acids by Quinone Methide Derivatives. *Chemistry – A European Journal* **21**, 13127-13136, 2015.

54 Modica, E., Zanaletti, R., Freccero, M. & Mella, M. Alkylation of Amino Acids and Glutathione in Water by o-Quinone Methide. Reactivity and Selectivity. *J. Org. Chem.* **66**, 41-52, 2001.

55 Poole, L. B. The Basics of Thiols and Cysteines in Redox Biology and Chemistry. *Free Radical Biol. Med.* **0**, 148-157, 2015.

56 Wang, H., Wahi, M. S. & Rokita, S. E. Immortalizing a Transient Electrophile for DNA Cross-Linking. *Angew. Chem. Int. Ed.* **47**, 1291-1293, 2008.

57 Nelson, S. M., Ferguson, L. R. & Denny, W. A. Non-covalent ligand/DNA interactions: Minor groove binding agents. *Mutat. Res-Fund. Mol. M.* **623**, 24-40, 2007.

58 Cohen, G. M.; Cullis, P. M.; Hartley, J. A.; Mather, A.; Symons, M. C. R.; Wheelhouse, R. T. Targeting of cytotoxic agents by polyamines: synthesis of a

chlorambucil-spermidine conjugate. *J. Chem. Soc., Chem. Commun.*, 298-300, 1992.

59 Cullis, P. M., Merson-Davies, L. & Weaver, R. Conjugation of a polyamine to the bifunctional alkylating agent chlorambucil does not alter the preferred crosslinking site in duplex DNA. *J. Am. Chem. Soc.* **117**, 8033-8034, 1995.

60 M. Cullis, P., Merson-Davies, L. & Weaver, R. DNA alkylation sites of nitrogen mustards conjugated to polyamines and their implications for polyamine-DNA interactions. *Chem. Commun.*, 1699-1700, 1998.

61 Mandal, S., Mandal, A., Johansson, H. E., Orjalo, A. V. & Park, M. H. Depletion of cellular polyamines, spermidine and spermine, causes a total arrest in translation and growth in mammalian cells. *Proc. Nat. Acad. Sci. U.S.A.* **110**, 2169-2174, 2013.

62 Boger, D. L., Yun, W., Han, N. & Johnson, D. S. CC-1065 CBI analogs: an example of enhancement of DNA alkylation efficiency through introduction of stabilizing electrostatic interactions. *Biorg. Med. Chem.* **3**, 611-621, 1995.

63 Besley, S., Cullis, P. M., Partridge, R., Symons, M. C. R. & Wheelhouse, R. T. Motion of polyammonium ions on aqueous solutions of DNA. *Chem. Phys. Lett.* **165**, 120-124, 1990.

64 Wang, P.; Liu, R.; Wu, X.; Ma, H.; Cao, X.; Zhou, P.; Zhang, J.; Weng, X.; Zhang, X.-L.; Qi, J.; Zhou, X.; Weng, L. A potent, water-soluble and photoinducible DNA cross-linking agent. *J. Am. Chem. Soc.* **125**, 1116-1117, 2003.

65 Verga, D.; Nadai, M.; Doria, F.; Percivalle, C.; Di Antonio, M.; Palumbo, M.; Richter, S. N.; Freccero, M. Photogeneration and Reactivity of

Naphthoquinone Methides as Purine Selective DNA Alkylating Agents. *J. Am. Chem. Soc.* **132**, 2010.

66 Wang, Y.; Liu, S.; Lin, Z.; Fan, Y.; Wang, Y.; Peng, X. Photochemical generation of benzyl cations that selectively cross-link guanine and cytosine in DNA. *Org. Lett.* **18**, 2544-2547, 2016.

67 Wemmer, D. E., Srivenugopal, K. S., Reid, B. R. & Morris, D. R. Nuclear magnetic resonance studies of polyamine binding to a defined DNA sequence. *J. Mol. Biol.* **185**, 457-459, 1985.

68 Neidle, S. & Abraham, Z. Structural and Sequence-Dependent Aspects of Drug Intercalation Into Nucleic Acid. *Crit. Rev. Biochem. Mol. Bio.* **17**, 73-121, 1984.

69 Woodson, S. A. & Crothers, D. M. Binding of 9-aminoacridine to bulged-base DNA oligomers from a frame-shift hot spot. *Biochemistry.* **27**, 8904-8914, 1988.

70 Lindahl, T. & Nyberg, B. Rate of depurination of native deoxyribonucleic acid. *Biochemistry.* **11**, 3610-3618, 1972.

71 Lindahl, T. Instability and decay of the primary structure of DNA. *Nature* **362**, 709-715, 1993.

72 Sowers, L. C., David Sedwick, W. & Shaw, B. R. Hydrolysis of N3-methyl-2′-deoxycytidine: Model compound for reactivity of protonated cytosine residues in DNA. *Mut. Res-Fund. Mol. M.* **215**, 131-138, 1989.

73 Gates, K. S., Nooner, T. & Dutta, S. Biologically Relevant Chemical Reactions of N7-Alkylguanine Residues in DNA. *Chem. Res. Toxicol.* **17**, 839-856, 2004.

74 Loeb, L. A. & Preston, B. D. Mutagenesis by apurinic/apyrimidinic sites. *Annu. Rev. Genet.* **20**, 201-230, 1986.

75 Boiteux, S. & Guillet, M. Abasic sites in DNA: repair and biological consequences in Saccharomyces cerevisiae. *DNA Repair* **3**, 1-12, 2004.

76 Schroeder, G. K., Lad, C., Wyman, P., Williams, N. H. & Wolfenden, R. The time required for water attack at the phosphorus atom of simple phosphodiesters and of DNA. *Proc. Natl. Acad. Sci. U. S. A.* **103**, 4052-4055, 2006.

77 Lindahl, T. & Andersson, A. Rate of chain breakage at apurinic sites in double-stranded deoxyribonucleic acid. *Biochemistry.* **11**, 3618-3623, 1972.

78 Gates, K. S. An Overview of Chemical Processes That Damage Cellular DNA: Spontaneous Hydrolysis, Alkylation, and Reactions with Radicals. *Chem. Res. Toxicol.* **22**, 1747-1760, 2009.

79 Dutta, S., Chowdhury, G. & Gates, K. S. Interstrand Cross-Links Generated by Abasic Sites in Duplex DNA. *J. Am. Chem. Soc.* **129**, 1852-1853, doi:10.1021/ja067294u (2007).

80 Greenberg, M. M. Abasic and Oxidized Abasic Site Reactivity in DNA: Enzyme Inhibition, Cross-Linking, and Nucleosome Catalyzed Reactions. *Acc. Chem. Res.* **47**, 646-655, doi:10.1021/ar400229d (2014).

81 Wilson, D. M., Takeshita, M., Grollman, A. P. & Demple, B. Incision Activity of Human Apurinic Endonuclease (Ape) at Abasic Site Analogs in DNA. *J. Biol. Chem.* **270**, 16002-16007, 1995.

82 An, R.; Jia, Y.; Wan, B.; Zhang, Y.; Dong, P.; Li, J.; Liang, X. Non-Enzymatic Depurination of Nucleic Acids: Factors and Mechanisms. *PLOS ONE,* **9**, e115950, 2015.

83 Gelfand, C. A., Plum, G. E., Grollman, A. P., Johnson, F. & Breslauer, K. J. Thermodynamic Consequences of an Abasic Lesion in Duplex DNA Are Strongly Dependent on Base Sequence. *Biochemistry.* **37**, 7321-7327, 1998.

84 Fukui, K. & Tanaka, K. The acridine ring selectively intercalated into a DNA helix at various types of abasic sites: double strand formation and photophysical properties. *Nucleic Acids Res.* **24**, 3962-3967, 1996.

85 Berthet, N., Constant, J.-F., Demeunynck, M., Michon, P. & Lhomme, J. Search for DNA Repair Inhibitors: Selective Binding of Nucleic Bases−Acridine Conjugates to a DNA Duplex Containing an Abasic Site. *J. Med. Chem.* **40**, 3346-3352, 1997.

BLESSING DEEYAA
Phone: 678-350-4604. Email: bddeeyaa@gmail.com

EDUCATION

Johns Hopkins University, Baltimore, Maryland
Ph.D. Chemistry February 2017
M.A. Chemistry August 2013
Thesis Project: Conjugation of mono-functional quinone methides to DNA ligands for promotion of reversible alkylation

Georgia State University, Atlanta, Georgia
M.S. Chemistry July 2011
Thesis Project: Evaluation of DNA strand scission induced by a bis-9-aminomethylanthracene photosensitizing agent under conditions of high ionic strength

B.S. Chemistry, Minor in Biological Science May 2010

RESEARCH EXPERIENCE

Johns Hopkins University Baltimore, MD
Graduate Research Assistant; Advisor: Dr. Steven Rokita 2012-2017

- Completed multi-step synthesis of quinone methide precursors for DNA alkylation studies
- Purified and characterized synthesized products using silica column chromatography, chromatotron chromatography, preparatory TLC, NMR and HR-MS
- Identified reversible DNA adducts of quinone methides using radiolabeled ^{32}P oligonucleotides via gel electrophoresis, enzymatic digestion, HPLC and UPLC-MS

National Institute of Standards and Technology Gaithersburg, MD
Milligan Fellow, Materials Measurements Laboratory Summer 2011
Group Leader: Dr. Kathryn Beers

- Synthesized polyethylene glycol (PEG) hydrogels of varying crosslink densities
- Measured the stress relaxation of swollen hydrogels at varying indentation depths
- Determined the self-diffusion and mutual diffusion coefficient of water in swollen PEG hydrogels

Georgia State University Atlanta, GA
Graduate Research Assistant; Advisor: Dr. Kathryn Grant 2009-2010

- Analyzed anthracene binding modes and affinity to DNA helices using UV-visible spectroscopy, DNA thermal denaturing, and fluorescence spectroscopy
- Conducted photo-oxidation of plasmid DNA, induced by irradiation of a bis-anthracene dye with UV light
- Assessed DNA damage in the presence of NaCl, KCl, and several transition metals

Georgetown University, Research Experience for Undergraduate (NSF-REU) Washington, DC
Research Assistant; Advisor: Dr. Sarah Stoll Summer 2009

- Synthesized and characterized europium selenide nanoparticle precursor
- Conducted experiments under anaerobic conditions by means of Schlenk line and glove box
- Characterized an europium selenide complex using IR, NMR, X-ray crystallography, and thermal gravimetric analysis

AWARDS AND HONORS

- Howard Hughes Medical Institute Biotechnology Scholar 2010 – 2011
- Louis Stokes Alliance for Minority Participation Scholar 2009 –2010
- Dolphus E. Milligan Graduate Fellowship 2011, 2013-2015
- NOBCChE Advancing Science Travel Award 2015, 2016
- Johns Hopkins University Diversity Recognition Award 2016

PUBLICATIONS

- Chan, E.P., Deeyaa, B.D., Johnson, P.M., Stafford, C.M., (2012) Poroelastic relaxation of polymer-loaded hydrogels. *Soft Matter*.

PROFESSIONAL PRESENTATIONS

- **Deeyaa, B.D.**, Rokita, S.E., "Electron Rich Quinone Methide Promotes Sequence Selective Reversible DNA Alkylation" Technical Talk, National Organization for the Professional Advancement of Black Chemists and Chemical Engineers 43rd National Conference, Raleigh, NC, November 11th, 2016.
- **Deeyaa, B.D.**, Rokita, S.E., "Conjugation of Quinone Methides to DNA Ligands for Promotion of Reversible DNA Alkylation" Technical Talk, National Organization for the Professional Advancement of Black Chemists and Chemical Engineers 42nd National Conference, Orlando, FL, September 24th, 2015.
- **Deeyaa, B.D.**, Rokita, S.E., "Reversible DNA Alkylation by Mono-Quinone Methides" Contributed Poster, National Organization for the Professional Advancement of Black Chemists and Chemical Engineers 41st National Conference, New Orleans, LA, September 24th, 2014.
- **Deeyaa, B.D.**, Rokita, S.E., "Reversible DNA Alkylation by Pyrrolizidine Alkaloids" Contributed Poster, University of Maryland, College Park "Frontiers at the Chemistry-Biology Interface Symposium" College Park, MD, May 4th, 2013.
- **Deeyaa, B.D.,** Fernández, M.-J., Lorente, A., & Grant, K.B. "DNA Photocleavage by a Bis-9- Aminomethylanthracene Dye at pH 7.0: Ionic Strength Effects," Contributed Poster (Abstract 13), "Southeast Regional Undergraduate Research Conference: 42nd Annual Conference of Student Affiliates Chapters of the American Chemical Society," Kennesaw, GA, April 9, 2010.

REFERENCES

Ph.D. Advisor: Professor Steven Rokita, rokita@jhu.edu, 410-516-5793
M.S. Advisor: Professor Kathryn Grant, kbgrant@gsu.edu, 404-413-5522